Bulletin of the Earthquake
Research Institute
Vol. 39 (1961), pp. 133-248

7. *A Study of the Textural Characteristics of Pyroclastic Flow Deposits in Japan.*

By Isamu Murai,

Earthquake Research Institute.

(Read Dec. 20, 1960.—Received April 30, 1961.)

Contents

Abstract 134
Introduction 136
Acknowledgments 140
Terminology 141
Classification of pyroclastic flows 143
Materials for the study 147
Size characteristics of pyroclastic flow deposits 158
  General statement 158
  Methods of mechanical analyses 159
  Parameters of particle size distribution 185
  Summary of results 190
    1) Lack of sorting 191
    2) Homogeneity 199
    3) Median diameters 200
    4) Shape of particle size distribution 203
    5) Subdivisions of pyroclastic flow deposits based upon size characteristics 211
    6) Comparison of the size characteristics of dry mud-flow deposits and auto-brecciated lava flows 213
Roundness of particles 214
Types of vesicular shards and pumice 220
Constituent characteristics 223
Bulk density of essential fragments 228
Succession of eruptive events 230
Chemical properties of pyroclastic flow deposits 232
Discussions on the mode of origin and mechanism of pyroclastic flows 238
  Gas-emission process 238
  Dual character of pyroclastic flows 242
  Sorting agency 244

Intermediate cases between pyroclastic flows and dry mud-flows 246
Concluding remarks 247

Abstract

Phenomena of pyroclastic flows (nuées ardentes or glowing avalanches in a broad sense) involve all kinds of flows of incandescent fragmental materials of juvenile origin, graduating from the Pelean type eruptions attending protrusion of domes to eruptions that produce vast ash-flow sheets. Textural and constituent characteristics vary widely in accordance with differences in the types of pyroclastic flows. It is possible to consider that the nature and mode of origin of pyroclastic flows are precisely reflected in these characteristics of the deposits. The writer tried a quantitative study of these characteristics of pyroclastic flow deposits in Japan. His study was carried out on samples collected from non-welded deposits or non-welded parts of welded deposits. 192 samples of pyroclastic flow deposits and 35 samples of pyroclastic fall deposits were collected from various volcanic regions in Japan, and mechanical analyses of these samples were performed. Among these samples, 59 samples of pyroclastic flow deposits were selected as representative of every unit of flows. Moreover, 5 samples of pyroclastic fall deposits which were caused by preceding eruptions immediately before the discharge of pyroclastic flows were selected to compare their characteristics with those of pyroclastic flows. On these samples, measurements of the roundness of constituent particles, the bulk density of essential fragments, the relative abundance of a peculiar type of glass shards and pumice or scoria crowded with fine tubular vesicles, and of the relative proportion of each element of the constituents were carried out. Besides these, 15 samples of dry mud-flow deposits and 5 samples of auto-brecciated lava flows were collected, and their size characteristics were analysed in order to compare them with those of pyroclastic flow deposits.

The most distinct features of pyroclastic flow deposits are the poorly sorted size characteristics. Data of mechanical analyses of every kind of pyroclastic flow deposits usually show a chaotic mingling of particles graduating from large blocks to fine dust, contrasting strikingly with the well-sorted size characteristics of pyroclastic fall deposits. The shape of the particle size distribution curves of every kind of pyroclastic flow deposit shows a close resemblance, each with the other. Each curve has tailingout parts both in coarser and finer fractions, a gentle mode in medium fractions, and a sub-mode, conspicuous or faint, in coarser fractions. Such size characteristics are

always found in all deposits of pyroclastic flows. There exists, however, considerable room for variation within the framework of size distribution curves. Pyroclastic flows are grouped into several subdivisions based upon the differences in the mode of origin and mechanism of emplacement as well as the differences in size characteristics and other textural characteristics of their deposits as follows: (1) nuée ardente of Pelée type and Sakurajima type, (2) intermediate type pyroclastic flow, (3) St. Vincent ash-flow, (4) Krakatoa type ash-flow (fine-grained and medium-grained), (5) Valley of Ten Thousand Smokes type ash-flow (or fissure eruption type ash-flow).

The size characteristics of dry mud-flow deposits and auto-brecciated lava flows are similar to those of pyroclastic flow deposits, but usually more poorly sorted and of coarser grain. Their size distribution curves tend to conform to Rosin's law of crushing. On the contrary, those of pyroclastic flow deposits show some disparities from Rosin's law, indicating the efficiency of sorting at the time of eruption and during flowage. It is possible to consider that sorting in a vertically rising column of ash or during the flowage of expanding cloud, as well as explosive disintegration and attrition or collision on the way of the ascent of frothing magma and during flowage, control the size characteristics of pyroclastic flow deposits. Although particles of all sizes are transported *en masse* in a state of turbulent flow as indicated by the distinct ill-sorted features of the deposits, the sorting agency has some effects upon their size characteristics.

Judging from the results of measurements of the roundness of particles and types of pumice and glass shards, together with the results of inspections of other features of pyroclastic flow deposits, it is clarified that in eruptions of the intermediate type pyroclastic flows and nuées ardentes, most of the vesiculation takes place during flowage, while in eruptions of the Krakatoa type ash-flows, it occurs within the vent, conduit or chamber, and in eruptions of the St. Vincent type ash-flows, vesiculation begins partly within the vent and occurs mostly at the time of discharge. In general, discharge of pyroclastic flows follows preliminary explosions. It is inferred that eruptions of pyroclastic flows take place after the removal of a confining load at the top of the vent by preliminary explosions.

It is possible to consider that magmas which produce pyroclastic flow eruptions have a relatively large amount of volatiles, and differences in the gas-emission process in the erupting magmas cause various types of pyroclastic flows. Rock types of the deposits seem to belong to the hypersthenic rock series which is produced by the contamination of the original magma and granitic substances. Perhaps such contamination may cause concentration of volatiles in magmas which is inferred to be responsible for the eruptions of pyroclastic flows.

Introduction

A characteristic eruption took place at Mt. Pelée on Martinique which is one of the Windward Islands of the West Indies on May 8th, 1902. A dark eruption-cloud was discharged laterally from the flank of the dome rising in the pre-existing summit crater, rushing down *en masse* along the mountain-slope of the volcano at a surprisingly high speed. St. Pierre, situated on the southwest foot of the volcano, was wiped away by this devastating hot cloud. The eruptive activity continued for the following several months, and similar peculiar eruptions occurred repeatedly. This type of eruption had not been recognized by any geologist until that time. The seething hot cloud cosisting of clastic materials and gases did not rise vertically into the air, but was swept down along the mountain-side. Lacroix (1903) introduced "nuée ardente" as a geological term for these disastrous eruptions on May 8th, 1902 and for the subsequent eruptions at Mt. Pelée[1].

Another similar peculiar eruption took place on May 7th, 1902 at the Soufrière on St. Vincent which also lies within the Windward Islands. The eruption occurred through an open crater on the summit, and a column of ash and steam rose to an enormous height. During the early climactic phase of the eruption, incandescent avalanches rose from the crater and poured over the mountain-slope. These avalanches also came to bear the same name "nuées ardentes". The characteristics of these two types of eruptions occurring almost at the same time in the Windward Islands were described in detail in the comprehensive reports assembled by Lacroix (1904, 1908) and Anderson and Flett (1903)[2]. Since then, phenomena of nuées ardentes have attracted the attention of many geologists and volcanologists. Detailed studies on eruptions of nuées ardentes occurring in this century, as well as those on pyroclastic deposits which were considered to be the products of nuées ardentes, have been induced by the two well-known papers. The two eruptions that occurred in the Windward Islands in 1902 have

1) Alfred LACROIX, "L'eruption de la montagne Pelée en janvier 1903," *Acad. Sci., (Paris), Comptes rendus,* **136** (1903), 442-445.

2) Alfred LACROIX, "La Montagne Pelée et ses éruptions," *Paris, Masson et Cie,* (1904), 662.

Alfred Lacroix, "La Montagne Pelée apres ses éruptions," Acid. Sci., Paris, (1908), 74-93.

Tempest ANDERSON and J. S. FLETT, "Report on the eruption of the Soufrière in St. Vincent in 1902, and on a visit to Montagne Pelée in Martinique, Pt. I," *Philos. Trans. Royal Soc. London, ser. A,* **200** (1903), 353-553.

been considered as the classic examples of nuées ardentes or glowing avalanches.

In 1929–1932, similar eruptions took place at Mt. Pelée. Perret (1935), who witnessed more than 100 nuées ardentes from Pelée, discussed the nature of these eruptions in detail[3]. It became clear that similar eruptions had occurred repeatedly since the historic ages at the Merapi Volcano in Central Java. In 1930–1935, violent nuées ardentes occurred at the Merapi Volcano, which were reported in detail by Stehn (1936) and Neumann van Padang (1933)[4]. Van Bemmelen (1949) summarized the nuée ardente phenomenon on the basis of his observations in Indonesia, principally at Merapi[5]. Nuées ardentes occurred at Mt. Lamington in New Guinea in 1951–1952, which were reported by Fisher (1945) and Taylor (1954 and 1956)[6]. Macdonald and Alcaraz (1956) described nuées ardentes that took place at the Hibok-Hibok Volcano in the Philippines in 1948–1953[7]. Thus the data of nuées ardentes phenomena have been augmented by many accounts of these eruptions.

Besides, many examples of nuées ardentes products have been recognized through detailed studies on pyroclastic deposits in every volcanic region in the world. Now, it is well known that nuées ardentes or glowing avalanches have been discharged throughout the geologic column as far distant as the pre-Cambrian. Deposits of nuées ardentes are distributed widely along orogenic belts in the world. Fenner (1920, 1923, 1937 and 1950) studied the origin of the tuff deposits emplaced in the Valley of Ten Thousand Smokes, Katmai, at the time of the 1912 erup-

3) F. A. PERRET, "The eruption of Mt. Pelée 1929-1932," *Carnegie Inst. Washington, Pub.* No. 457 (1935), 125.

4) M. NEUMANN van PADANG, "De Uitbarsting van den Merapi (Midden Java) in de jaren 1930-1931," *Vulkan. en Seismol. Mededeel*, No. 12 (1933), Batavia, 135.

C. E. STEHN, "Beobachtungen an Glutwolken wahrend der erhohted Tatigkeit des Vulkans Merapi in Mittel-Java in den Jahren 1933-1935," *Handel. v/h 7 de Ned.-Indie Natuurwet Congres, Batavia*, (1936), 647-656.

5) R. W. van BEMMELEN, "Geology of Indonesia, v. 1A, General geology of Indonesia and adjacent archipelagoes," *The Hague, Government Printing Office*, (1949), 732.

6) N. H. FISHER, "Report of the subcommittee on volcanology 1951," *Bull. Volcanol., ser., 2,* **15** (1954), 71-80.

G. A. TAYLOR, "Volcanological observations Mount Lamington, 29th May 1952," *Bull. Volcanol., ser. 2,* **15** (1954), 81-97.

G. A. TAYLOR, "An outline of Mount Lamington eruption phenomena," *8th Pacific Sci. Cong., Philippines 1953,* **2** (1956), 83-88.

7) G. A. MACDONALD and A. ALCARAZ, "Nuées ardentes of the 1948-1953 eruption of Hibok-Hibok," *Bull, volcanol., ser. 2,* **18** (1956), 169-178.

tion. He wrote a number of papers in which he set out volcanological evidences and inferred from these the nature and mechanism of incandescent tuff-flows[8]. Moore (1934) described the recent pumice deposits of the Crater Lake region and discussed their origin. He concluded that one of them, named the "Older Pumice", was apparently different in origin from pumice deposits of the normal air-fall type, being regarded as a product of nuée ardente, judging from the size characteristics, distribution and other sedimentary features[9]. Marshall (1932, 1935 and 1953) discussed the origin of rhyolite tuff deposits named "ignimbrite", distributed in an extensive sheet-like form in the Taupo-Rotorua region, New Zealand. He assumed that ignimbrites were formed by nuée ardente type flows which were erupted as a highly mobile emulsion of incandescent ash, gas and other pyroclastic material[10]. Williams (1941) discussed the mechanism of the formation of calderas, and pointed out the fact that calderas of the "Krakatau type" were formed by collapse following the eruption of a tremendous amount of pumice, usually in the form of nuées ardentes[11]. Recently, Hay (1959) studied the deposits of glowing avalanches discharged from the Soufrière of St. Vincent on May 7th, 1902, discussing the mechanism of avalanches produced from a vertically rising column of ash and steam[12].

In Japan, deposits of nuées ardentes have been reported from several volcanic regions. In 1929, a great eruption took place on the

8) C. N. FENNER, "The Katmai region, Alaska, and the great eruption of 1912," *Jour. Geol.*, **28** (1920), 569-606.

C. N. FENNER, "The origin and mode of emplacement of the great tuff deposits in the Valley of Ten Thousand Smokes," *Natl. Geog. Soc. Contributed Tech. Papers, Katmai Ser.*, No. 1, (1923), 74.

C. N. FENNER, "Tuffs and other volcanic deposits of Katmai and Yellowstone Park," *Trans. Am. Geophys. Union, 18th Ann. Mtg., pt. 1*, (1937), 236-239.

C. N. FENNER, "The chemical kinetics of the Katmai eruption," *Am. Jour. Sci.*, **248** (1950), 593-627, 697-725.

9) B. N. MOORE, "Deposits of possible nuée ardente origin in the Crater Lake region, Oregon," *Jour. Geol.*, **42** (1934), 358-375.

10) Patrick Marshall, "Notes on some volcanic rocks of the North Island of New Zeland," *New Zealand Jour. Sci. and Tech.*, **13** (1932), 198-200.

Patrick MARSHALL, "Acid rocks of Taupo-Rotorua volcanic district," *Trans. Royal Soc. New Zealand*, **64** (1935), 323-366.

Patrick MARSHALL, "Ignimbrites," *7th Pacific Soc. Cong., New Zealand 1949*, **2** (1953), 407-411.

11) Howel WILLIAMS, "Calderas and their origin," *Bull. Dept. Geol. Sci., Univ. Calif.*, **25** (1941), 239-346.

12) Richard L. HAY, "Formation of the crystal-rich glowing avalanche deposits of St. Vincent, B.W.I.," *Jour. Geol.*, **67** (1959), 540-562.

Komagatake Volcano in southern Hokkaido. During the paroxysmal phase of the eruption, a large quantity of pumice blocks and ash materials effused from the crater and descended down the mountain-slope in a state of pumice-flow. Detailed studies on the mechanism of the eruption as well as on the nature of the deposits of pumice-flow were carried out by many geologists and volcanologists[13]. Kuno (1941) pointed out the fact that the sedimentary features and the size characteristics of the pumice-flow deposits are quite different from those of the normal projected air-fall pumice deposits[14]. Kuno (1953) indicated that most Japanese calderas belong to the "Krakatau type calderas" of Williams, being surrounded by extensive areas of unstratified pumice-flow deposits or welded tuffs[15]. Investigations of pyroclastic deposits resulting from eruptions of nuées ardentes in Japan have been advanced by Matsumoto, Kuno, Ishikawa, Yagi, Taneda, Minato, Yamasaki, Aramaki, Katsui, et al.[16] Taneda (1954 and 1957) and Taneda, Miyachi and Nishihara (1957) studied the "Shirasu" deposits in southern Kyushu, concluding that they might be regarded as nuées ardentes products showing size characteristics similar to those of the "Older Pumice" of the Crater Lake

13) Hiromichi TSUYA, etc. 7, "The eruption of Komagatake, Hokkaido, in 1929," *Bull. Earthq. Res. Inst., Tokyo Univ.*, **8** (1930), 237-319.

Shukusuke KOZU, "The great activity of Komagatake in 1929," *Min. Petr. Mitt.*, **45** (1934), 133-174.

14) Hisashi KUNO, "Characteristics of deposits formed by pumice flows and those by ejected pumice," *Bull. Earthq. Res. Inst., Tokyo Univ.*, **19** (1941), 144-149.

15) Hisashi KUNO, "Formation of calderas and magmatic evolution," *Trans. Am. Geoph. Union*, **34** (1953), 267-280.

16) Tadaiti MATUMOTO, "The four gigantic caldera volcanoes of Kyushu," *Japanese Jour. Geol. Geogr.*, **19** (1943), Special number, 57.

Tadaiti MATUMOTO, Toshio ISHIKAWA, and Masao MINATO, "Some problems of welded-lava and welded-tuff related with the sunken calderas in Japan," *8th Pacific Sci. Cong., Philippines 1953, Proc.*, **2** (1956), 130-138.

Toshio ISHIKAWA, Masao MINATO, Hisashi KUNO, Tadaichi MATSUMOTO, and Kenzo YAGI, "Welded tuffs and deposits of pumice flow and nuée ardente in Japan," *Intern. Geol. Cong.* (1956).

Masao YAMASAKI, "The volcanic activity in the later stages of the development of Nantai, Nikko," *Bull. Volcanol. Soc. Jap., 2nd Ser.* **2** (1957), 63-76. (Japanese with English abstract.)

Shigeo ARAMAKI, "The 1783 activity of Asama Volcano, Pt. I," *Jap. Jour. Geol. Geogr.*, **27** (1956), 189-229.

Shigeo ARAMAKI, "The 1783 activity of Asama Volcano, Pt. II," *Jap. Jour. Geol. Geogr.*, **28** (1957), 11-33.

Yoshio KATSUI, "Geology and petrology of the Volcano Mashû Hokkaido, Japan," *Jour. Geol. Soc. Jap.*, **61** (1955), 481-495. (Japanese with English abstract.)

region[17].

The study of nuées ardentes or glowing avalanches and their deposits is still in its infancy, althrough major progress is being made as mentioned. The outline of nuées ardentes eruptions has already been drawn through such researches mentioned above. A great number of problems about the origin and mechanism of these phenomena, however, are still left unsolved, and every argument is more or less inferential. A lot of detailed study on nuée ardente deposits, as well as the augmenting of data of actual observations of future eruptions of nuées ardentes, is needed. Complete solutions of many unsolved problems will come about only through careful progressive research. It has been noticed by some volcanologists that the mode and mechanism of nuées ardentes are related to the viscosity and gas content of erupting magmas and the condition of gas-emission. Aramaki (1957) pointed out that there exists a certain relationship between the mode of emplacement and the nature of nuée ardente deposits. This fact may suggest the course of the future studies. Quantitative study on the texture, structure and constituent of nuée ardente deposits, together with analytical study on the chemical and mineralogical composition and petrological features of the deposits, is necessary. It can be expected that analytical methods used in sedimentary petrology may be effective in solving problems on the phenomenon of nuée ardente. The writer is proceeding systematically with his quantitative study on the textural and constituent characteristics of pyroclastic flow deposits distributed in every volcanic region in Japan, to obtain some useful data for deciphering the mode of origin and mechanism of pyroclastic flows or nuées ardentes. Part of his work has already been published in several preliminary reports[18].

17) Sadakatu TANEDA, "Geological and petrological studies on the 'Shirasu' in south Kyushu, Japan, Part I, Preliminary note," *Kyushu Univ. Fac. Sci. Mem., ser. D. Geology,* **4** (1954), 167-177.

Sadakatu TANEDA, "Geological and petrological studies of the 'Shirasu' in south Kyushu, Japan, Part II, Preliminary note," *Kyushu Univ. Fac. Sci. Mem. ser. D, Geology,* **7** (1957), 91-105.

Sadakatu TANEDA, Sadanori MIYACHI, and Moto-o NISHIHARA "Geological and petrological studies of the 'Shirasu' in south Kyushu, Japan, Part III, The 'Shirasu' in the Tsuruda-Hiwaki-Koriyama area, north of Kagoshima City," *Kyushu Univ. Fac. Sci. Mem., ser. D, Geology,* **6** (1957), 107-127.

18) Hiromichi TSUYA, Isamu MURAI, and Yoshichi HOSOYA, "Size characteristics of the pumice deposits distributed in the vicinity of Komoro on the southwest foot of Asama Volcano," *Bull. Earthq. Res. Inst., Tokyo Univ.,* **36** (1958), 413-431. (Japanese with English abstract.)

Isamu MURAI and Hiromichi TSUYA, "Size characteristics of the 'Shirasu' deposit distributed in the southern part of Kyushu Island," *Bull. Earthq. Res. Inst., Tokyo Univ.,* **37** (1959), 637-647. (Japanese with English abstract.)

Isamu MURAI, "On the mud-flows of the 1926 eruption of Volcano Tokachi-daké, Central Hokkaido, Japan," *Bull. Earthq. Res. Inst., Tokyo Univ.,* **38** (1960), 55-70.

Acknowledgements

The writer wishes to express his sincere thanks to Prof. Hiromichi Tsuya of the Earthquake Research Institute, University of Tokyo, for introducing him to this study as well as for constant guidance in the course of the work. His grateful thanks are also due to Prof. Takao Sakamoto and Prof. Hisashi Kuno of the Faculty of Science of the the same University, for invaluable criticism and advice. Special thanks due to Prof. Seitaro Tsuboi of the same University for his critical reviewing of the manuscript. He greatly appreciates the valuable advice by Mr. Shigeo Aramaki and Ph. D. Takayasu Uchio of the same University. He is indebted to Mr. Masao Yamasaki, assistant professor of Kanazawa University, for kindly supplying unpublished data. He is also indebted to Mr. Yoshichi Hosoya of the Komoro Branch of the Earthquake Research Institute for his great help in carrying out laboratory work as well as in the preparation of the figures included in this paper.

Terminology

Nuée ardente: As already mentioned, Lacroix (1903) introduced this word as a geological term for the peculiar eruptions of Mt. Pelée in 1902–1903. Since then, this term has been adopted for all eruptions of similar types. The eruptions of the Soufrière, Katmai, Merapi, etc. were described in the same terminology "nuée ardente". Furthermore, "nuée ardente" has been adopted to designate eruptions which are considered to have been responsible for extensive tuff deposits or welded tuffs. Thus, the usage of the term "nuée ardente" has become ambiguous. It has been used for all kinds of eruptions which produced laterally moving masses of incandescent fragmentary materials of juvenile origin and gases. There exist wide variations of the mode and magnitude of eruptions and the nature of discharged materials among the eruptions termed nuées ardentes. Consequently, some confusion frequently exists in the accounts of these phenomena. In order to eliminate such ambiguity in the terminology, the usage of the term "nuée ardente" must be confined to eruptions of the Pelée type and their confederates. Aramaki (1957) used the term "pyroclastic flow" as a synonym of

Isamu MURAI, "Pyroclastic deposits distributed on the east foot of Volcano Myoko," *Bull. Earthq. Res. Inst.*, **38** *Tokyo Univ.*, (1960), 307-315.

Isamu MURAI, "Pumice-flow deposits of Komagatake Volcano, Southern Hokkaido," *Bull. Earthq. Res. Inst., Tokyo Univ.*, **38** (1960), 451-466.

"nuée ardente" or "glowing avalanche" in the broad sense. This term was already used by Gilbert (1938) and Williams (1941)[19]. The writer adopts this term in the following sections of this paper.

Ash-flow: The nomenclature of deposits emplaced by pyroclastic flows may be very controversial. A great number of terms, i.e. incandescent tuff flow, volcanic sand flow, pumice flow, scoria flow, block and ash flow, hot ash flow, ignimbrite, tuff lava, mud lava, welded tuff, etc., have been used to designate these deposits. It is generally considered that the most distinct features of these deposits are the non-sorted size characteristics, the constituent particles of which range in all sizes from huge blocks to fine dust. Most of the pyroclastic flow deposits, welded ones and their non-welded equivalents, contain a large quantity of fine materials and fall into the category of ash, consisting of a large percentage of particles of ash size (4 to 1/4 mm in diameter) and fine ash size (less than 1/4 mm in diameter), referring to the Wentworth and Williams' size scale (1932)[20]. Smith (1960) defined the term "ash flow deposits" as those consisting of 50 per cent or more in weight of ash and fine ash exclusive of foreign inclusions[21]. This term includes almost all of the pyroclastic flow deposits, although some consist mainly of particles larger than ash and will not conform to the arbitrary 50 per cent minimum for particles of juvenile origin less than 4 mm in diameter. The writer adopts the term "ash-flow" in his scheme of the classification of pyroclastic flows to designate the eruptions of pyroclastic flows which produce fine-grained pumiceous pyroclastic deposits. The term "ash-flow deposit" may be used as a substitute for many terms such as tuff flow, pumice flow, welded tuff, etc.

Mud-flow: Lack of sorting has been considered as a characteristic feature and a good criterion for recognition of pyroclastic flow deposits. It is generally believed that such size characteristics may be the result of deposition from a turbulent flow or an avalanche. A similar non-sorted feature is also recognized in mud-flow deposits. These two types of deposits are sometimes confused with each other because of their similarity in appearance. The usage of the term "mud-flow" is quite ambiguous. Volcanic mud-flows include all kinds of phenomena which

19) C. M. GIBERT, "Welded tuff in Eastern California," *Bull. Geol. Soc. Am.*, **49** (1938), 1829-1862.

Howel WILLIAMS, *op. cit.* (1941).

20) C. K. WENTWORTH and Howel WILLIAMS, "The classification and terminology of the pyroclastic rocks," *Bull. Natl. Research Council*, **89** (1932), 19-53.

21) Robert L. SMITH, "Ash flows," *Bull. Geol. Soc. Am.*, **71** (1960) 795-842.

originate as the result of eruptions through crater lakes (e.g. the 1919 eruption of the Klut Volcano in Java), causing the melting of ice and snow (e.g. the 1877 eruption of the Cotopaxi Volcano in Ecudor), and eruptions following or accompanied by heavy rains. They also include those which are caused not by eruptions, but by the collapse of the dam of a crater lake, by heavy rains falling on unconsolidated ejecta and by the rapid melting of ice and snow[22]. Further, the term "mud-flow" has been used for avalanches of disintegrated materials caused by the collapse of a part of a volcanic cone destroyed by a violent explosion. For example, those of the 1888 eruption of the Bantai Volcano were described as mud-flows. Flows of essential fragments and water caused by the entering of pyroclastic flows into streams are also classified as mud-flows. The word "lahar" is used as a synonym of volcanic mud-flow. This word comes from an Indonesian word for volcanic materials transported by water. Van Bemmelen (1949) defined this term as "a mudflow, containing debris and angular blocks of chiefly volcanic origin. . . ." As mentioned here, the term "mud-flow" has been used in the broad sense. Furthermore, some pyroclastic flow deposits have been confusedly given the same term occasionally. In order to eliminate such ambiguity of this term, a proper classification of mud-flows may be neccessary. In this paper, however, the writer omits the argument on such classification and discusses only the deposits of avalanches caused by the collapse of part of the volcanic cone destroyed by a violent explosion, descending down the mountain-slope by graviational force without the agency of water, for the purpose of comparing their size characteristics with those of pyroclastic flow deposits. In the following sections in this paper he uses the term "dry mud-flow" for such a tpye of flow of disintegrated materials.

Classification of Pyroclastic Flows

Since 1902 many examples of pyroclastic flows have been witnessed, and a large number of pyroclastic flow deposits have been recognized through the whole geologic column in the volcanic regions of the world. Some discussions and inferences on the origin and mechanism of pyroclastic flows have been presented, based upon results from actual investigations of the eruptions as well as studies of the discharged

22) C. A. Anderson, "The Tuscan formation of northern California," *Bull. Dept. Geol. Sci., Univ. Calif.*, **23** (1933), 215-276.

materials. Present concepts of the mode of eruption of pyroclastic flows depend almost entirely on the well-known published accounts of the 1902 eruptions of Mt. Pelée and the Soufrière and the eruption in 1912 in the Valley of Ten Thousand Smokes. These accounts have been augmented by several detailed observations of the later eruptions of pyroclastic flows which occurred on Mt. Pelée, Merapi, Mt. Lamington, Hibok-Hibok, etc. Now it is clarified that the phenomena of pyroclastic flows involve all kinds of flows of high-temperature essential fragmentary materials, graduating from the Pelean type eruptions emanating from the side of a dome to eruptions that produce vast ash-flow sheets. Among such various kinds of pyroclastic flows, there exist wide variations in the mode of eruption and nature of the discharged materials. Various classifications of pyroclastic flows have been proposed by many geologists and volcanologists. Lacroix (1930), Escher (1933), Neumann van Padang (1933), Fenner (1937), Cotton (1944), van Bemmelen (1949), MacGregor (1952 and 1955), Williams (1957) and Aramaki (1957) tried to analyze the mechanism of pyroclastic flows and proposed various schemes on the classification of this phenomenon[23].

Among these, Lacroix's classification is the most fundamental one, in which he established four subdivisions of pyroclastic flows or nuées ardentes in the broad sense. Lacroix carefully investigated the peculiar eruptions of Mt. Pelée in 1902–1903, which he named "nuées ardentes peléennes". These eruptions took place during the slow protrusion of viscous lava, forming a steep-sided dome. He distinguished two kinds

23) Alfred LACROIX, "Remarques sur les matériaux de projection des volcans et sur la genèse des roches pyroclastiques qu'ils constituent," *Centenaire Soc. Geol. France, Livre Jubliaire 1830-1930*, **2** (1930), 431-472.

B. G. ESCHER, "On a classification of central eruptions according to gas pressure of the magma and viscosity of the lava," *Leidsche Geol. Mededeel.*, **6** (1933), 45-49.

M. NEUMANN van PADANG, *op, cit.*, (1933).

C. N. FENNER, *op. cit.*, (1937).

C. A. COTTON, "Volcanoes as landscape forms," *Christchurch and London, Whitcomb and Tombs*, (1944 and 1952), 416.

R. W. van BEMMELEN, *op cit.*, (1949).

A. G. MACGREGOR, "Eruptive mechanisms—Mt. Pelée, the Soufrière of St. Vincent (West Indies) and the Valley of Ten Thousand Smokes (Alaska)," *Bull. Volcanol., ser. 2*, **12** (1952), 49-74.

A. G. MACGREGOR, "Classification of nuée ardente eruptions," *Bull. Volcanol., ser. 2*, **16** (1955), 7-10.

Howel WILLIAMS, "Glowing avalanche deposits of the Sudbury basin," *Ontario Dept. Mines 65th Ann. Rept.*, **65** (1957), 57-89.

Shigeo ARAMAKI, *op. cit.*, (1957).

of nuées ardentes at Mt. Pelée. One was initiated by the lateral explosive propulsion of the materials of a lava dome due to violent explosion through the flank of the dome. He termed this type "nuée ardente Peléenne d'explosion dirigée". The other originated through the collapse of part of the dome with a mild lateral explosion or without attendant explosions, which Lacroix termed "nuée ardente peléenne d'avalenche". The former is the most destructive type, such as the eruption that swept down from Mt. Pelée on May 8th, 1902. The latter is commonly recognized on the Merapi Volcano, and Escher called it the Merapi type. The pyroclastic flows at the Soufrière of St. Vincent differed from those of Mt. Pelée in being initiated by a vertical explosive eruption through an open crater. Lacroix termed this type "nuée ardente d'explosions vulcaniennes", and Escher called this "Glutwolken of the St. Vincent type". The last of Lacroix's subdivision is "nuée ardente du Massif du Katmai", named as it was first recognized from Fenner's study of the deposits emplaced in the Valley of Ten Thousand Smokes in the Katmai Region, Alaska, during the eruptions of 1912. Fenner (1937) termed this type a "Katmaian eruption". (See Table 1.)

Table 1. Classifications of pyroclastic flows.

Lacroix (1930)	Escher (1933) Fenner (1937)	Williams (1957)	Aramaki (1957)
Nuée ardente peléenne d'explosion dirigée	Pelée type	} Pelean type	Nuée ardente in the strict sence
Nuée ardente peléenne d' avalanche	Merapi type		Intermediate type
Nuée ardente d'explosion vulcanienne	St. Vincent type	Vertical explosion type (Krakatoan type)	} Pumice flow
Nuée ardente du Massif du Katmai	Katmaian type	Fissure eruption type (Valley of Ten Thousand Smokes type)	

MacGregor (1952 and 1955) proposed a detailed classification which was based upon the mode of initiation, source, specific type of eruption and magma. Williams (1957) distinguished three principal types of pyroclastic flows or glowing avalanches, namely, those attendant on the rise of Pelean domes, those formed by vertical explosions from craters and those produced by the discharge of effervescing magma from swarms of vertical fissures.

Most of the classifications of pyroclastic flows are based upon results

of direct observations on the mode of eruptions on the spot, although there are few examples of occurrences of pyroclastic flows ever witnessed. MacGregor (1952) stated that "the classification of nuées ardentes and tuff-flows should not be used as a kind of substitute for lithological classification of volcanic debris". Barksdale (1951), MacGregor (1952) and Neumann van Padang (1933) mentioned that deposits having lithologically similar features may be formed by different eruptive mechanisms. On the other hand, Williams (1957) discussed in detail the characteristics of deposits of the three principal types of pyroclastic flows. His precise accounts suggest the existence of some relationship between the types of pyroclastic flows and the textural and constituent characteristics of the deposits. Aramaki (1957) stated that there exists a certain relationship between the mode of emplacement and the nature of the deposits. He proposed a new classification of pyroclastic flows, mainly from the result of his study on the pyroclastic flow deposits discharged during the 1783 eruption of Mt. Asama.

There may be no marked discrepancy between Aramaki's classification based essentially upon the viscosity of essential fragmentary materials in the deposits and the others based mainly upon the mode and nature of eruptions. It may be wrong to discuss the nature and mechanism of eruptions of pyroclastic flows without investigating the characteristics of their deposits. For convenience in proceeding with his study, which is set out from quantitative inspections of the textural characteristics of pyroclastic flow deposits, the writer tries to draw a scheme of classification of pyroclastic flows by amending the previous ones. (See Table 2.) The classification is established on the basis of the nature of the representative eruptions of pyroclastic flows actually investigated by

Table 2. Proposed scheme of classification of pyroclastic flows.

Classification of pyroclastic flows		Pepresentatives
Nuée ardente	Pelée type (Merapi type)	Pelée (1902-03, 1929-32), Merapi (1930-31), Hibok-Hibok (1948-53), Lamington (1951-52).
	Sakurajima type	Sakurajima (1914, 1939), Asama-Kambara Nuée Ardente (1783).
Intermediate type		Tokachidake (1926), Asama-Agatsuma Pyroclastic Flow (1783).
Ash-flow	St. Vincent type	St. Vincent (1902), Komagatake (1929).
	Krakatoa type	Krakatoa (1883).
	V. T. T. S. type	Valley of Ten Thousand Smokes (1912).

geologists, as well as on the basis of the nature of their deposits, althouth there are rather few representatives. Detailed discussions on the nature of each type of pyroclastic flow and the characteristics of the deposit are presented in the later chapters. There are a large number of examples of pyroclastic flow deposits produced by pre-historic eruptions, and it is possible to deal with their characteristics consistenly in the framework of this classification. The writer classifies three subdivisions of pyroclastic flows, which generally correspond to three types of pyroclastic flows in Aramaki's classification (1957). The writers distinguishes two types of nuées ardentes; one takes place during the protrusion of viscous lava as a steep-sided dome, and the other is generated by the discharge of magma from a crater. Intermediate type pyroclastic flow shows intermediate nature between nuée ardente and ash-flow. The term "intermediate type" was proposed by Aramaki (1957), and the writer adopts this term in his classification. The writer adopts the term "ash-flow" to designate the pyroclastic flow which produces fine-grained pumiceous deposits. He distinguishes three types of ash-flows; one is produced by the vertical explosion through an open crater, being attendant on the rising of a lofty ash column, as explained by Hay (1959); the second one is caused also by the vertial explosion through a crater, but the magnitude of the eruption is by far greater in comparison with the former type, causing the collapse of a volcanic cone to form a characteristic depression, as stated by Williams (1941); and the last one is generated by the discharge of acidic magma through fissures.

Materials for the Study

The writer visited almost all the Japanese volcanoes where pyroclastic flow deposits, discharged mainly in the Holocene, have been recognized. He investigated the features of these deposits on the spot, and collected materials in order to examine their textural and constituent characteristics. Besides, he studied several examples of pyroclastic fall deposits, dry mud-flow deposits and auto-brecciated lava flows to compare their characteristics with those of pyroclastic flow deposits. The volcanoes visited by the writer shown in Fig. 1. There are a few other volcanoes having deposits of pyroclastic flows or mud-flows where he could not visit. He will investigate these volcanoes in the near future. The names of the volcanoes and brief descriptions of the pyroclastic flow deposits investigated by the writer are listed in Table 3. Localities

Table 3. List of the pyroclastic flows and their preceding falls in Japan which the writer studied.

Name of volume	Symbol	Remark	Rock type	SiO_2%	Volume	Welding	Sp. no.	Type of pyroclastic flow
Kutcharo	Kc	u	V	71.58(2)	80–100 km³	−	1,2,5,6,7,10	K
		m	V			−	3,4,8,9	K(f)
		l	V			+		K(f)
Mashu	Ms		V	65.53	5	−	1,2,3	K
Akan	Ak	u	V	65.87	60	−	1,2	K(f)
		l	V			+		K(f)
Akan (Meakandake)	Ak-cc		V		1	−	3,4	I
Daisetsuzan	D		VI			+	1,2	S
	D-fa		VI			−	3,4	
Tokachi Welded Tuff	TkW		XVI	71.57	60	+	1	K(f) or V
Tokachidake	Tk	1926-s	V	53.93	0.0035	−	5,6,7,8	I
		1926-p	V		0.0175	−	1,2,3,4	I
Shikotsu	S	u	VI	69.05	90–100	−	1～11	K
		l	VI			+		K
	S-fa		VI	72.41	25	−	12	
Kuttara	Kt	u	V	64.27(4)	10	−	1,2	S
		l	V			+		
Toya	Ty	u	V		40	−	1,5,6,7,9	K
		l	V			−	2,3,4,8	K
	Ty-fa		V			−	11,12	
	Ty-o		V			−	10	S
Komagatake	Km	1929	V	59.15	0.15	−	1,2,3,4,5,6	S
	Km-fa	1929-fa	V		0.4	−	11	
	Km-o-K	Kurumizaka-fl	V		0.4	−	8	S
	Km-o-H	H.-shaped-cr.-fl	V		2.5	−	7,9,10	S
Towada	Tw		V	69.53(3)	50	−	1 19	K
	Tw-fa		V			−	23,24	
	Tw-o		V	60.44		−	20,21,22	S*
Osoreyama	Os		V			−	1	S*
Hakkodasan	Hd		V	68.51		+	1	K
Tazawa Welded Tuff	Tz		VI	74.16(2)	150	+	1	K or V
Onikobe	On		V			+～−	1,2,3	K
Hijiori	Hj		VII		1.4	−	1,2	S
Numajiri Welded Tuff	Nm		V		1.15	+	1	I
Takaharayama	Th		V			−	1	K(f) or V

Table 3. (Continued)

Name of volume	Symbol	Rock type	SiO_2%	Volume	Remark	Welding	Sp. no.	Type of pyroclastic flow
Nantaisan	Nn-p	VI	62.86(2)	0.8 km³		+~−	2,3,4,5,6	S
	Nn-p-fa	VI		0.6		−		
	Nn-s		64.43	0.14		+~−	1	S
	Nn-s-fa			2.5		−	7	
Harunasan	Hr-u	VI		0.1		−	4	S
	Hr-u-fa	VI		0.6		−	5	
	Hr-l	VI		0.5		−	1,2,3	S*
Kusatsu-Shiranesan	KS	V		3	main part	+	1	S
		V			l	−	2,3,4	S*
Myoko	My	V	63.51	1.2		−	1~11	N-P
Asamayama	Am-up	V		1.0		−	17~23	S
	Am-up-fa	V				−	39	
	Am-lp	V	66.71	3·3		−	1~16	S
	Am-S	V		0.015	Shiraito-fl	−	35	I
	Am-O	V		0.6	Oiwake-fl	+~−	24~30	I
	Am-K	V		0.01~0.001	Kambara-na	−	34	N-S
	Am-A	V	60.8	0.1	Agatsuma-fl	+	31,32,33	I
	Am-1958	V				−	36,37,38	S
Hakone	Hn	V	60.87(2)	15	s	−	8,9,10	K
		V			p	−	1~7	K
Hakone Central Cone	Hn-cc	V				−	11,12,13	I
Ko-Fuji	KF	V				−	1~10	I
Aso	As	VI	62.88(4)	180	u	−	1,2	K
Aira	Ai	VI	74.53		u	−	5	K
		VI		150	m	−	1,2,6,7,11~13	K
		VI			l (or Ata-fl)	−	8,9,10	K(f)

Rock types were determined by Kuno's classification (1950) based upon mafic mineral assemblage. fl:pyroclastic flow, fa: pyroclastic fall, na:nuée ardente, s:scoria, p:pumice, o:pyroclastic flow of older stage, u:upper part, m:middle part, l:lower part, N-P:nuée ardente of Pelée type, N-S:nuée ardente of Sakurajima type, I:intermediate type pyroclastic flow, S:St. Vincent type ash-flow, S*:variety of St. Vincent type ash-flow having an intermediate nature between ash-flow and dry mud-flow, K:Krakatoa type ash-flow, f:fine-grained, V:V.T.T.S. type ash-flow. Values of SiO_2% attended by parenthese, figures in which are the numbers of data, are average values.

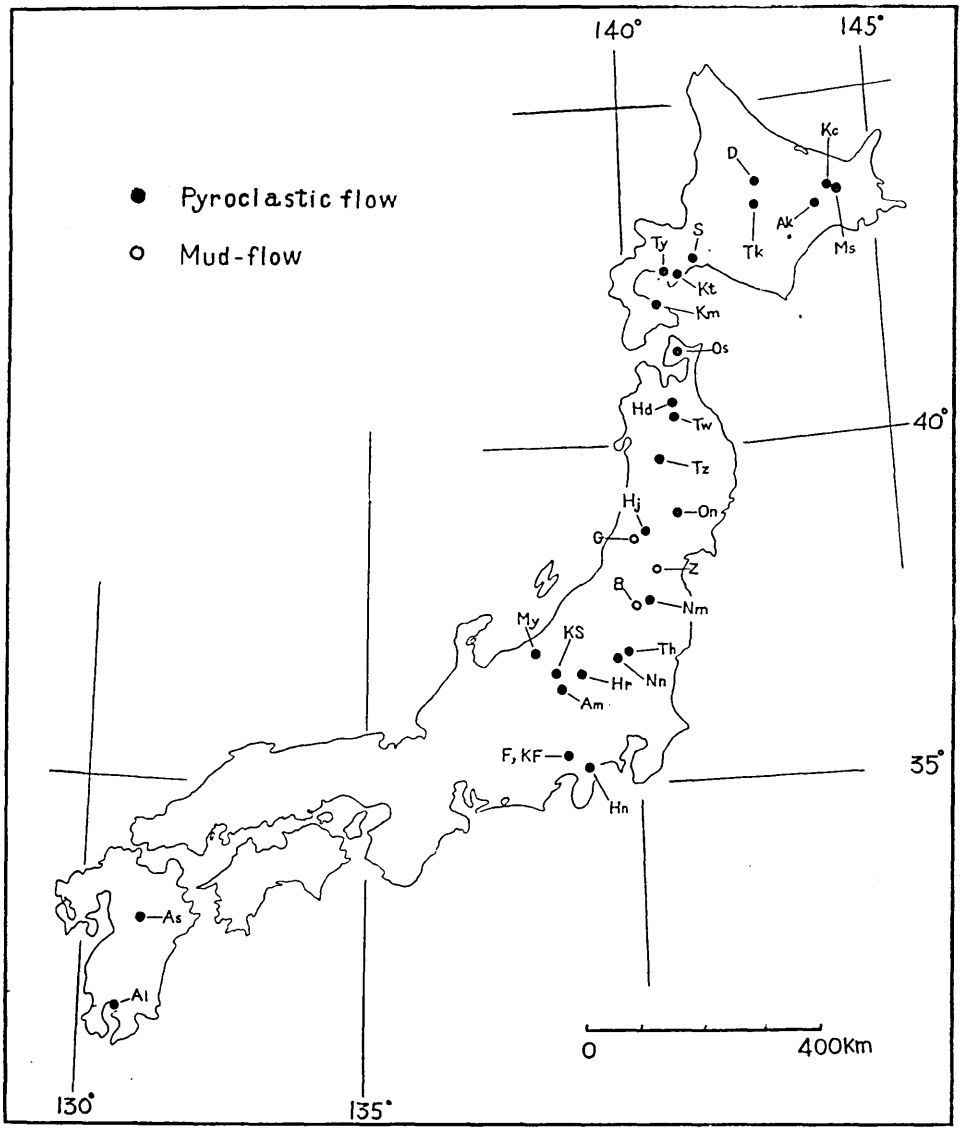

Fig. 1. Distribution map of the volcanoes, having deposits of pyroclastic flows and mud-flows, from which the samples were collected.

from which the materials were collected are shown in Figs. 2a–2k and Table 17. As shown in Table 3, the writer obtained many examples of pyroclastic flow deposits produced by the St. Vincent type and the Krakatoa type ash-flows. Almost entirety of the ash-flow deposits of

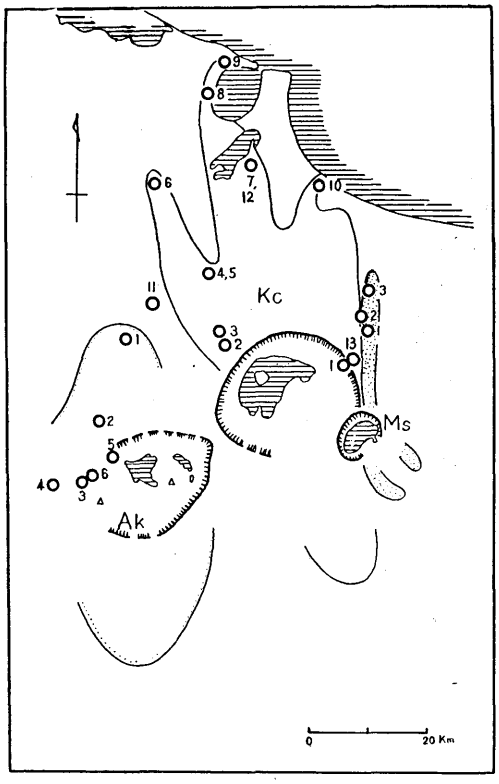

Fig. 2. Map showing the general distribution of pyroclastic flow deposits and the localities of samples collected for mechanical analyses.

Fig. 2a. The Kutcharo, Masyu and Akan Volcanoes.

Fig. 2b. The Shikotsu, Kuttara and Toya Volcanoes.

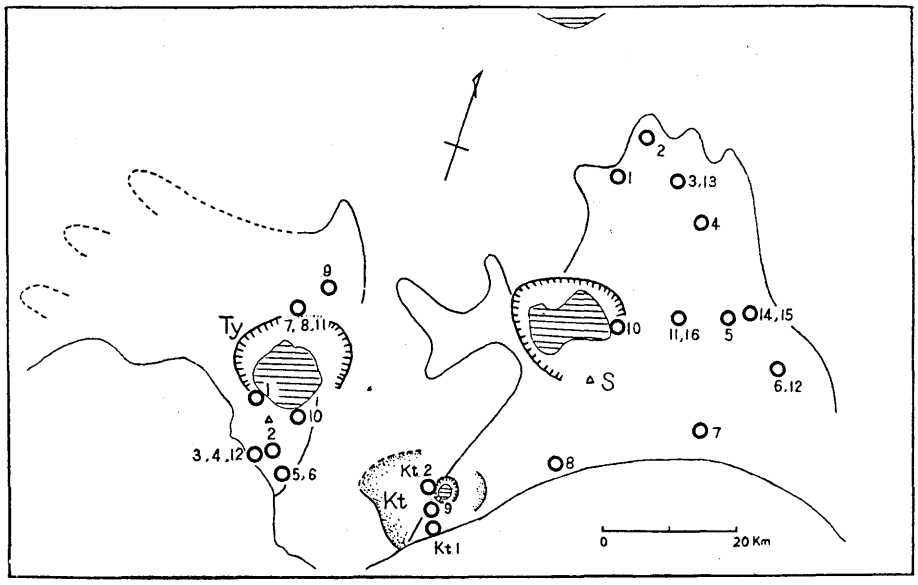

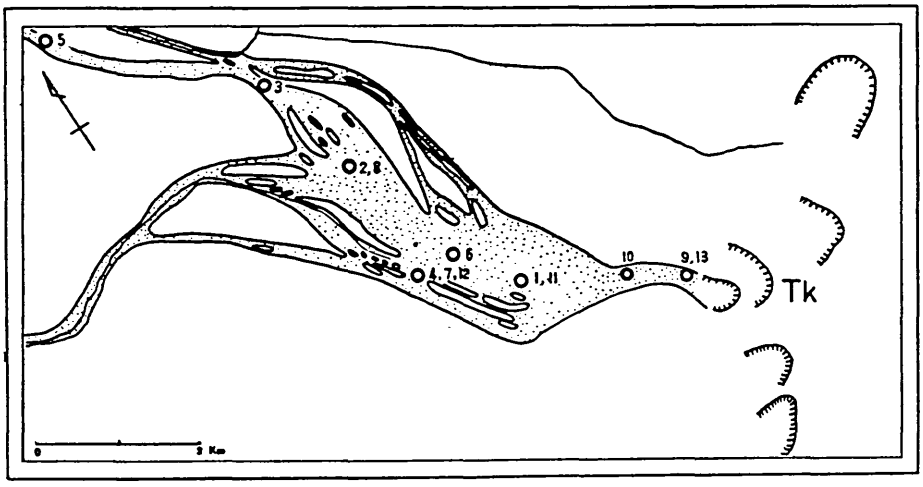

Fig. 2c. The Tokachidake Volcano. (After Tada and Tsuya, 1929.)

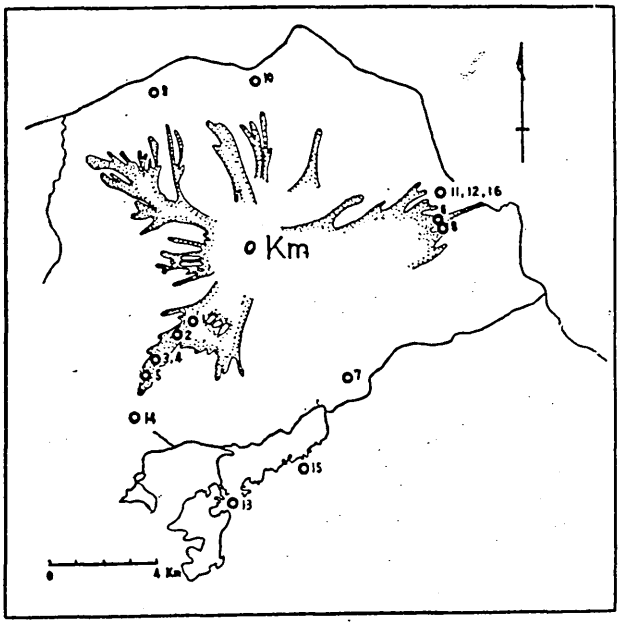

Fig. 2d. The Komagatake Volcano, Hokkaido. (After Tsuya, 1930)

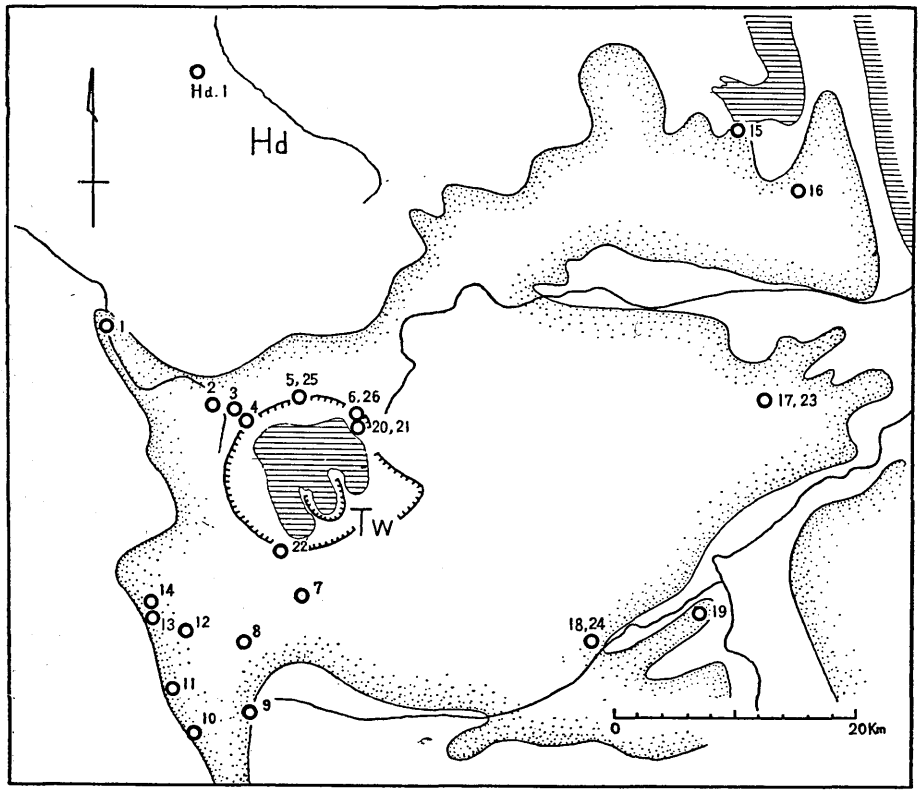

Fig. 2e. The Hakkoda and Towada Volcanoes. (Modified from K. Yagi, etc., 1960.)

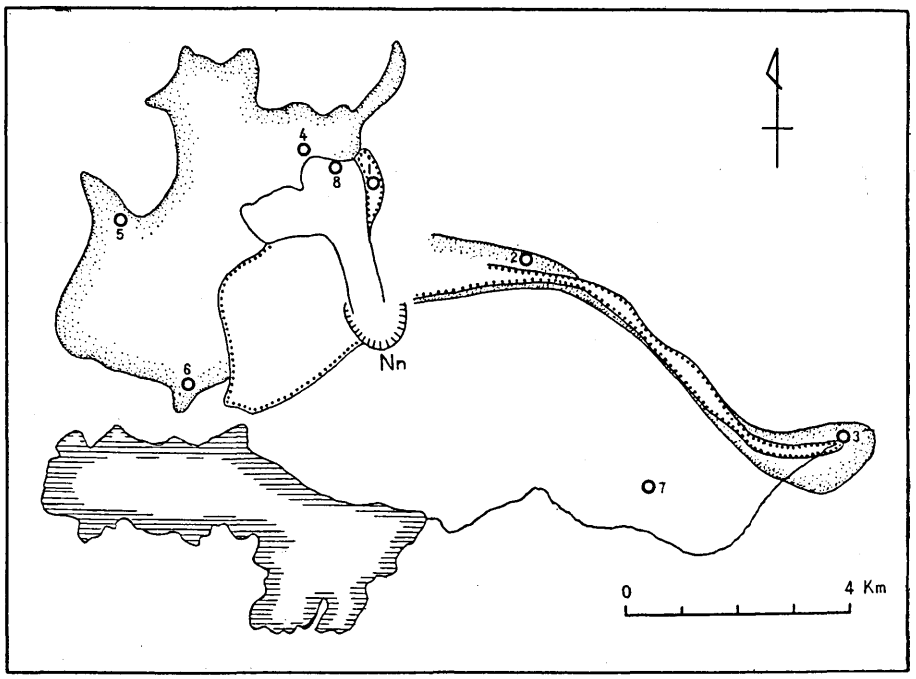

Fig. 2f. The Nantai Volcano, Nikko. (Modified from Yamasaki, 1957 and 1958.)

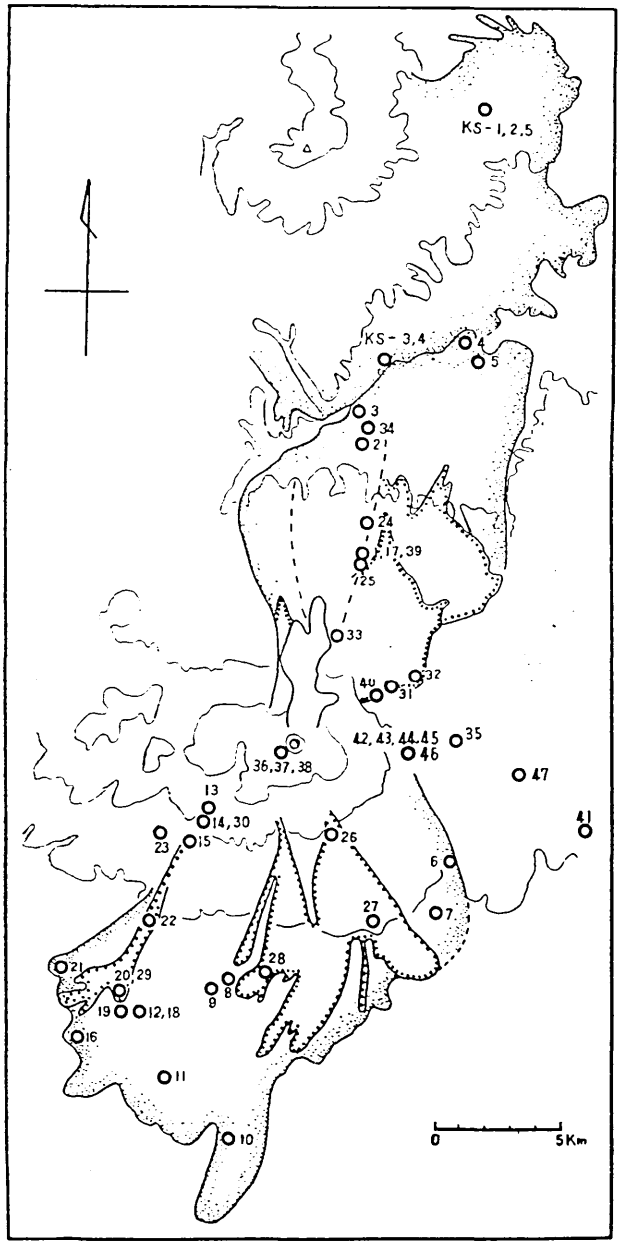

Fig. 2g. The Asama and Kusatsu-Shirane Volcanoes.
(Modified from T. Yagi, 1933; Aramaki, 1956; and Ota, 1956.)

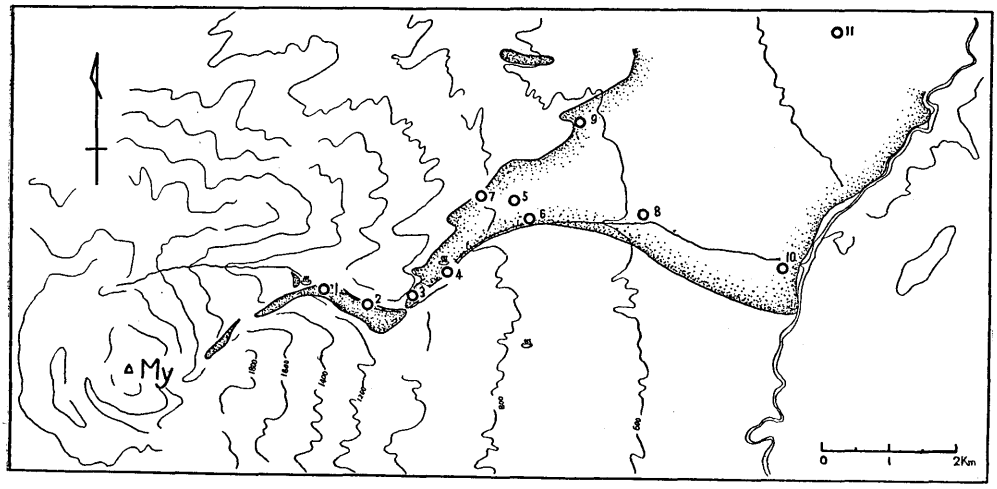

Fig. 2h. The Myoko Volcano.

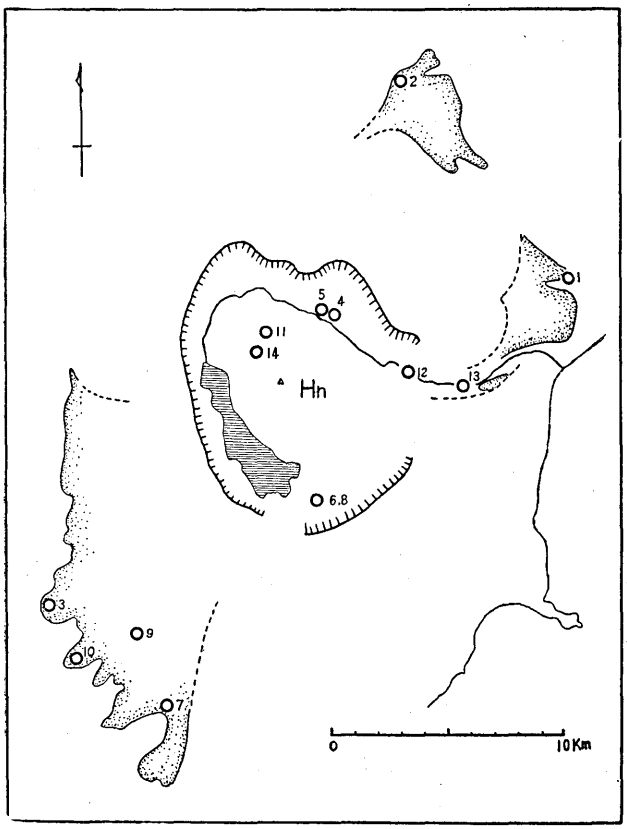

Fig. 2i. The Hakone Volcano. (After Kuno, 1950 and 1954.)

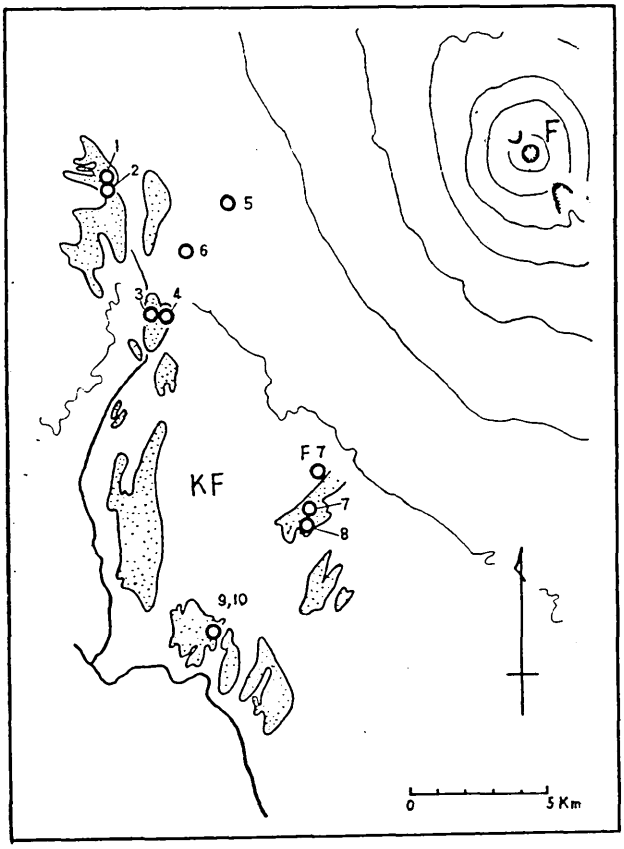

Fig. 2j. The Ko-Fuji Volcano. (Drawn from unpublished data of Tsuya.)

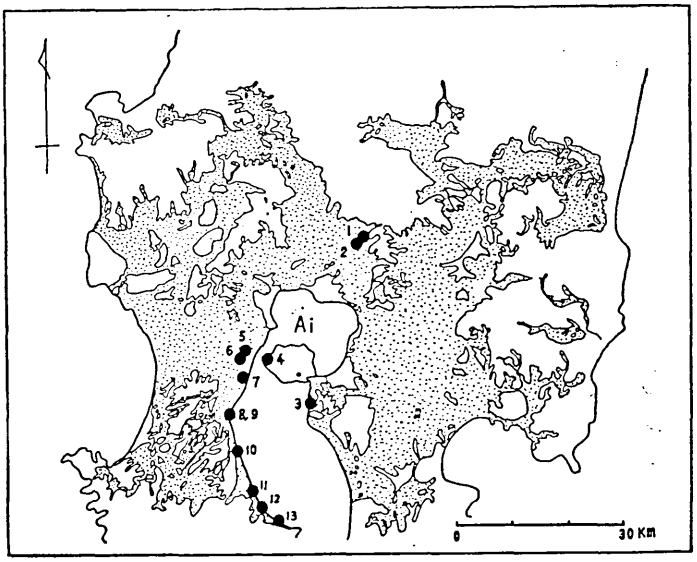

Fig. 2k. The Aira Volcano. (After Matsumoto.)

small volume distributed on many volcanoes in Japan are considered as the products of the former type of ash-flow, and the ash-flow deposits of large volume distributed in the surrounding areas of most calderas in Japan are the products of the later type as indicated by Kuno (1953). The writer also had several examples of the intermediate type pyroclastic flow deposits and a few ones of the nuée ardente deposits. He, however, could not obtain sure examples of ash-flow deposits of the fissure eruption type, in Japan. The 1912 eruption of the Valley of Ten Thousand Smokes has been considered to be the representative of this type of ash-flow. Fenner (1923, etc.); Williams, Curties and Tuhle (1956); and Williams (1957) considered that the deposits of the Valley were erupted from fissures. Moreover, the vast ash-flow sheets, such as those in the Taupo-Rotorua district in New Zealand (Marshall, 1932 etc.), the Great Basin and neighbouring provinces in U.S.A. (Mansfield and Ross, 1935; Gilbert, 1938; Callaghan, 1939; Enlows, 1955; Sabins, 1957; Mackin, 1960), the Brisbane area in eastern Australia (Richards and Bryan, 1933), Sumatra (van Bemmelen, 1949; Westerveld, 1942, etc.). Costa Rica (Williams, 1952), and El Salvador (Williams and Meyer-Abich, 1955), are generally considered as the products of ash-flows through fissures.[24] Some of "green tuffs" and rhyolitic tuff sheets in the Tertiary formations in Japan may be the similar deposits, the witer consideres.

24) C. N. FENNER, *op. cit.*, (1923, etc.).

Howel WILLIAMS, "Volcanic history of the Meseta Central Occidental, Costa Rica," *Bull. Dept. Geol. Sci., Univ. Calif.*, **29** (1952), 145-180.

Howel WILLIAMS, "Preliminary notes on geological work done on Mount Katmai and in the Valley of Ten Thousand Smokes," *U. S. Natl. Park Service Interim Rept. on Katmai Project*, (1954), 55-61.

Howel WILLIAMS, G. H. CURTIS, and Werner JUHLE, "Mount Katmai and the Valley of Ten Thousand Smokes, Alaska (a new interpretation of the great eruptions of 1912)," *8th Pacific Sci. Cong., Philippines 1953 Proc.*, **2** (1956), 129.

Howel WILLIAMS and Helmut MEYER-ABICH, "Volcanism in the southern part of El Salvador—with particular reference to the collapse of basins of Lake Coatepeque and Ilopango," *Bull. Dept. Geol. Sci. Univ. Calif.*, **32** (1955), 1-64.

Howel WILLIAMS, *op. cit.*, (1957).

Patrick MARSHALL, *op. cit.*, (1932, etc.).

G. R. MANSFIELD and C. S. ROSS., "Welded rhyolitic tuffs in southeastern Idaho," *Trans. Am. Geophys. Union, 16th Ann. Mtg., pt. 1*, (1935), 308-321.

C. M. GILBERT, *op. cit.*, (1938).

E. CALLAGHAN, "Volcanic sequence in the Marysvale region in southwest-central Utah," *Trans. Am. Geopys. Union, 20th Ann. Mtg., pt. 3*, (1939), 428-452.

H. E. ENLOWS, "Welded tuffs of Chiricahua National Monument," *Bull. Geol. Soc. Am.*, **66** (1955), 1215-1246.

Size Characteristics of Pyroclastic Flow Deposits.

General Statement

It is generally believed that the most distinct features of pyroclastic flow deposits are non-stratification and non-sorting (or ill-sorting) as can be seen at any outcrops of the deposits. There is no grading of any kind in the deposits, and fragments range in size from large blocks sometimes exceeding scores of meters in diameter to minute vesicular dust. This contrasts strikingly with the well-sorted features of air fall pyroclastic deposits. The difference may be clarified in diagrams of particle size distributions drawn from the results of mechanical analyses. In the case of pyroclastic flow, it is considered that large blocks, smaller fragments and fine dust travel *en masse* for long distances from the source in a state of turbulent flow. Such motion of the pyroclastic flow may give rise to the characteristic ill-sorted features of the deposits. On the contrary, in the case of pyroclastic fall, ejecta hurled up high into the air are transported by the atmospheric current under the agency of an eolian differentiation, the larger and the denser fragments falling first and closest to the vent while the smaller and the more vesicular fragments fall farther from the vent. Consequently, deposits of pyroclastic falls are well sorted and show distinct lateral and vertical regular grading in texture and composition.

Deposits of dry mud-flows exhibit distinct features of unstratification and ill-sorting, similar to those of pyroclastic flow deposits, although

---

Floyd F. SABINS JR., "Geology of the Cochise Head and western part of the Vanar Quadrangles, Arizona," *Bull. Geol. Soc. Am.*, **68** (1957), 1315-1342.

J. Hoover MACKIN, "Structural significance of Tertiary volcanic rocks in southwestern Utah," *Am. Jour. Sci.*, **258** (1960), 81-131.

H. C. RICHARDS and W. H. BRYAN, "The problem of the Brisbane tuff," *Pr. Roy. Soc. Queensland*, **45** (1933), 50-61.

R. W. van BEMMELEN, *op. cit.*, (1949).

J. WESTERVELD, "Welded rhyolitic tuffs or 'ignimbrites' in the Pasoemah region, West Palembang, South Sumatra," *Leidsche Geol. mededeel.*, **13** (1942), 202-217.

J. WESTERVELD, "On the origin of the acid volcanic rocks around Lake Toba, North Sumatra," *Verh. Kon. Ned. Akad. van Wetensch., Afd. Natuurk., Tweede Sectie*, **43** (1947), 1-51.

J. WESTERVELD, "Quaternary volcanism on Sumatra," *Bull. Geol. Soc. Am.*, **63** (1952), 561-594.

J. WESTERVELD, "Eruptions of acid pumice tuffs and related phenomena along the great Sumatran fault-trough system," *7th Pacific Sci. Cong., New Zealand 1949, Proc.*, **2** (1953), 411-438.

there exists a pronounced difference in composition between these two types of deposits. This indicates the fact that the mode of emplacement and mechanism of flowage may be similar in both cases. Auto-brecciated parts of lava flows also show similar features to those of pyroclastic flow deposits.

Data on the size characteristics of various kinds of pyroclastic flow deposits suggest that there is considerable room for variation within the framework of size distribution curves. This may be clearly indicated in diagrams of size distribution curves and in diagrams of parameters of size distributions. The variations among size distribution curves represent the difference in the proportion of coarse to fine materials and in the degree of sorting, and originally may result from the difference in the mode of origin and mechanism of pyroclastic flow eruption. Accordingly, detailed studies on many examples of the deposits should yield some useful data for deciphering the origin and mechanism of this phenomenon.

Methods of Mechanical Analyses

The writer collected samples, each about 1 to 4 kg in weight, for analyses of textural characteristics of the deposits. As the methods of mechanical analyses have already been explained in detail by the writer

Table 4. Results of mechanical analyses of pyroclastic flow deposis deposits. The result of the analysis of a given sample is noted in the column beneath its sample with weight per cent of each fraction.

ϕ	Kc 1	2	3	4	5	6	7	8	9	10
～−6	0.2	2.2			0.4	0.3	0.4			
−6～−5	1.0	4.6	0.3		0.8	1.1	1.4		0.1	0.2
−5～−4	1.6	6.2	0.9	0.4	2.1	1.9	2.5	0.1	0.1	1.1
−4～−3	5.2	6.7	1.3	0.5	4.0	3.1	2.9	0.3	0.2	2.4
−3～−2	6.3	7.5	2.2	1.1	5.0	4.4	3.6	0.7	0.6	2.6
−2～−1	7.0	7.6	3.4	2.4	5.5	4.6	4.2	0.8	1.0	4.6
−1～−0	15.6	11.8	12.3	7.3	11.9	9.1	9.1	3.4	3.3	9.7
0～ 1	14.6	15.2	19.4	14.5	17.1	17.6	16.6	8.7	9.3	17.7
1～ 2	10.3	10.0	13.0	13.7	12.2	14.4	14.0	10.3	13.1	13.5
2～ 3	6.9	8.5	11.0	14.3	10.7	15.1	14.9	18.0	18.0	12.4
3～ 4	6.0	6.0	12.9	15.1	10.6	14.6	14.0	21.0	23.6	14.5
4～ 5	4.6	4.9	8.8	12.8	7.7	9.3	8.7	16.1	13.7	9.8
5～ 6	6.5	4.0	5.5	7.3	4.3	3.5	4.0	9.7	6.2	4.5
6～ 7	7.3	2.4	5.3	4.4	3.9	0.7	2.2	6.4	2.6	2.6
7～ 8	4.4	1.4	2.5	2.5	2.5	0.1	0.9	2.8	2.8	1.3
8～ 9	1.2	0.8	0.7	0.9	0.9	0.1	0.2	1.0	2.8	0.8
9～	1.3	0.2	0.5	2.8	0.4	0.1	0.4	0.7	2.6	2.3

Table 4. (Continued)

ϕ	Ms 1	2	3	Ak 1	2	3	4	D 1	2
~−8								2.5	
−8~−7			0.2					3.7	
−7~−6		0.5	0.2			1.7		4.4	1.6
−6~−5		1.8	1.6	0.1		2.1	3.5	4.0	4.4
−5~−4	1.3	3.3	2.5	1.1		2.5	8.7	4.1	5.7
−4~−3	5.4	4.2	3.8	2.6	2.3	3.8	9.5	4.6	5.6
−3~−2	8.1	4.7	4.6	3.9	3.7	5.2	9.7	5.1	5.9
−2~−1	10.9	5.5	4.8	5.2	5.5	5.9	6.8	4.9	4.8
−1~−0	14.9	11.2	8.4	10.9	7.3	7.1	12.0	11.1	10.9
0~ 1	15.7	15.0	13.5	19.0	16.9	19.6	16.5	19.2	19.6
1~ 2	12.0	11.8	10.2	14.8	14.5	21.6	11.9	12.6	13.8
2~ 3	9.2	11.7	11.4	12.3	13.5	15.8	7.1	7.3	8.8
3~ 4	7.3	10.9	11.5	14.3	14.0	9.7	4.6	4.8	5.7
4~ 5	5.5	7.4	8.3	9.7	10.0	3.6	3.5	3.7	4.0
5~ 6	3.5	5.7	6.5	2.9	5.5	0.6	2.5	2.8	3.0
6~ 7	1.9	3.0	5.0	1.5	3.2	0.3	1.8	2.5	2.8
7~ 8	2.0	2.1	3.5	0.7	1.9	0.3	1.1	1.5	1.6
8~ 9	2.1	0.8	1.9	0.5	0.5	0.1	0.7	0.6	0.5
9~	0.2	0.4	2.1	0.5	1.2	0.1	0.1	0.6	1.3

ϕ	TkW 1	Tk 1	2	3	4	5	6	7	8
~−9				1.3					1.2
−9~−8		1.2	2.0	1.4		1.0	0.8		5.5
−8~−7		5.2	1.7	1.9		2.0	2.9	4.0	5.8
−7~−6		5.4	2.1	2.2		3.3	4.3	5.3	5.1
−6~−5		3.4	7.2	3.2		4.6	4.7	3.4	3.5
−5~−4	0.2	4.1	11.5	6.1		5.8	3.8	2.0	4.2
−4~−3	2.5	4.1	10.1	8.2		6.1	6.2	4.0	5.0
−3~−2	3.0	6.0	8.2	7.9	1.2	8.1	7.3	6.0	5.4
−2~−1	3.1	7.4	7.0	7.1	1.5	8.4	6.3	6.5	6.2
−1~ 0	11.3	10.5	9.2	10.2	3.5	10.0	10.6	8.8	9.1
0~ 1	15.5	17.9	15.7	17.0	10.4	14.2	16.6	17.0	14.3
1~ 2	15.0	16.8	12.0	14.8	15.3	12.3	15.0	15.7	12.7
2~ 3	16.7	10.2	7.5	9.5	18.3	8.9	9.5	12.4	8.8
3~ 4	15.5	4.2	2.8	4.5	18.9	6.0	6.1	7.2	5.9
4~ 5	9.0	1.0	1.3	1.9	15.9	3.8	2.9	3.8	3.8
5~ 6	3.4	0.7	0.5	0.7	5.4	1.9	1.3	1.2	1.6
6~ 7	1.9	0.7	0.4	1.4	3.3	1.4	1.2	1.2	0.7
7~ 8	1.0	0.5	0.5	0.4	2.4	0.8	0.3	0.6	0.8
8~ 9	0.6	0.3	0.2	0.2	2.1	1.3	0.1	0.7	0.2
9~	1.3	0.2	0.1	0.1	1.8	0.2	0.1	0.2	0.2

Table 4. (Continued)

ϕ	S 1	2	3	4	5	6	7	8	9	10	11
~−6						0.2					0.4
−6~−5			0.3	0.3	1.4	0.5	0.5				0.7
−5~−4	0.7	0.8	1.0	0.9	3.6	1.5	4.5	2.2	1.5	3.1	1.1
−4~−3	1.7	2.2	3.7	2.4	5.2	2.9	6.0	7.5	2.6	4.8	2.0
−3~−2	3.4	3.8	6.0	5.1	6.6	4.5	7.8	9.0	4.0	6.3	3.1
−2~−1	5.9	5.7	7.7	7.0	6.5	5.4	7.6	10.0	4.7	7.0	4.8
−1~ 0	7.8	7.9	9.4	8.4	8.5	6.8	7.5	12.5	5.3	9.5	8.1
0~ 1	12.7	11.9	11.1	11.9	10.7	9.2	9.9	11.7	9.7	11.6	14.8
1~ 2	12.5	12.0	11.9	13.0	12.0	12.0	10.3	9.5	12.3	12.3	14.7
2~ 3	15.6	13.9	13.2	14.8	11.3	16.2	10.2	9.4	15.9	13.0	12.0
3~ 4	14.3	15.6	13.0	13.7	11.2	14.8	9.8	8.5	17.1	10.9	9.8
4~ 5	10.8	11.4	8.7	8.6	8.8	10.4	8.3	7.0	12.7	7.5	8.5
5~ 6	6.6	5.8	5.0	6.1	5.4	6.8	7.2	4.4	5.5	4.2	7.0
6~ 7	3.4	3.3	3.3	3.1	3.8	3.2	4.7	3.0	4.4	2.5	5.3
7~ 8	2.1	2.4	1.4	1.9	1.9	2.6	2.9	1.6	2.5	2.2	3.1
8~ 9	0.4	1.5	0.8	0.6	1.0	0.6	1.8	1.3	0.6	1.7	1.6
9~	2.1	1.8	3.5	2.2	2.0	2.4	1.0	2.4	1.2	3.4	3.0

ϕ	Kt 1	2	Ty 1	2	3	4	5	6	7	8	9	10
~−6		0.6									0.7	
−6~−5	1.7	1.2									2.3	
−5~−4	4.8	4.5	0.3	0.3		0.4	2.2	5.2	2.9		3.5	2.5
−4~−3	5.2	7.4	2.8	2.7		2.5	8.1	7.6	7.8		1.8	5.8
−3~−2	5.5	6.7	3.9	4.6	1.7	5.0	10.5	9.2	11.0	0.3	3.6	7.4
−2~−1	4.8	5.6	9.2	6.4	5.2	7.9	11.4	10.8	12.1	1.7	6.2	8.0
−1~ 0	8.0	8.3	14.2	8.7	8.9	8.8	11.7	11.9	15.4	3.9	14.2	18.9
0~ 1	24.3	16.7	17.3	12.0	11.7	11.4	10.8	10.3	13.9	8.1	20.3	20.3
1~ 2	18.9	23.6	13.3	11.9	13.2	9.8	7.7	7.3	8.7	12.9	15.9	10.9
2~ 3	8.5	8.6	12.5	13.0	16.6	11.2	6.1	6.7	6.6	17.6	11.1	8.4
3~ 4	4.2	5.1	11.8	15.1	17.0	13.0	8.8	7.3	5.5	20.8	7.2	6.6
4~ 5	3.1	3.3	7.0	10.6	11.4	11.5	8.0	7.0	4.4	16.4	4.7	3.5
5~ 6	3.3	2.3	2.6	5.8	6.0	6.8	4.9	6.0	3.6	7.4	1.8	2.4
6~ 7	3.0	1.7	1.7	3.9	3.3	5.1	3.6	4.4	2.4	4.0	1.5	2.3
7~ 8	2.4	1.3	0.4	2.0	2.3	2.9	2.9	2.9	1.4	3.1	1.5	1.3
8~ 9	0.9	0.8	0.6	1.1	0.7	1.3	0.8	1.3	1.8	2.3	1.7	0.6
9~	1.4	2.3	2.4	1.9	2.0	2.4	2.0	1.1	2.2	1.5	2.0	1.1

Table 4. (Continued)

ϕ	Km 1	2	3	4	5	6	7	8	9	10
～−8	2.0	1.2				1.5				
−8～−7	2.8	1.8		1.6	1.6	6.8		1.4	1·4	
−7～−6	3.1	3.0	0.4	3.2	4.1	8.1	1.8	2.4	3.5	3.2
−6～−5	3.5	3.6	2.9	6.7	8.1	7.9	3.9	3.9	4.6	4.8
−5～−4	4.4	4.7	7.5	12.8	9.2	8.6	5.6	7.6	5.7	6.8
−4～−3	7.2	6.7	6.8	7.4	6.2	6.8	6.5	8.2	5.2	6.4
−3～−2	6.1	5.8	5.6	3.5	4.5	3.9	5.5	6.1	4.6	4.0
−2～−1	3.1	3.5	3.8	3.8	3.3	2.7	4.7	4.0	5.0	3.1
−1～ 0	12.3	11.5	9.8	9.5	8.7	8.3	12.2	11.8	15.6	9.0
0～ 1	26.0	26.7	27.8	22.3	22.3	19.0	27.6	22.2	23.9	25.0
1～ 2	13.0	13.8	15.7	12.3	13.9	10.9	16.3	14.5	12.9	14.0
2～ 3	5.0	5.5	6.1	4.8	5.3	4.2	5.9	5.7	6.8	6.3
3～ 4	2.1	2.7	2.8	1.8	2.4	2.4	1.3	2.5	3.3	2.7
4～ 5	1.7	1.9	1.9	1.5	1.7	1.3	1.4	1.9	3.1	1.8
5～ 6	2.3	1.9	1.7	2.3	2.8	1.3	1.2	2.0	2.2	4.1
6～ 7	2.5	2.8	3.5	3.5	2.8	3.0	2.2	2.8	1.5	4.6
7～ 8	2.2	2.0	2.4	1.7	1.9	2.6	2.2	1.7	0.5	2.2
8～ 9	0.3	0.7	1.1	1.0	0.8	0.6	0.5	1.0	0.1	1.1
9～	0.2	0.2	0.2	0.3	0.4	0.1	1.5	0.3	0.2	0.9

ϕ	Tw 1	2	3	4	5	6	7	8	9	10	11	12
～−7									0.7			0.2
−7～−6									1.1			0.6
−6～−5	0.7		3.1			1.2			2.3	0.3	0.3	1.7
−5～−4	3.2	0.9	5.2	1.3	1.2	2.0			4.3	2.0	1.1	3.7
−4～−3	6.9	1.9	6.3	2.4	5.5	2.6	1.0	1.6	9.6	3.6	1.9	6.0
−3～−2	9.8	3.2	6.8	3.3	8.4	4.5	1.3	3.3	11.3	5.1	2.5	7.1
−2～−1	11.1	6.0	9.3	3.5	8.3	8.3	3.9	4.7	9.8	5.7	4.7	7.4
−1～ 0	12.7	10.8	11.6	6.6	8.5	9.9	8.4	6.3	9.6	7.2	6.9	9.9
0～ 1	17.9	12.2	13.9	14.1	11.8	12.5	14.3	11.1	14.9	13.8	11.9	15.2
1～ 2	12.7	14.5	10·2	17.0	10.9	10.3	14.3	12.3	12.1	13.5	10.9	11.8
2～ 3	8.3	11.7	7.2	13.2	8.2	7.1	12.1	9.9	6.3	8.8	9.6	7.7
3～ 4	6.5	9.5	6.6	9.9	8.4	6.8	11.4	9.4	4.1	8.0	11.5	6.0
4～ 5	4.7	8.3	6.1	5.9	8.6	8.3	10.0	9.1	3.7	7.4	11.5	5.5
5～ 6	2.5	6.7	5.0	5.8	7.4	8.8	8.5	9.9	3.0	8.2	9.5	4.9
6～ 7	1.3	6.1	3.9	6.4	5.6	7.5	6.9	9.1	2.8	7.5	7.5	4.3
7～ 8	0.5	4.4	3.0	4.4	3.3	5.4	4.0	6.9	2.1	4.8	4.7	3.5
8～ 9	0.4	1.6	0.9	1.8	1.6	1.8	1.7	3.1	0.5	1.3	2.3	1.8
9～	0.8	2.2	0.9	4.8	2.3	3.0	2.2	3.3	1.8	2.8	3.2	2.7

Table 4. (Continued)

ϕ	Tw 13	14	15	16	17	18	19	20	21	22	Os 1	Hd 1
～−8	0.7											
−8～−7	1.4				0.1	0.3		0.7	0.8			1.1
−7～−6	2.9	0.3			0.2	0.7		1.5	1.4			1.9
−6～−5	4.3	3.2	0.1		2.0	1.9	0.5	5.5	1.8		0.3	1.7
−5～−4	6.4	7.0	4.6	0.1	5.0	3.6	2.5	11.8	2.1	6.4	1.7	1.4
−4～−3	7.8	9.8	8.0	1.1	7.1	5.7	3.9	14.1	2.7	10.4	3.7	0.7
−3～−2	8.8	10.5	10.0	2.6	7.8	6.4	4.3	14.4	4.0	10.9	4.8	1.3
−2～−1	9.5	9.9	9.5	4.1	9.1	7.1	5.0	11.3	7.6	9.0	7.2	1.9
−1～ 0	9.4	10.0	10.8	9.4	8.7	9.1	5.3	9.5	11.3	10.4	9.4	9.7
0～ 1	12.1	12.7	8.7	14.4	12.8	14.5	9.5	8.8	15.4	12.5	14.0	21.4
1～ 2	11.7	12.1	6.8	12.3	15.5	13.5	12.5	6.9	15.6	8.7	15.6	12.4
2～ 3	6.3	6.2	6.0	11.3	9.5	7.9	9.3	4.8	12.8	7.4	13.3	7.2
3～ 4	3.9	3.3	6.5	11.7	5.2	5.9	9.2	3.1	9.5	6.6	10.9	6.1
4～ 5	3.0	1.9	6.7	10.7	4.2	6.0	10.5	2.8	6.2	6.2	7.1	6.0
5～ 6	3.1	4.0	6.0	8.1	3.5	5.2	9.7	1.7	3.5	5.2	4.0	5.5
6～ 7	4.0	3.6	4.6	6.2	3.6	4.8	8.3	0.9	2.2	3.7	3.4	4.7
7～ 8	2.4	2.4	4.0	3.9	3.0	3.6	5.8	0.9	1.1	1.6	2.4	4.4
8～ 9	1.0	0.6	2.3	2.0	1.7	2.3	1.8	0.4	0.6	0.8	0.9	3.7
9～	1.3	2.5	5.4	2.1	1.0	1.5	1.9	0.9	1.4	0.2	1.3	8.9

ϕ	Tz 1	On 1	2	3	Hj 1	2	Nm 1	Nn 1	2	3	4	5	6
～−9							1.0						
−9～−8							2.0						
−8～−7							3.0	1.3	0.3	2.0		2.0	1.7
−7～−6							4.2	5.7	3.9	3.8	0.8	3.2	6.0
−6～−5	1.3	1.3	4.2	1.2		0.5	5.0	13.5	8.1	6.5	1.5	4.8	8.1
−5～−4	1.1	2.2	6.4	2.1	1.7	3.3	5.4	12.6	9.7	7.9	1.0	4.2	8.2
−4～−3	1.6	4.8	5.1	2.5	5.7	7.0	4.5	8.4	13.5	6.9	1.1	3.0	7.2
−3～−2	1.0	6.7	3.5	2.9	7.7	7.9	4.2	5.8	12.4	5.9	1.4	2.1	5.8
−2～−1	2.3	6.1	2.8	3.5	7.8	7.6	4.7	5.7	9.4	4.3	3.0	1.4	5.5
−1～ 0	16.5	6.4	4.2	11.2	12.2	8.9	14.5	7.3	9.0	11.3	19.0	7.5	7.9
0～ 1	20.9	18.7	5.6	16.6	22.8	17.8	18.7	5.0	8.9	18.5	23.5	15.8	13.2
1～ 2	13.3	18.9	7.6	10.4	19.1	15.3	10.9	4.5	7.3	11.2	13.3	12.7	10.2
2～ 3	10.0	10.8	10.9	8.3	12.3	11.7	6.0	5.0	6.2	5.9	7.7	8.9	7.9
3～ 4	8.7	6.6	16.2	8.1	5.9	7.2	4.6	5.6	5.6	3.5	7.1	8.1	6.3
4～ 5	7.1	4.8	12.2	6.4	2.1	3.5	4.5	4.7	3.5	2.8	8.2	8.1	4.2
5～ 6	5.5	4.3	9.6	4.0	0.8	2.8	3.7	3.6	0.9	3.3	7.0	7.0	3.2
6～ 7	3.6	2.9	6.5	3.8	0.7	2.9	1.9	3.0	0.9	3.1	3.6	5.8	2.4
7～ 8	2.5	2.3	2.8	4.2	0.3	1.8	0.5	2.2	0.2	1.8	1.1	3.4	1.2
8～ 9	1.6	1.0	1.0	4.6	0.3	1.0	0.2	1.5	0.1	0.5	0.6	1.6	0.4
9～	3.0	2.2	1.4	10.2	0.6	0.8	0.5	4.6	0.1	0.8	0.1	0.4	0.6

Table 4. (Continued)

ϕ	Th 1	Hr 1	2	3	4	KS 1	2	3	4
~−7			0.7						
−7~−6		2.7	2.3						2.2
−6~−5	0.1	5.5	4.8		0.9	2.6	0.7	8.5	3.1
−5~−4	0.2	7.3	8.4		4.2	6.1	4.6	7.5	4.2
−4~−3	1.4	9.2	11.8		6.3	7.3	6.7	5.9	4.5
−3~−2	3.1	10.6	11.0		6.9	4.0	7.1	4.7	4.3
−2~−1	3.5	10.0	8.6	0.5	5.9	1.1	8.1	3.7	4.4
−1~ 0	5.1	10.7	9.4	1.2	9.4	4.9	10.5	11.1	10.5
0~ 1	15.9	13.9	14.6	4.5	16.9	14.7	16.5	18.0	17.6
1~ 2	16.7	12.1	12.7	11.1	17.9	15.8	15.5	13.8	15.7
2~ 3	15.7	7.7	7.0	14.0	12.1	12.0	11.5	9.0	11.2
3~ 4	16.5	4.5	3.8	17.2	7.3	9.0	8.1	6.0	6.5
4~ 5	8.8	2.2	2.0	16.8	4.0	6.4	4.3	3.8	3.6
5~ 6	3.6	1.6	0.9	11.0	2.5	4.3	2.2	2.7	0.8
6~ 7	2.4	0.8	0.7	7.8	2.5	3.7	2.1	2.3	1.8
7~ 8	2.5	0.4	0.8	5.7	1.5	3.5	1.3	1.8	0.6
8~ 9	1.5	0.1	0.3	3.4	0.7	1.9	0.3	0.4	0.9
9~	3.0	0.7	0.2	6.8	1.0	2.7	0.5	0.8	8.1

ϕ	My 1	2	3	4	5	6	7	8	9	10	11
~−10	1.1		1.0								
−10~− 9	2.2	1.5	2.2		0.6					1.7	
−9~− 8	2.6	2.5	3.9	2.0	1.8		2.0	0.8		2.3	
−8~− 7	2.8	3.2	2.7	3.0	2.9	1.8	3.0	2.5	1.5	3.1	3.5
−7~− 6	4.2	4.0	4.4	4.1	4.0	3.4	5.5	3.9	3.0	3.7	4.0
−6~− 5	5.3	6.2	6.3	4.2	6.5	3.6	7.1	5.0	4.1	3.7	4.5
−5~− 4	6.6	6.3	8.1	4.8	8.5	3.9	6.3	5.1	4.6	4.0	5.5
−4~− 3	4.8	5.2	7.4	4.9	8.0	6.0	4.2	4.7	5.9	3.3	6.0
−3~− 2	2.9	4.8	6.7	5.0	6.0	10.0	3.9	4.5	6.9	4.1	6.5
−2~− 1	4.4	5.1	7.0	5.8	5.5	10.1	4.7	4.9	7.0	5.1	6.7
−1~ 0	9.6	7.8	8.8	8.6	6.4	9.1	8.0	8.8	10.5	9.2	10.2
0~ 1	13.5	12.6	9.8	12.0	11.8	13.1	12.9	12.5	13.5	13.7	12.1
1~ 2	12.8	11.5	8.7	12.9	11.2	11.0	12.6	10.8	13.0	13.4	12.2
2~ 3	10.0	9.5	7.0	11.9	5.5	9.5	10.0	9.3	10.4	10.0	10.9
3~ 4	6.9	7.4	5.3	9.3	7.3	6.9	7.9	7.9	8.2	8.4	7.2
4~ 5	4.5	5.4	4.4	6.8	5.0	5.2	5.2	6.8	5.4	6.5	4.9
5~ 6	2.1	3.2	2.6	2.8	2.2	2.7	2.6	5.3	2.5	3.3	1.8
6~ 7	1.7	2.1	0.8	0.7	1.4	1.6	1.9	3.4	1.3	2.0	1.4
7~ 8	1.0	0.9	0.7	0.5	0.4	0.9	1.1	1.1	1.2	1.1	1.0
8~ 9	0.6	0.3	0.9	0.6	0.4	1.0	0.8	0.8	0.7	0.6	0.9
9~	0.4	0.5	0.3	0.1	0.6	0.2	0.3	1.9	0.3	0.8	0.7

Table 4. (Continued)

ϕ	Am 1	2	3	4	5	6	7	8	9	10	11	12	13
～−7										0.3			
−7～−6		0.8				1.6		0.7	0.2	1.0			
−6～−5	1.5	2.0	1.5	0.5		2.6	1.5	2.3	1.8	1.4	1.0	0.4	
−5～−4	3.0	3.3	5.8	2.2	0.1	2.9	4.6	3.5	4.0	2.6	1.7	1.9	0.1
−4～−3	4.3	4.1	7.9	4.4	1.6	5.4	5.9	5.3	5.1	5.2	3.4	1.4	0.7
−3～−2	4.4	5.0	7.2	5.6	0.5	6.8	6.7	6.4	6.2	7.5	4.3	3.6	1.5
−2～−1	5.6	5.8	6.1	6.1	1.3	7.2	5.5	7.2	6.4	8.0	4.8	5.1	2.1
−1～ 0	11.9	13.3	9.1	9.8	11.7	13.8	15.8	9.8	11.2	12.1	11.8	9.8	7.3
0～ 1	23.0	21.4	18.4	18.9	19.8	21.2	22.0	21.3	19.8	18.1	19.6	20.3	19.9
1～ 2	14.0	14.3	14.4	13.3	15.6	14.6	12.4	14.9	15.8	13.4	14.8	16.5	22.7
2～ 3	9.4	9.3	9.6	10.3	11.8	8.7	7.9	8.9	11.0	8.2	10.3	12.1	19.9
3～ 4	9.0	7.8	6.9	9.6	13.2	6.0	5.6	5.0	7.2	5.7	7.1	10.5	13.6
4～ 5	7.2	5.7	5.4	7.6	12.2	3.6	4.2	4.7	3.5	5.6	6.2	7.7	7.4
5～ 6	2.5	2.9	3.4	4.8	6.2	1.9	2.1	4.0	2.3	5.1	5.4	4.2	2.3
6～ 7	2.0	1.8	2.1	3.2	3.3	1.5	1.9	3.0	2.5	3.1	4.0	2.6	1.0
7～ 8	1.0	1.3	1.5	2.0	1.9	0.6	1.1	1.7	1.8	1.3	2.8	1.6	0.7
8～ 9	0.2	0.7	0.4	0.8	0.5	0.3	0.5	0.4	0.8	0.7	1.5	1.0	0.5
9～	1.0	0.5	0.3	0.9	0.3	0.3	2.3	0.9	0.4	0.7	1.3	1.3	0.3

ϕ	Am 14	15	16	17	18	19	20	21	22	23	24	25	26
～−9													0.3
−9～−8													2.0
−8～−7				0.5		0.2		0.3	0.8		0.6		3.1
−7～−6	0.2			2.3	2.3	2.3	2.2	1.9	1.3		1.2	5.5	4.8
−6～−5	1.1			4.7	4.7	3.5	6.6	4.5	1.9		3.4	9.5	6.6
−5～−4	2.0	0.5		6.3	5.5	4.1	7.5	5.5	2.2	2.7	4.2	12.8	8.0
−4～−3	2.2	3.3		6.5	5.6	4.8	7.0	6.0	2.7	5.1	7.3	9.9	7.9
−3～−2	2.8	2.8		6.5	5.1	4.8	6.7	6.3	3.5	6.5	8.1	8.1	7.3
−2～−1	3.9	5.7	0.1	7.8	4.7	4.6	6.0	6.0	6.8	6.7	8.0	6.2	6.4
−1～ 0	11.3	11.9	0.2	11.6	10.7	11.3	11.2	12.5	15.5	12.7	9.5	7.9	8.4
0～ 1	22.8	21.8	4.4	18.4	15.6	18.0	17.9	18.8	22.4	21.5	16.4	11.9	12.2
1～ 2	19.3	17.5	13.2	11.4	13.2	14.4	12.9	12.7	15.9	19.8	14.0	9.9	10.4
2～ 3	11.9	12.5	19.5	7.5	10.0	9.7	8.5	8.2	10.1	13.3	10.9	7.0	8.1
3～ 4	6.3	8.4	19.2	4.6	6.9	5.5	4.5	4.5	5.2	6.1	6.7	4.5	5.2
4～ 5	4.2	5.1	12.0	3.9	4.3	4.6	2.3	2.8	3.0	2.2	4.4	2.5	3.8
5～ 6	3.3	3.3	9.2	2.9	3.1	4.2	1.9	2.6	2.5	0.9	2.3	1.5	2.3
6～ 7	1.4	2.2	7.4	2.7	3.6	3.5	1.7	2.4	2.3	0.9	1.7	1.1	1.6
7～ 8	1.7	1.9	5.6	1.0	2.7	2.4	1.4	3.0	1.6	0.7	0.5	0.9	0.8
8～ 9	1.7	2.0	3.3	1.0	1.2	1.2	0.6	1.0	1.1	0.2	0.5	0.5	0.5
9～	1.9	1.1	5.9	0.4	0.8	0.9	1.1	1.0	1.2	0.7	0.3	0.3	0.3

Table 4. (Continued)

ϕ	Am 27	28	29	30	31	32	33	34	35	36	37	38
～−9			0.3				3.7					
−9～−8	2.3	4.3	0.5		1.5		3.1					
−8～−7	6.5	6.7	2.2		3.5	4.2	2.2					
−7～−6	11.0	8.2	4.1		5.0	5.8	1.2					
−6～−5	13.2	8.8	6.6		5.8	6.2	1.6	6.7	10.7			
−5～−4	10.5	8.2	7.5		5.7	6.1	2.7	7.1	8.8			2.5
−4～−3	6.5	7.0	7.5		4.6	5.6	4.3	6.9	6.8		2.4	7.9
−3～−2	5.7	6.0	6.1	0.7	4.2	5.5	5.4	5.5	5.1	1.8	6.9	10.3
−2～−1	4.6	5.1	5.2	1.2	4.0	5.9	5.8	4.8	3.9	7.2	9.2	11.7
−1～ 0	5.8	6.4	8.5	2.4	7.9	8.7	11.0	12.1	11.2	10.8	9.5	13.1
0～ 1	11.2	11.7	14.8	10.2	17.8	15.0	19.7	20.5	20.3	18.3	16.0	17.6
1～ 2	9.0	10.6	14.2	17.8	13.2	10.8	16.4	12.1	12.9	19.1	19.0	15.9
2～ 3	6.2	7.4	10.7	23.4	7.9	6.9	9.6	7.1	8.0	17.8	16.6	10.1
3～ 4	3.7	4.6	5.8	21.2	5.3	5.9	7.1	5.0	5.9	11.7	9.9	5.1
4～ 5	2.1	2.2	2.8	13.0	4.6	5.4	4.4	4.3	3.7	7.2	5.0	2.3
5～ 6	0.9	1.2	1.0	7.6	3.6	4.4	1.1	3.4	1.6	4.1	1.8	1.2
6～ 7	0.5	0.9	1.2	2.0	2.7	2.4	0.3	2.7	0.7	0.7	1.4	0.8
7～ 8	0.1	0.5	0.5	0.2	2.0	0.9	0.2	1.2	0.2	0.7	1.1	0.7
8～ 9	0.1	0.1	0.2	0.2	0.5	0.2	0.1	0.3	0.1	0.3	0.7	0.4
9～	0.1	0.1	0.3	0.1	0.2	0.1	0.1	0.3	0.1	0.3	0.5	0.4

ϕ	Hn 1	2	3	4	5	6	7	8	9	10	11	12	13
～−9											5.1	2.0	
−9～−8											6.6	8.5	3.3
−8～−7	0.3										8.7	6.3	3.3
−7～−6	0.8	0.2				0.1	0.4	3.8		0.4	7.3	5.0	4.0
−6～−5	2.1	0.5	0.4		0.1	1.4	1.6	6.0	1.0	4.1	5.0	6.9	4.8
−5～−4	4.6	1.5	1.2		0.3	3.4	6.8	6.7	3.3	5.9	4.8	8.8	5.6
−4～−3	5.5	4.0	2.6	4.1	2.1	7.1	8.0	7.5	7.2	9.5	6.3	5.9	6.0
−3～−2	6.7	6.1	5.1	8.9	7.1	9.3	9.0	8.3	10.1	10.6	7.2	5.9	6.7
−2～−1	7.2	8.7	13.4	12.5	11.2	10.0	9.5	8.4	10.9	11.3	9.3	10.7	9.5
−1～ 0	11.8	12.0	21.4	15.0	15.4	10.6	13.4	8.2	13.7	11.3	13.5	10.2	16.0
0～ 1	20.0	20.7	23.4	15.2	21.3	17.3	19.0	14.3	15.5	10.6	10.8	9.1	11.9
1～ 2	13.7	16.1	17.7	11.8	17.0	12.5	13.5	10.6	12.0	8.4	6.4	6.9	10.2
2～ 3	8.5	10.2	6.9	9.5	11.5	7.5	6.7	6.6	9.6	6.2	3.8	5.3	7.4
3～ 4	4.8	6.2	2.4	7.8	5.1	6.1	2.7	4.0	7.4	3.7	2.3	3.8	4.9
4～ 5	3.8	3.6	1.2	3.8	2.5	3.8	1.5	2.9	4.3	4.7	1.4	2.0	3.0
5～ 6	2.6	2.7	0.8	3.7	0.8	2.9	1.5	3.4	2.1	3.2	0.3	0.6	1.4
6～ 7	3.2	3.4	1.4	2.7	1.5	2.9	1.9	3.7	1.3	2.9	0.3	0.5	1.0
7～ 8	2.2	1.7	0.4	2.1	1.7	1.8	2.3	2.3	1.0	2.1	0.4	0.5	0.6
8～ 9	0.6	0.2	0.4	1.5	1.3	0.8	0.4	0.8	0.3	1.4	0.3	0.3	0.3
9～	1.6	2.2	2.3	1.4	1.1	2.5	1.8	2.5	0.3	3.7	0.2	0.8	0.1

Table 4. (Continued)

ϕ	KF 1	2	3	4	5	6	7	8	9	10	As 1	2
～−9	1.3		1.0									
−9～−8	4.3	1.8	1.8									
−8～−7	6.4	6.4	3.9	1.7	2.0	1.8	1.4	1.2		0.7		
−7～−6	7.4	8.1	6.5	4.5	3.2	7.2	5.8	6.0	2.1	5.5		0.3
−6～−5	7.3	8.7	8.6	7.1	6.0	9.5	7.6	8.9	7.1	12.3		0.5
−5～−4	7.0	8.2	11.2	9.0	8.8	9.8	9.5	11.2	10.2	17.3		0.9
−4～−3	6.9	6.8	10.9	11.0	11.6	8.5	8.0	10.5	9.9	11.9	0.8	1.3
−3～−2	6.5	5.2	8.4	9.7	10.5	8.0	6.8	8.4	8.6	8.3	1.7	1.2
−2～−1	5.3	6.6	6.0	7.3	8.9	7.4	5.9	7.0	9.1	6.6	2.1	1.6
−1～ 0	6.7	6.4	7.0	8.6	8.3	7.5	7.1	9.6	9.6	6.3	4.4	2.2
0～ 1	9.7	8.4	9.0	9.3	9.5	9.0	9.0	9.4	13.0	8.8	7.8	6.1
1～ 2	8.0	8.8	8.3	9.0	9.0	8.0	8.2	6.9	12.8	8.4	10.0	9.1
2～ 3	6.9	11.3	6.2	7.2	8.1	7.0	7.0	5.6	8.8	5.8	11.2	14.3
3～ 4	4.7	7.1	4.5	5.6	5.9	6.0	6.0	4.6	4.9	3.4	13.3	18.1
4～ 5	3.8	2.7	3.1	3.6	4.0	4.3	5.3	4.0	1.7	1.7	15.5	14.3
5～ 6	2.9	1.3	1.7	2.3	1.9	2.3	3.6	2.2	0.4	1.0	11.4	12.5
6～ 7	2.0	1.1	0.5	1.5	0.9	1.4	2.9	1.5	0.4	0.4	8.6	7.1
7～ 8	1.2	0.4	0.4	0.6	0.6	0.7	2.0	0.7	0.3	0.2	5.8	2.7
8～ 9	0.7	0.3	0.3	0.4	0.4	0.7	1.1	0.4	0.3	0.2	1.5	1.1
9～	1.0	0.4	0.7	1.6	0.4	1.3	2.8	1.9	0.8	1.2	5.9	6.7

ϕ	Ai 1	2	3	4	5	6	7	8	9	10	11	12	13
～−8	1.1												
−8～−7	0.9												0.9
−7～−6	1.2		1.1			1.1	0.4		0.2		0.3		0.4
−6～−5	0.9	2.0	2.4		1.2	2.4	2.4		1.5		1.8	2.0	1.5
−5～−4	1.2	6.0	5.2	1.5	1.4	5.8	6.7		4.8	1.0	2.2	5.4	3.7
−4～−3	2.7	6.5	11.9	1.6	1.5	5.4	5.7		8.2	1.0	2.7	2.9	4.3
−3～−2	5.0	7.2	12.3	1.1	1.2	4.5	4.6	1.0	9.3	1.3	3.3	3.1	3.9
−2～−1	5.1	8.2	11.9	1.7	5.2	5.8	5.2	1.7	7.0	2.4	4.3	2.9	3.3
−1～ 0	8.2	7.1	13.0	2.8	14.0	10.1	8.9	4.2	2.1	5.9	9.3	7.1	7.7
0～ 1	13.0	13.3	15.3	6.5	17.8	13.2	13.4	14.1	8.7	13.8	15.5	12.6	14.8
1～ 2	15.7	12.9	12.9	9.8	14.3	13.7	14.0	18.8	13.5	18.9	17.6	16.3	15.1
2～ 3	13.8	11.8	6.1	11.8	12.6	12.4	12.5	17.1	12.9	19.9	17.7	15.7	14.7
3～ 4	11.9	10.0	2.2	16.8	10.6	10.3	10.6	12.3	11.2	15.8	12.5	13.6	12.4
4～ 5	7.2	4.9	1.0	16.3	7.3	5.3	7.3	7.9	6.8	8.6	5.7	8.9	7.3
5～ 6	4.8	2.5	1.0	11.1	4.4	3.0	2.9	5.5	3.2	4.3	2.1	4.1	2.8
6～ 7	1.6	1.7	0.5	6.9	3.7	2.6	2.3	4.1	2.5	2.5	2.3	2.7	2.1
7～ 8	0.3	1.4	0.4	3.6	1.6	0.5	1.1	3.3	2.9	1.1	1.0	0.9	0.8
8～ 9	0.3	0.3	0.2	2.0	0.2	0.9	0.5	1.7	1.3	0.3	0.7	0.9	0.1
9～	5.1	4.2	2.6	6.5	3.0	3.0	1.5	8.3	3.9	3.2	1.0	0.9	4.2

Table 5. Results of mechanical analyses of pyroclastic fall deposits.

ϕ	Kc 11	12	13	Ms 4	Ak 5	D 3	4	S 12	13	14	15	16
− 6∼−5.5				—			2.6					
−5.5∼− 5				4.8								
− 5∼−4.5			5.0	7.0		2.9	12.0	—		—	13.5	1.7
−4.5∼− 4			7.2	7.7				1.8		2.5	12.2	4.6
− 4∼−3.5			7.7	7.8		6.4	7.6	4.5		6.3	11.2	6.0
−3.5∼− 3			8.6	8.5			10.0	10.0		11.4	12.1	10.1
− 3∼−2.5	1.2		10.3	8.5		5.9	10.0	12.7		13.6	9.8	11.2
−2.5∼− 2			10.9	8.1		10.8	8.9	13.9		12.5	6.4	11.9
− 2∼−1.5	4.1		9.7	6.9		14.2	6.7	12.7	0.8	10.7	6.5	10.2
−1.5∼− 1			8.4	5.9		11.6	4.9	11.7		12.0	4.4	10.3
− 5∼−0.5	9.2	0.2	6.8	4.9		8.2	11.8	8.7	1.7	12.2	3.2	9.3
−0.5∼ 0			5.8	5.0		9.2		7.5		9.5	5.1	8.2
0∼ 0.5	12.5	1.2	5.5	7.2	0.3	14.0	12.5	6.5	9.1	5.0	8.1	6.5
0.5∼ 1	17.5		3.2	7.0		7.3		4.5		1.5	4.3	3.2
1∼ 1.5	18.8	8.9	3.0	5.7	0.6	3.7	5.9	2.5	8.9	1.1	2.4	1.9
1.5∼ 2	13.4			3.2					13.0			
2∼ 2.5	11.5	10.4	2.1	1.3	21.6	2.1	2.2	1.0	14.5	0.6	0.4	1.0
2.5∼ 3		15.6							16.5			
3∼ 3.5	4.1	19.9	1.9	0.2	24.0	1.4	1.7	0.5	15.7	0.4	0.2	0.8
3.5∼ 4		15.1							8.8			
4∼ 4.5	2.4	9.9	1.0	0.1	16.0	1.0	1.0	0.5	5.1	0.4	0.1	1.1
4.5∼ 5		5.3										
5∼ 6	1.8	4.7	2.9	0.2	13.3	0.8	0.7	1.0	1.2	0.3	0.1	2.0
6∼ 7	1.3	3.1			11.7		0.7		1.0			
7∼ 8	1.0	1.9			8.0		0.4		0.7			
8∼ 9	0.7	0.7			3.7		0.2		1.1			
9∼	0.5	3.1			0.8		0.2		1.9			

ϕ	Ty 11	12	Km 11	12	Tw 23	24	25	26	Nn 7	Hr 5	KS 5
− 6∼−5.5			15.0	—	2.7	—		2.7		—	
−5.5∼− 5			22.4	24.5		5.6				7.8	
− 5∼−4.5			24.8	19.7	9.4	33.9		10.0	—	17.4	
−4.5∼− 4			21.6	15.0		16.5	2.7		12.4	17.3	
− 4∼−3.5	3.0	4.0	10.1	18.0	6.2	11.7		6.7	17.4	13.3	1.8
−3.5∼− 3					8.4	8.6	9.3	8.2	19.7	12.4	
− 3∼−2.5	9.5	10.5	1.8	8.4	9.0	11.5	7.9	8.4	15.7	9.1	7.7
−2.5∼− 2					8.6		10.4	9.4	10.5	6.2	
− 2∼−1.5	7.5	13.5	1.0	5.7	7.4	5.7	12.4	9.1	6.5	7.5	6.2
−1.5∼− 1	8.2				6.8		12.4	9.5	5.0		8.1
− 1∼−0.5	9.5	7.0	1.0	4.3	6.8	2.8	11.8	8.7	7.1	3.6	11.7
−0.5∼ 0	10.0	7.4			7.4		10.8	8.2			16.3
0∼ 0.5	18.8	13.9	1.0	2.7	7.8	1.9	11.2	8.9	3.0	2.7	26.8
0.5∼ 1	24.0	21.2			6.2		6.7	5.9			14.4
1∼ 1.5	7.9	12.3	0.5	1.1	5.3	0.6	3.6	3.2	0.9	1.4	5.0
1.5∼ 2		5.5									
2∼ 3	1.0	2.4	0.3	0.2	2.0	0.4	0.6	0.5	0.6	0.4	0.8
3∼ 4	0.3	0.9	0.2	0.2	1.3	0.3	0.3	0.3	0.4	0.3	0.6
4∼ 5	0.2	0.8	0.2	0.2	1.3	0.2	0.2	0.2	0.4	0.2	0.3
5∼	0.1	0.4			3.4	0.3	0.1	0.1	0.4	0.4	0.3

Table 5. (Continued)

ϕ	Am 39	40	41	46	47	KF 11	F 1	2	3	4	5	6
− 6～−5.5	2.3	—										
−5.5～− 5	19.0	4.5										
− 5～−4.5	19.2	11.3				—	—	—				
−4.5～− 4	17.9	12.7				1.2	5.2	2.5				
− 4～−3.5	8.6	14.6	14.3			3.8	9.5	6.3	2.2	1.9		1.5
−3.5～− 3	4.3	16.4				13.5	23.8	7.7		14.1		23.8
− 3～−2.5	5.4	11.2	23.8	20.0		20.8	27.2	10.8	12.3	14.7	9.6	21.9
−2.5～− 2		4.9				22.2	15.1	11.1		16.1		16.6
− 2～−1.5	2.5	4.2	17.9	18.4		13.6	6.7	9.2	12.0	16.5	7.6	11.9
−1.5～− 1				18.5		7.2	3.6	7.8	13.8	16.4	10.8	7.7
− 1～−0.5	2.7	2.1	15.4	18.4		3.7	3.5	12.6	17.7	10.1	15.0	8.5
−0.5～ 0				13.2		2.3			18.0	6.1	21.5	
0～ 0.5	4.1	2.1	12.6	5.0	—	2.7	2.1	9.7	15.0	3.9	22.7	4.9
0.5～ 1				1.5	3.0				5.8		9.9	
1～ 1.5	4.2	2.3	1.6	3.5	5.7	1.3	1.5	6.8	2.8	0.1	2.6	2.2
1.5～ 2					15.5							
2～ 2.5	3.7	3.1	0.3	1.1	30.8	1.7	0.9	4.9	0.2	0.03	0.2	0.8
2.5～ 3					21.8							
3～ 3.5	3.0	3.8	1.3	0.3	10.0	1.9	0.5	3.3	0.1	0.04	0.05	0.1
3.5～ 4					4.4							
4～ 5	1.9	3.1	1.6	0.1	4.5	2.2	0.3	1.6	0.07	0.02	0.03	0.05
5～ 6	1.2	3.7	4.9		4.3	1.9	0.1	1.7	0.03	0.01	0.02	0.05
6～ 7			3.4			0.9		1.5				
7～ 8			1.5			0.5		1.5				
8～ 9			1.3			0.4		0.4				
9～			0.1			0.2		0.6				

in another paper, full description of them is omitted here. Mechanical analyses were carried out through several steps in order to obtain accurate results of thorough analyses of every size fraction. Each sample was divided into three parts, one was reserved for preservation, another was prepared for analyses of the coarse fractions, and the rest was used for analyses of the fine and medium fractions. The analyses were carried out by means of the decantation, sieving and pipette methods in sequence. All results obtained through such steps of laboratory work were corrected for the coarser fractions by referring to photographs of the outcrops from which the samples were picked up. The resuls of mechanical analyses of the pyroclastic flow deposits are shown in Table 4, where each figure listed in the column represents the weight per cent of each fraction sized out by mechanical analyses. Figs. 3a–3k show cumulative curves of particle size distribution of the pyroclastic flow deposits. The results of mechanical analyses of the pyroclastic fall deposits are shown in Table 5 and Fig. 4. The results of mechanical analyses of the dry mud-flow deposits and the auto-brecciated lava flows are shown in Table 6 and Figs. 5a and 5b. The diameters of particles ξ in millimeters are replaced here by ϕ as expressed in the equations $\xi=(1/2)^{\phi}$ or $\phi=-\log_2 \xi$, for convenience.

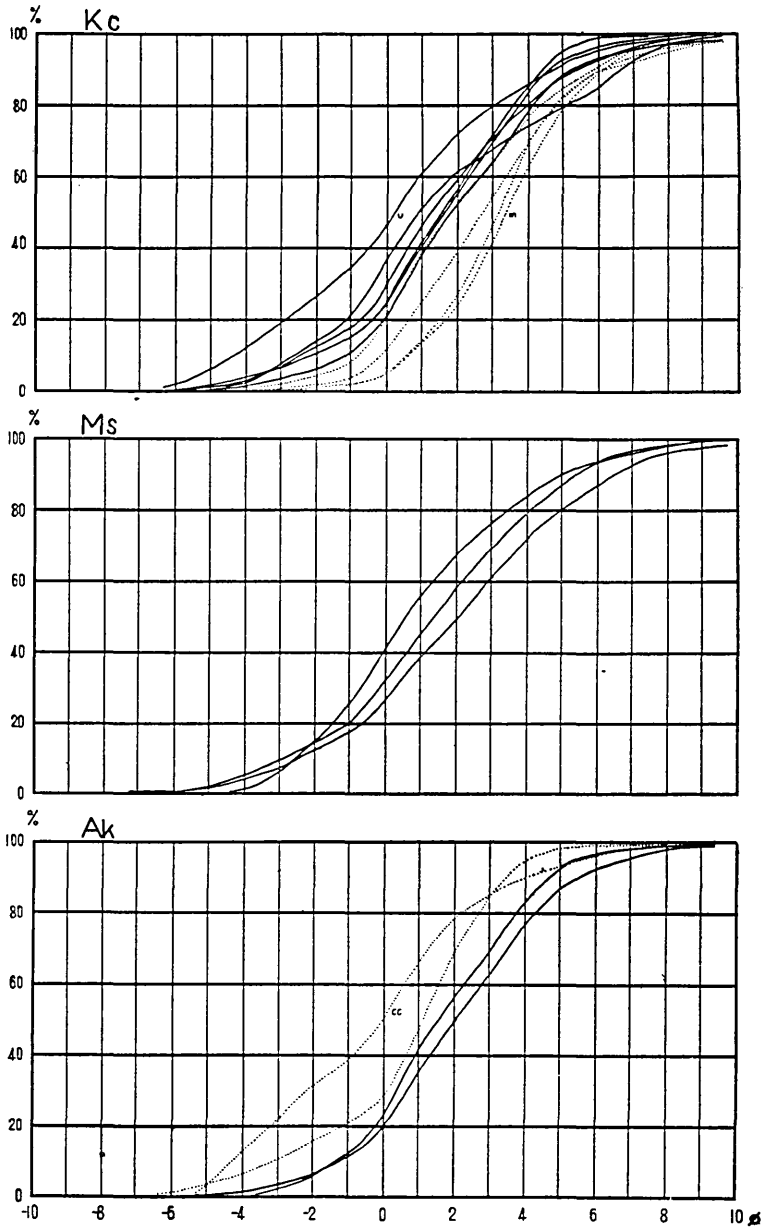

Fig. 3. Cumulative curves of the particle size distribution of pyroclastic flow deposits.

Fig. 3a. Upper: the Kutcharo Volcano, middle: the Mashu Volcano, lower: the Akan Volcano.

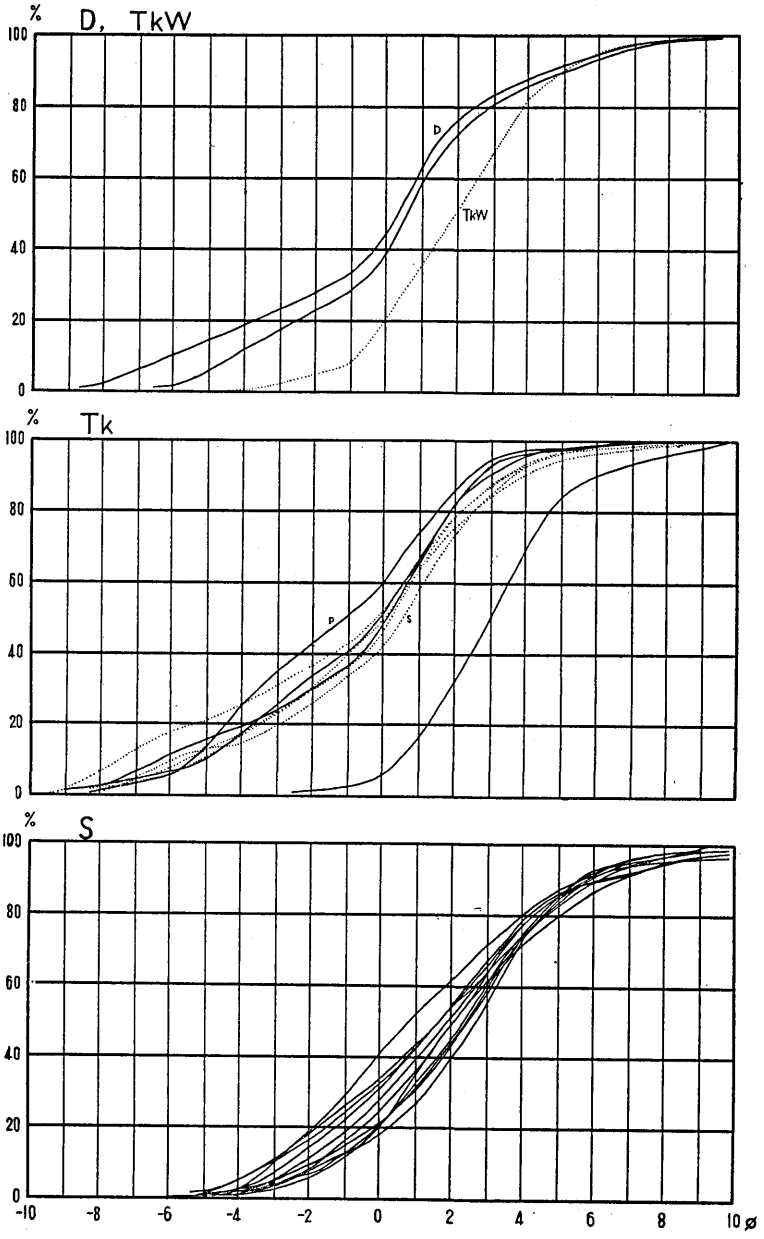

Fig. 3b. Upper: the Daisetsu Volcano and the Tokachi Welded Tuff, middle: the Tokachidake Volcano, lower: the Shikotsu Volcano.

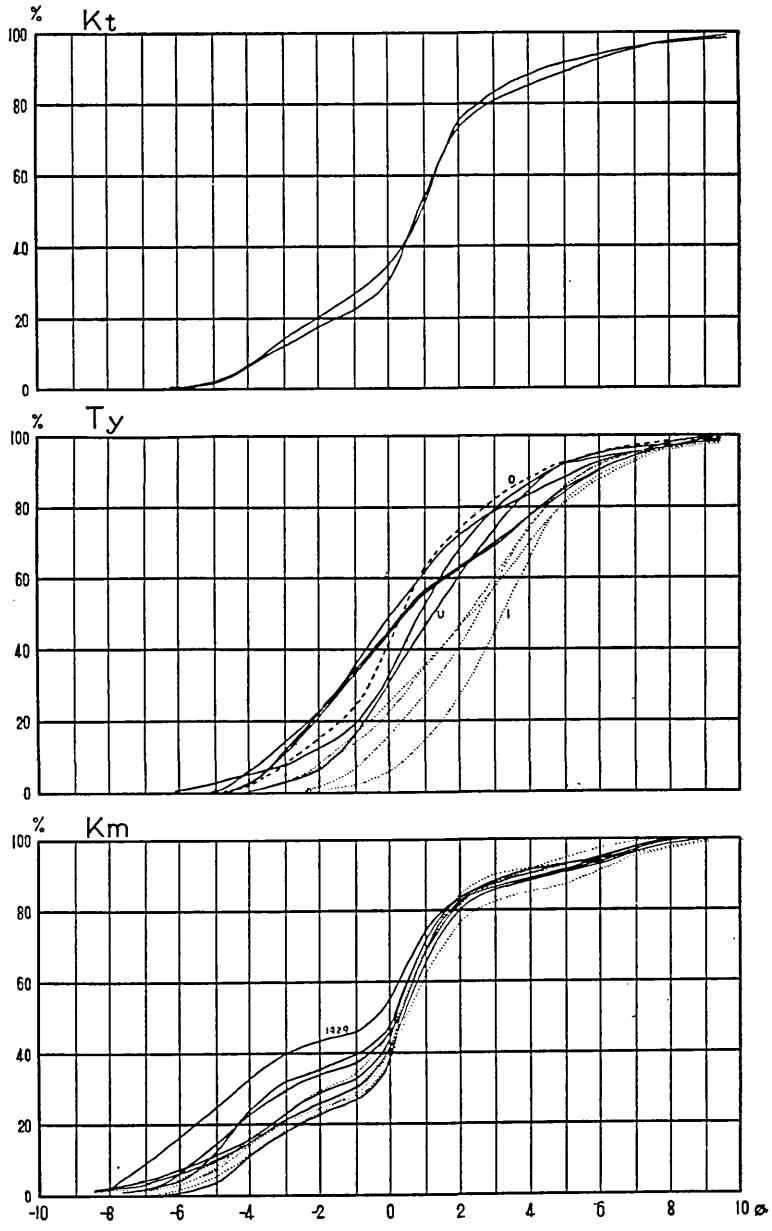

Fig. 3c. Upper: the Kuttara Volcano, middle: the Toya Volcano, lowere: the Komagatake Volcano.

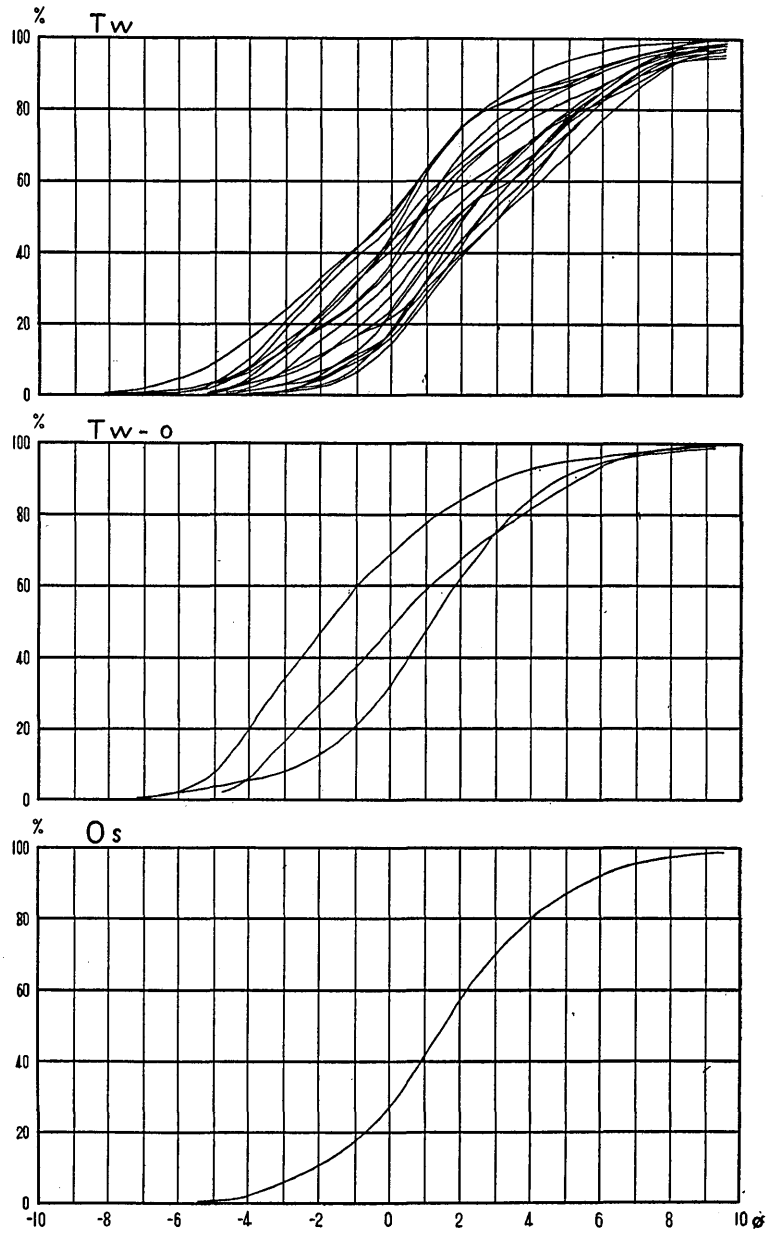

Fig. 3d. Upper: the Younger Ash-flow of the first stage of the Towada Volcano, middle: the Older Ash-flow of the first stage of the Towada Volcano, lower: the Osoreyama Volcano.

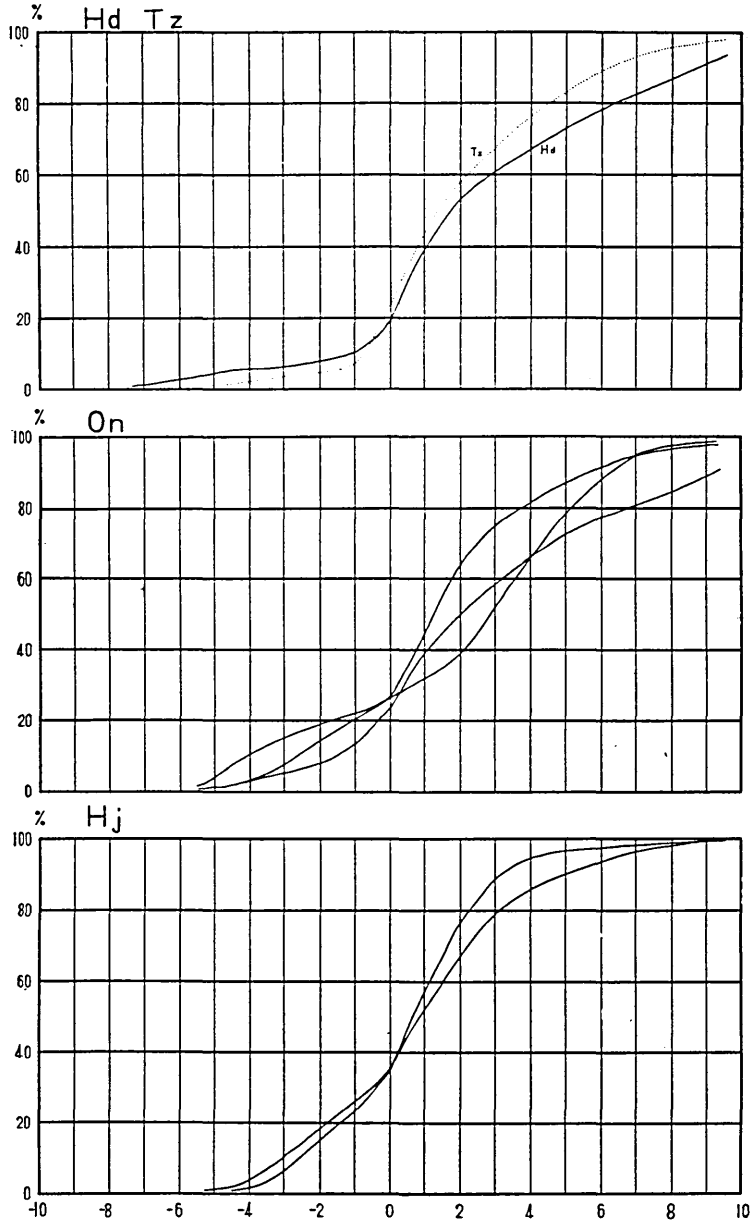

Fig. 3e. Upper: the Hakkoda and Tazawa Welded Tuffs, middle: the Onikobe Volcano, lower: the Hijiori Ash-flow.

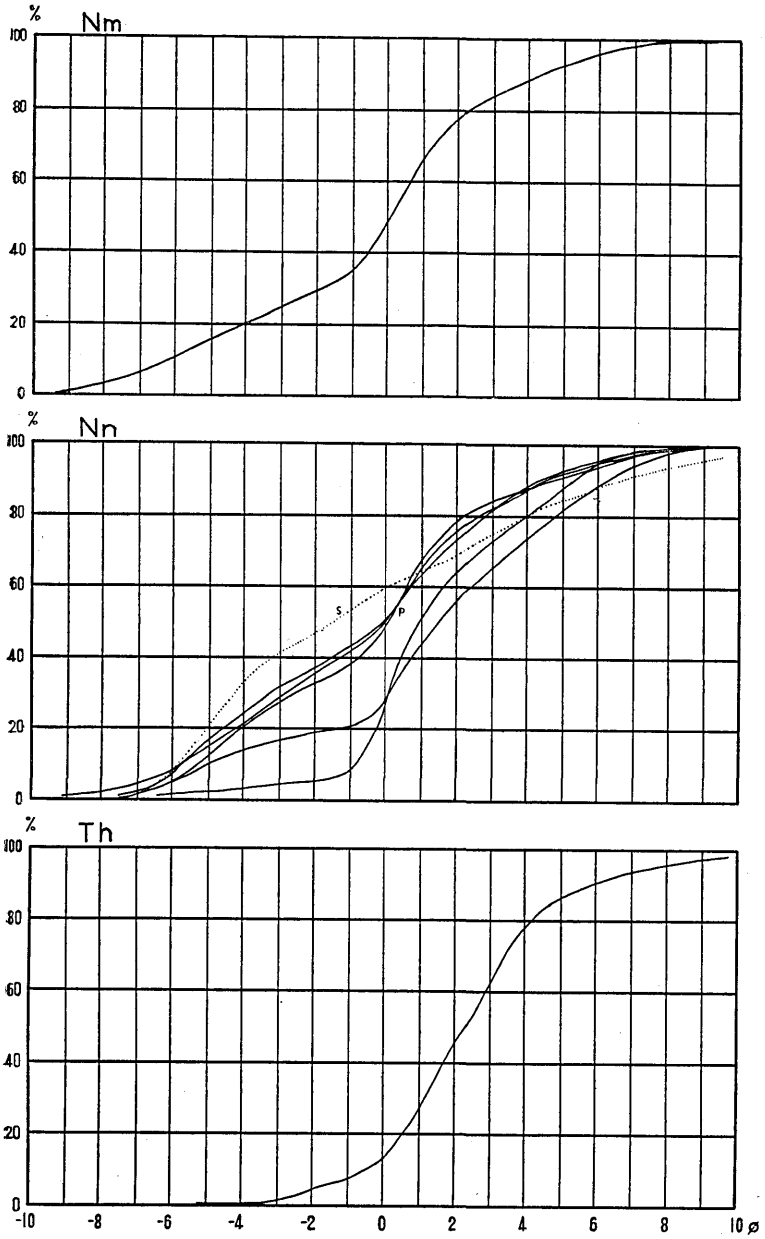

Fig. 3f. Upper: the Numajiri Welded Tuff, middle: the Nantai Volcano, lower: the Takahara Volcano.

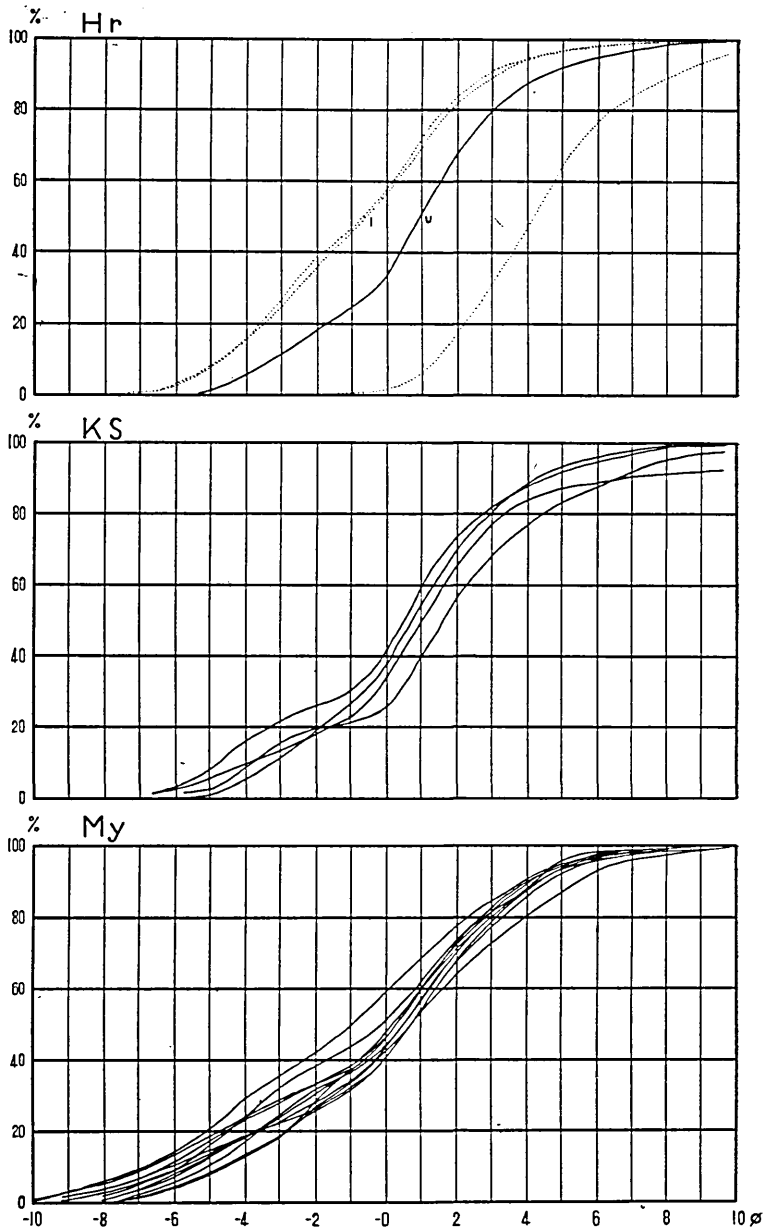

Fig. 3g. Upper: the Haruna Volcano, middle: the Kusatsu-Shirane Volcano, lower: the Myoko Volcano.

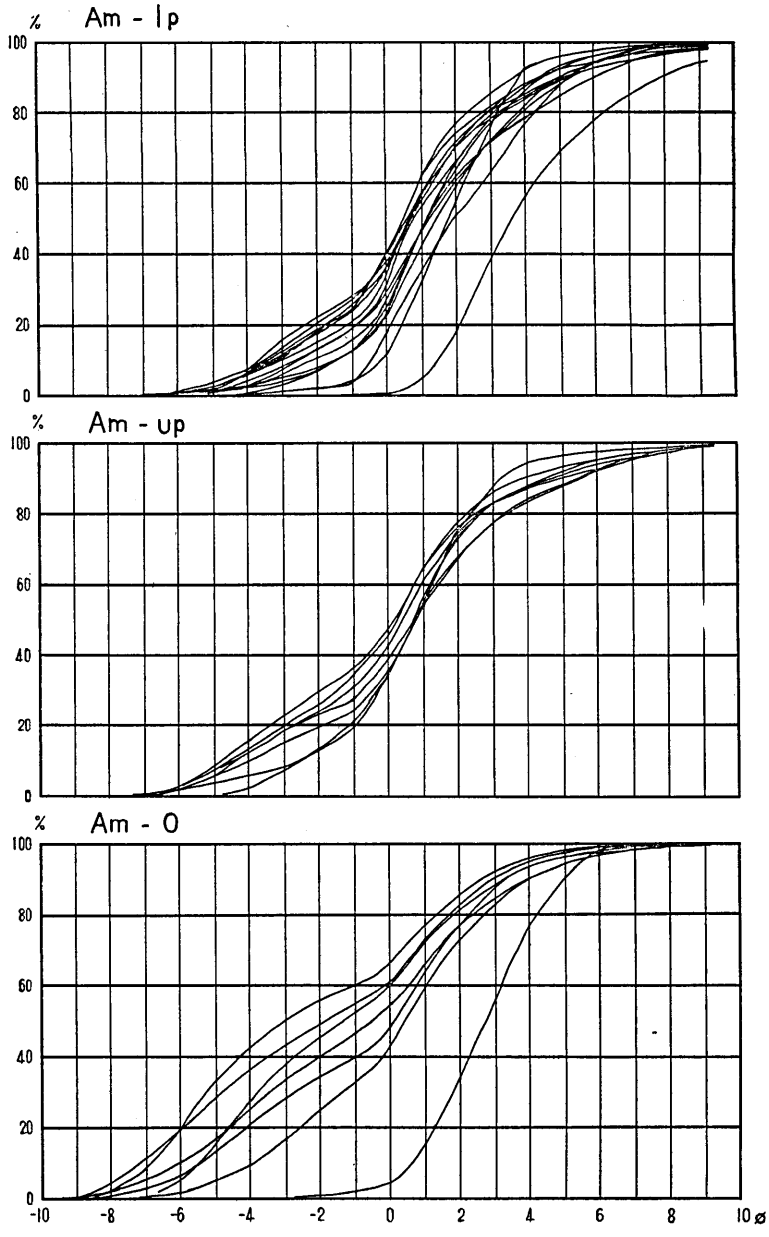

Fig. 3h. Pyroclastic flows of the Asama Volcano. Upper: the Lower Ash-flow, middle: the Upper Ash-flow, lower: the Oiwake Pyroclastic Flow.

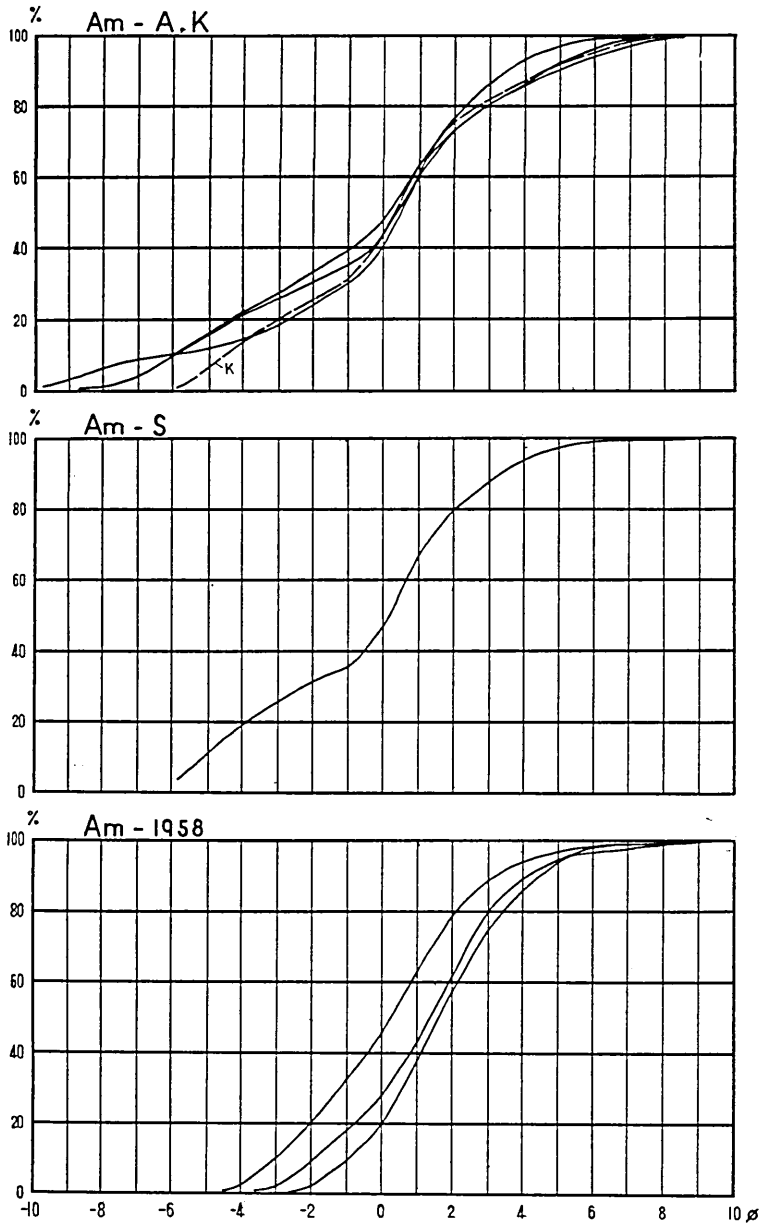

Fig. 3i. Pyroclastic flows of the Asama Volcano. Upper: the Agatsuma Pyroclastic Flow of the 1783 eruption, middle: the Shiraito Pyroclastic Flow, lower: the Ash-flow of the 1958 eruption.

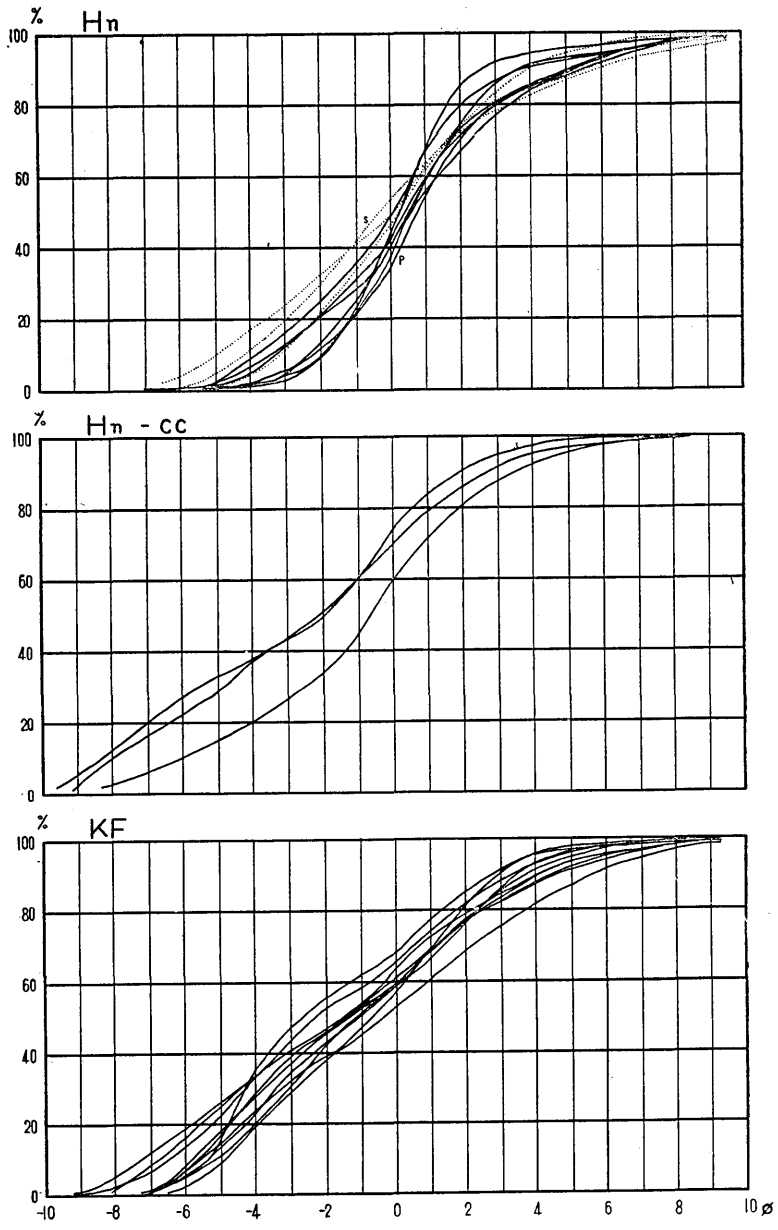

Fig. 3j. Upper: the Ash-flow of the second stage of the Hakone Volcano, middle: the Central Cone Pyroclastic Flow of the Hakone Volcano, lower: the Lower and Upper Pyroclastic Flows of the Ko-Fuji Volcano.

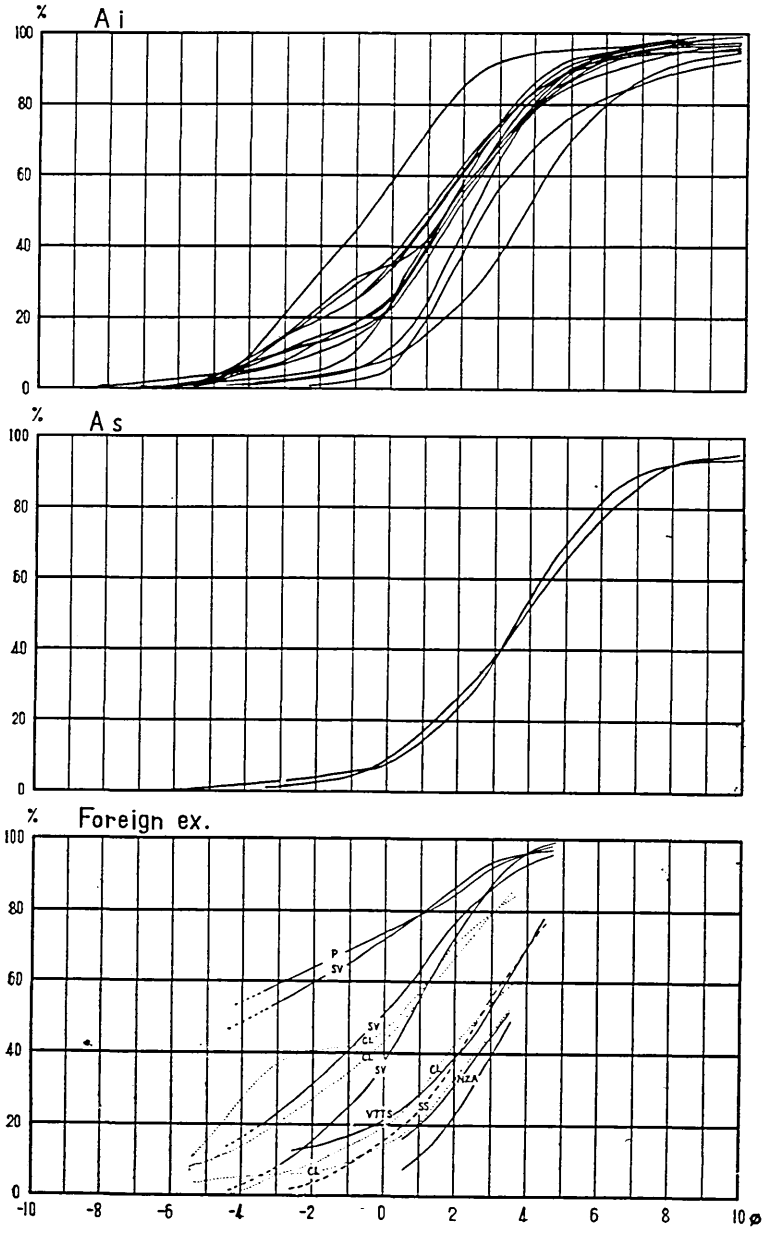

Fig. 3k. Upper: the Aira Volcano, middle: the Aso Volcano, lower: foreign examples of pyroclastic flows.

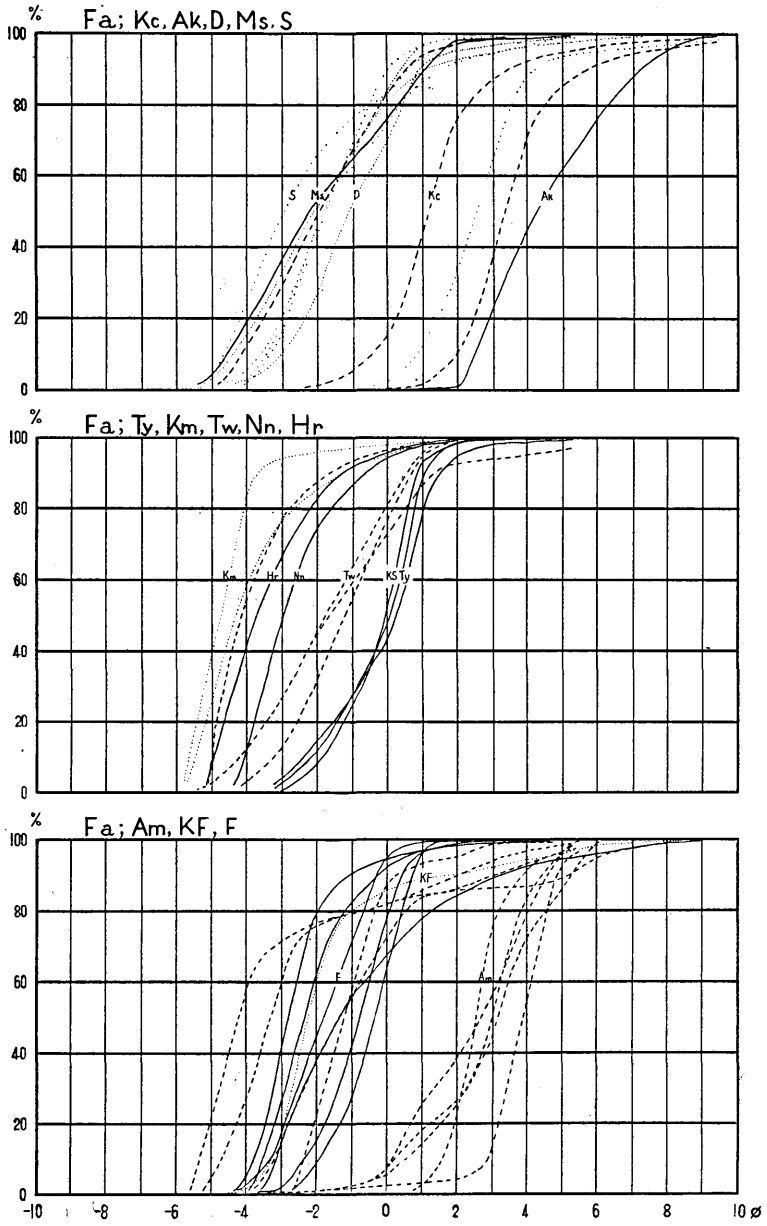

Fig. 4 Cumulative curves of the particle size distribution of pyroclastic fall deposits.

Table 6. Results of mechanical analyses of dry mud-flow deposits and auto-brecciated lava flows.

ϕ	Tk 9	10	11	12	13	Km 13	14	15	Z 1	2
~−9	3.5	3.7				1.2				
−9~−8	2.2	3.5			3.8	1.4	2.0	2.7		
−8~−7	1.0	3.0	0.8		3.6	2.6	3.6	4.4	0.6	
−7~−6	1.1	3.5	2.4		8.4	4.0	3.8	5.3	2.5	1.8
−6~−5	1.0	4.4	4.8	1.1	14.2	4.8	5.3	6.7	6.4	9.2
−5~−4	2.4	4.4	4.0	4.7	17.8	5.3	5.8	10.1	9.2	9.6
−4~−3	4.0	5.5	6.0	8.1	12.0	6.3	6.3	10.1	10.1	10.4
−3~−2	5.1	6.0	7.9	9.5	8.4	7.5	6.4	8.0	10.2	9.4
−2~−1	6.4	5.9	7.2	9.9	7.1	9.1	6.4	6.4	10.0	8.2
−1~ 0	12.5	8.3	7.1	13.3	7.6	13.5	8.5	7.6	11.8	7.9
0~ 1	15 2	12.2	8.0	14.0	5.8	17.6	13.6	9.0	13.0	7.2
1~ 2	15.2	10.0	7.9	9.6	3.2	10.9	11.6	7.8	8.4	5.1
2~ 3	11.7	8.4	6.9	6.9	2.4	6.7	9.0	5.1	5.5	4.1
3~ 4	7.0	5.8	6.2	5.3	1.9	3.4	6.2	3.9	3.4	3.7
4~ 5	3.0	3.6	4.5	4.2	1.2	2.4	4.5	4.1	2.1	3.9
5~ 6	1.7	2.9	3.9	3.4	0.6	1.1	2.3	3.3	1.7	4.0
6~ 7	1.4	1.9	3.7	3.1	0.8	1.0	1.9	2.9	1.4	4.5
7~ 8	2.1	1.5	4.1	2.2	0.7	0.5	1.4	1.3	0.9	4.5
8~ 9	1.8	1.6	3.5	0.8	0.2	0.3	1.0	0.3	0.8	2.5
9~	1.7	3.9	11.1	3.9	0.3	0.4	0.4	1.0	2.0	4.0

ϕ	G 1	B 1	2	3	Hn 14	Ak 6	Km 16	Z 3	Nn 8	F 7
~−12				0.7						
−12~−11			1.0	3.1						
−11~−10			1.7	4.2	11.4			2.5	2.0	
−10~− 9		1.0	2.3	6.7	18.0			1.7	5.7	
− 9~− 8		3.4	2.3	8.7	10.8		8.0	1.1	6.8	2.4
− 8~− 7	1.6	4.6	2.7	8.3	7.9	4.3	10.4	0.7	7.0	5.2
− 7~− 6	5.8	6.7	4.2	7.3	5.9	8.2	8.0	1.3	8.5	7.1
− 6~− 5	8.6	6.9	6.3	5.3	6.3	13.5	6.0	10.5	8.7	9.9
− 5~− 4	11.0	7.2	9.2	4.6	7.2	18.6	5.2	28.3	8.3	11.2
− 4~− 3	11.7	6.0	9.0	5.2	5.8	12.1	3.6	16.4	7.7	14.3
− 3~− 2	9.6	5.5	7.1	5.2	5.4	9.6	4.0	9.9	7.7	15.6
− 2~− 1	8.2	5.5	6.0	5.1	5.3	7.5	6.1	6.5	7.8	10.0
− 1~ 0	7.5	6.2	6.3	4.9	3.1	6.7	8.3	5.4	8.0	6.3
0~ 1	7.0	9.5	11.1	5.9	3.8	6.9	11.0	5.0	7.8	4.8
1~ 2	5.2	9.7	10.2	4.0	2.8	4.4	9.1	3.5	5.6	3.9
2~ 3	4.1	9.8	8.3	3.2	1.7	3.2	7.1	2.4	4.2	3.6
3~ 4	5.0	7.5	5.6	3.3	1.5	2.1	5.5	1.6	2.4	3.0
4~ 5	5.7	4.6	2.7	4.1	1.2	2.0	3.6	0.9	1.0	1.8
5~ 6	4.5	2.3	1.6	3.8	0.7	0.6	1.9	0.6	0.2	0.3
6~ 7	2.0	1.6	1.0	3.1	0.8	0.2	1.2	0.8	0.3	0.2
7~ 8	0.8	0.7	0.6	1.8	0.1	0.1	0.2	0.1	0.1	0.2
8~ 9	0.9	0.5	0.2	0.7	0.2		0.2	0.2	0.1	0.1
9~	0.8	0.8	0.6	1.2	0.1		0.6	0.6	0.1	0.1

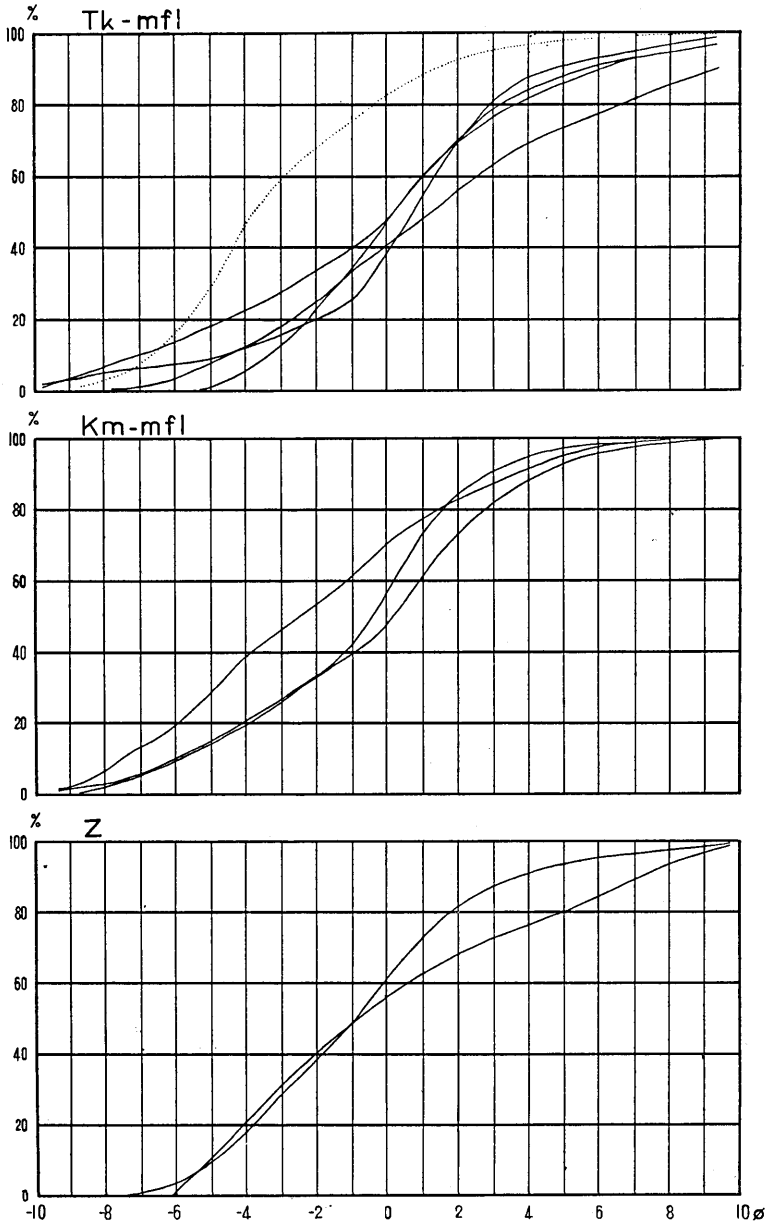

Fig. 5a. Cumulative curves of the particle size distribution of dry mud-flow deposits. Upper: the Tokachidake Volcano (solid line: May 24th, 1926, dotted line: Sept. 3rd, 1926), middle: the Komagatake Volcano, lower: the Zao Volcano.

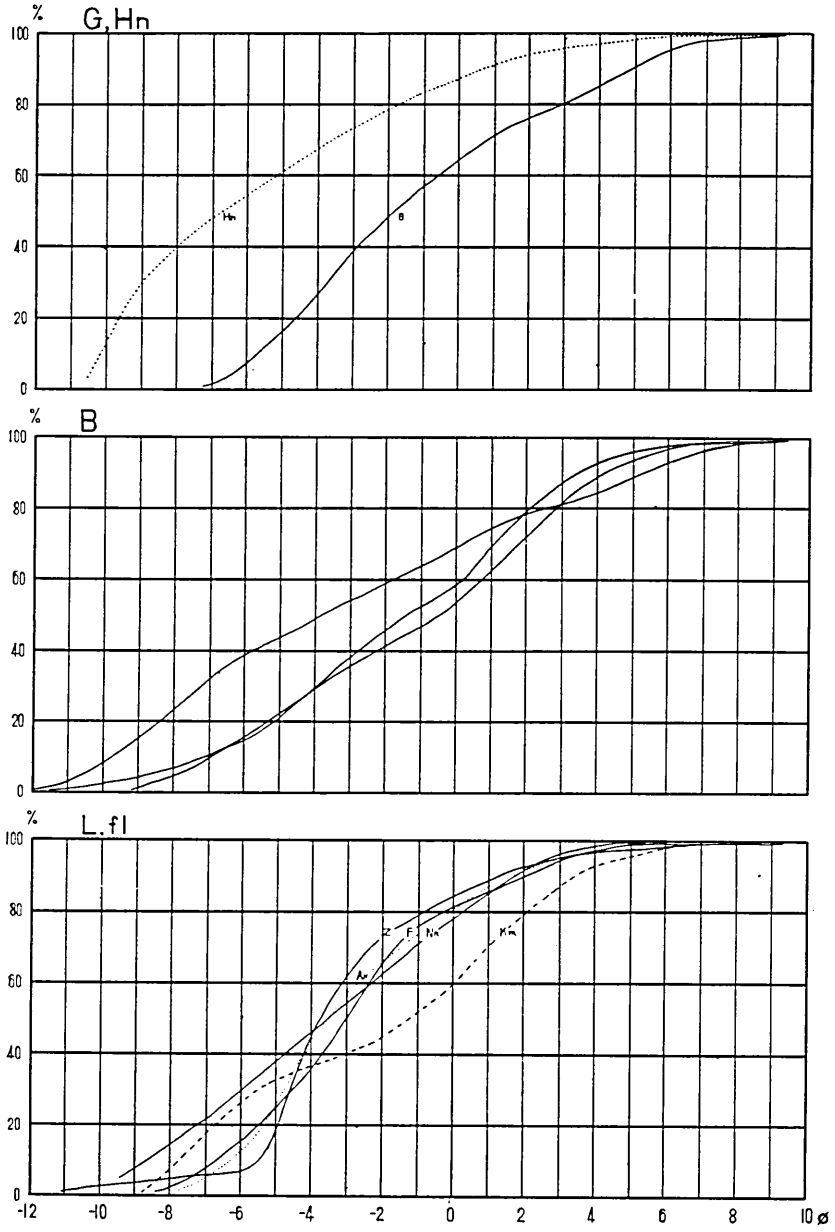

Fig. 5b. Cumulative curves of the particle size distribution of dry mud-flow deposits and auto-brecciated lava flows. Upper: mud-flows of the Gassan and Hakone Volcanoes, middle: the 1888 Mud-flow of the Bantai Volcano, lower: autobrecciated lava flows.

Parameters of Particle Size Distribution

In the discussion on the size characteristics of clastic deposits, descriptive measures of patrticle size distribution are used in general. The phi values of the percentiles, ϕ_5, ϕ_{16}, ϕ_{25}, ϕ_{50}, ϕ_{75}, ϕ_{84} and ϕ_{95}, the phi values for which the cumulative per cent of samples by weight is 5, 16, 25, 50, 75, 84 and 95 per cent respectively, are read on the cumulative curves, and approximate values for every parameter of the particle size distribution are calculated from the following relations.

$$Md_\phi = \phi_{50}\ ,\quad M_\phi = (\phi_{16}+\phi_{84})/2\ ,$$
$$Q' = (\phi_{75}-\phi_{25})/2\ ,\quad Q'' = (\phi_{75}+\phi_{25}-2\phi_{50})/Q'\ ,$$
$$\sigma_\phi = (\phi_{84}-\phi_{16})/2\ ,\quad \alpha_\phi = (M_\phi-\phi_{50})/\sigma_\phi\ ,$$
$$\alpha_{2\phi} = \{(\phi_5+\phi_{95})/2-\phi_{50}\}/\sigma_\phi\ ,$$
$$\beta_\phi = \{(\phi_{95}-\phi_5)/2-\sigma_\phi\}/\sigma_\phi\ .$$

M_ϕ, Q' and Q'' are the approximations of median, standard deviation and skewness respectively, obtained by the quartile method, while M_ϕ, σ_ϕ, α_ϕ and $\alpha_{2\phi}$, and β_ϕ are those of the mean, standard deviation, primary and secondary skewness and kurtosis of the Inman's phi measure system[25]. The values of these parameters are listed in Tables 7–12. It is generally considered that the measures of Inman's phi measure system represent a closer approximation to the values of true statistical parameters than those obtained by other measure systems. Therefore, Inman's system is widely used in the field of sedimentary petrology. The writer adopts these measures in this study.

Md_ϕ and M_ϕ are the measures of central tendency of the particle size distribution. The median is the diameter value in phi of the ordinate that divides an area surrounded by the frequency distribution curve and the abscissa into two equal areas, while the mean is the diameter value of the center of gravity of the frequency distribution. The phi deviation measure σ_ϕ may give the standard deviation of the size distribution curve in terms of Wentworth units (1922), since one phi unit is equivalent to one Wentworth division, and shows the magnitude of the horizontal scattering of the curve. The smaller the values of σ_ϕ, the better the sorting. The measures of skewness, α_ϕ and $\alpha_{2\phi}$, show the degree of asymmetry of the size distribution curve. In a symmetrical distribution the mean and the median coincide and the

25) D. L. INMAN, "Measures of describing the size distribution of sediments," *Jour. Sed. Petrol.*, **22** (1952), 125-145.

Table 7. Data of parameters of the particle size distribution of pyroclastic flow deposits.

Sp.	no.	$Md\phi$	Q'	Q''	$M\phi$	$\sigma\phi$	$\alpha\phi$	$\alpha_2\phi$	$\beta\phi$	Remark
Kc	1	0.87	2.37	0.67	1.98	3.75	0.30	0.28	0.45	u
	2	0.19	2.31	−0.16	0.04	2.93	−0.05	0.04	0.93	u
	3	1.77	1.81	0.28	2.27	2.51	0.20	0.25	0.72	m
	4	2.72	1.76	−0.06	2.77	2.61	−0.13	0.10	0.76	m
	5	1.26	1.87	0.37	1.56	2.88	0.10	0.01	0.78	u
	6	1.52	1.59	0.15	1.45	2.39	−0.03	−0.33	0.75	u
	7	1.65	2.16	0.40	1.61	2.44	−0.02	−0.30	0.93	u
	8	3.37	1.32	−0.02	3.31	2.13	−0.03	0.04	0.64	m
	9	3.13	1.26	−0.05	3.11	2.00	−0.01	0.10	1.06	m
	10	1.85	1.75	0.14	2.06	2.43	0.09	0.12	0.90	u
Ms	1	0.56	1.89	0.29	0.99	2.86	0.15	0.42	0.74	
	2	1.32	1.97	0.13	1.36	3.06	0.01	−0.05	0.73	
	3	2.02	2.19	0.05	2.05	3.38	0.01	−0.03	0.70	
Ak	1	1.46	1.65	0.27	1.70	2.30	0.10	−0.08	0.71	
	2	1.98	1.72	0.09	2.11	2.48	0.05	0.05	0.76	
	3	1.09	1.33	−0.14	0.51	2.39	−0.25	−0.56	0.61	cc
	4	0.01	2.16	−0.49	−0.40	3.12	−0.13	0.10	0.76	cc
D	1	0.25	2.28	−0.56	−0.78	3.87	−0.27	−0.23	0.73	
	2	0.53	1.91	−0.23	0.09	3.35	−0.13	0.30	0.74	
TkW	1	1.97	1.57	−0.10	1.88	2.22	−0.04	−0.05	0.84	
Tk	1	0.16	2.13	−0.69	−1.36	3.51	−0.43	−0.59	0.55	p
	2	−0.98	2.48	−0.39	−1.51	3.23	−0.16	−0.16	0.47	p
	3	0.04	2.23	−0.66	−0.90	3.11	−0.30	−0.49	0.73	p
	4	2.98	1.39	0.00	2.98	2.03	0.00	0.32	0.93	p
	5	0.06	2.31	−0.38	−0.58	3.50	−0.18	−0.18	0.66	s
	6	0.21	2.24	−0.61	−0.80	3.30	−0.30	−0.43	0.64	s
	7	0.61	2.06	−0.50	−0.34	3.24	−0.30	−0.53	0.78	s
	8	−0.10	2.90	−0.73	−1.74	4.37	−0.37	−0.41	0.47	s
S	1	2.37	1.81	−0.16	2.22	2.64	−0.06	−0.02	0.72	
	2	2.44	1.86	−0.22	2.18	3.90	−0.07	0.00	0.24	
	3	1.93	2.05	−0.20	1.70	4.36	−0.05	0.06	0.19	
	4	2.07	1.84	−0.15	1.89	2.86	−0.06	0.02	0.67	
	5	1.63	2.29	−0.10	1.33	4.52	−0.07	0.03	0.22	
	6	2.48	1.86	−0.29	2.04	2.90	−0.15	0.15	0.75	
	7	1.60	2.66	−0.11	1.44	3.76	−0.04	−0.01	0.48	
	8	0.72	2.34	0.25	1.08	4.71	0.07	0.22	0.13	
	9	2.65	1.70	−0.26	2.23	3.61	−0.12	−0.17	0.33	
	10	1.64	2.11	−0.11	1.49	3.19	−0.05	0.19	0.82	
	11	2.03	2.04	0.34	2.58	2.98	0.18	0.17	0.77	
Kt	1	0.83	1.33	0.00	0.65	2.82	0.07	0.18	0.98	u
	2	0.96	1.60	−0.66	2.35	2.90	0.48	0.08	0.88	u
Ty	1	1.15	1.72	0.28	1.43	2.45	0.11	0.27	0.73	u
	2	2.27	1.93	−0.18	2.06	2.79	0.08	−0.01	0.51	l
	3	2.59	1.64	−0.22	2.43	2.41	−0.07	0.11	0.73	l
	4	2.43	2.19	−0.18	2.16	3.14	−0.09	0.03	0.59	l
	5	0.47	2.69	0.41	1.12	3.64	0.18	0.31	0.49	u
	6	0.37	2.74	0.42	1.10	3.85	0.19	0.28	0.46	u
	7	0.04	2.07	0.30	−0.02	3.08	−0.02	0.58	0.78	u
	8	3.27	1.35	−0.59	3.20	2.03	−0.04	0.22	0.89	l
	9	0.87	1.50	0.26	1.15	2.39	0.12	0.25	1.35	u
	10	0.27	1.50	0.48	0.64	2.61	0.14	0.39	0.84	o

Table 7. (Continued)

Sp.	no.	$Md\phi$	Q'	Q''	$M\phi$	$\sigma\phi$	$\alpha\phi$	$\alpha_{2}\phi$	$\beta\phi$	Remark
Km	1	0.20	1.97	−0.93	−0.97	3.00	−0.39	−0.21	1.17	1929
	2	0.29	1.86	−0.84	−0.77	3.00	−0.35	−0.10	1.10	1929
	3	0.47	1.55	−0.58	−0.36	2.88	−0.29	0.16	0.98	1929
	4	0.06	2.60	−1.07	−1.26	3.39	−0.39	0.33	0.53	1929
	5	0.17	2.55	−1.02	1.26	3.56	−0.40	−0.03	0.73	1929
	6	−0.30	3.02	−1.08	−2.06	3.99	−0.44	0.05	0.67	1929
	7	0.33	1.48	−0.62	−0.65	3.64	−0.37	−0.16	1.21	H.-shaped-cr.-fl
	8	0.20	2.11	−0.82	−0.83	3.09	−0.33	0.05	0.91	Kurumizaka-fl
	9	0.22	1.72	−0.58	−0.77	3.09	−0.32	−0.20	0.80	H.-shaped-cr.-fl
	10	0.50	1.94	−0.61	−0.23	3.60	−0.20	0.03	0.74	H.-shaped-cr.-fl
Tw	1	0.29	1.81	1.68	0.33	2.81	0.01	0.16	0.59	
	2	2.04	2.15	0.29	2.58	3.18	0.18	0.22	0.57	
	3	0.53	2.37	0.24	0.91	3.71	−0.10	0.17	0.56	
	4	2.13	1.99	0.48	2.53	2.63	0.15	0.38	1.18	
	5	1.56	2.63	0.19	1.83	3.71	0.07	0.17	0.46	
	6	1.84	2.77	0.40	2.46	3.74	0.17	0.13	0.50	
	7	2.57	2.05	0.21	2.97	2.87	0.14	0.21	0.56	
	8	3.08	2.45	0.16	3.36	3.35	0.08	0.03	0.54	
	9	0.10	2.15	−0.30	0.14	3.31	0.01	0.29	0.73	
	10	1.89	2.32	0.70	2.47	3.60	0.16	0.10	0.52	
	11	3.02	2.29	−0.09	3.01	3.18	−0.05	−0.02	0.63	
	12	0.88	2.40	0.25	1.41	3.87	0.14	0.24	0.57	
	13	0.11	2.41	−0.25	−1.70	3.80	−0.16	0.15	0.71	
	14	0.06	2.25	−0.21	0.10	3.50	0.05	0.36	0.70	
	15	0.75	3.19	0.42	1.70	4.36	0.22	0.42	0.51	
	16	2.53	2.12	0.10	2.87	2.93	0.12	0.18	0.61	
	17	0.82	3.14	−0.23	0.72	3.49	−0.03	0.17	0.67	
	18	1.07	2.39	0.20	1.25	3.82	0.05	0.14	0.57	
	19	2.68	2.41	0.13	2.58	3.61	−0.03	0.15	0.54	
	20	0.22	2.59	0.07	0.59	3.65	0.10	0.23	0.43	o
	21	−1.83	2.15	0.38	−1.17	3.09	0.21	0.52	0.50	o
	22	1.18	1.75	0.03	1.18	2.69	0.00	−0.13	0.96	o
Os	1	1.57	1.82	0.04	2.08	2.80	0.18	0.11	0.79	
Hd	1	0.66	2.60	0.57	3.50	3.69	0.77	0.74	1.06	
Tz	1	1.37	1.86	0.59	2.34	2.71	0.40	0.58	0.82	
On	1	1.18	1.59	0.17	1.20	3.05	0.07	0.20	0.76	
	2	2.97	2.44	−0.44	1.31	4.24	−0.39	−0.45	0.41	
	3	1.96	2.68	0.59	3.58	4.13	0.41	0.35	0.63	
Hj	1	0.66	1.31	−1.13	0.29	2.19	−0.17	−0.17	0.67	
	2	0.84	1.86	0.18	2.81	2.86	−0.10	0.18	0.83	
Nm	1	0.07	2.33	−0.66	−0.94	3.91	−0.26	−0.26	0.63	
Nn	1	−1.46	3.83	0.34	−0.32	5.02	0.23	0.54	0.47	s
	2	0.03	2.71	−0.66	−0.71	4.10	−0.18	−0.12	0.60	p
	3	0.10	2.48	−0.74	−0.29	3.74	−0.10	0.00	0.68	p
	4	0.93	1.63	1.00	2.03	2.55	0.43	0.33	0.69	p
	5	1.43	2.22	0.46	0.93	4.38	0.12	−0.20	0.51	p
	6	−0.05	3.01	−0.38	−0.82	4.16	−0.19	−0.05	0.47	p
Th	1	2.25	1.52	0.00	2.34	2.16	0.05	0.32	1.26	
Hr	1	−0.53	2.18	−0.24	−0.88	3.09	−0.11	−0.03	0.59	l
	2	−0.67	2.23	−0.29	−1.03	3.00	−0.11	−0.03	0.58	l
	3	4.10	1.65	0.15	4.44	2.54	0.13	0.53	0.81	l
	4	0.97	1.70	−0.21	0.52	2.86	−0.16	0.51	0.80	u

Table 7. (Continued)

Sp.	no.	$Md\phi$	Q'	Q''	$M\phi$	$\sigma\phi$	$\alpha\phi$	$\alpha_2\phi$	$\beta\phi$	Remark
KS	1	1.58	1.89	0.22	1.01	4.01	−0.14	0.03	0.55	m
	2	0.73	1.84	0.14	0.44	2.86	−0.10	0.01	0.68	l
	3	0.22	2.27	−0.28	−0.38	3.63	−0.16	0.03	0.59	l
	4	0.96	1.70	0.09	0.71	3.26	−0.08	0.07	1.62	l
My	1	0.28	3.07	−0.76	−1.05	4.27	−0.31	−0.41	0.60	
	2	0.28	2.59	−0.36	−0.85	4.32	−0.26	−0.32	0.54	
	3	−0.98	3.03	−0.28	−1.39	4.24	−0.10	−0.16	0.59	
	4	0.63	2.61	−0.47	−0.43	3.96	−0.27	−0.42	0.51	
	5	−0.03	3.05	−0.56	−0.92	4.06	−0.22	−0.25	0.49	
	6	0.14	2.30	−0.15	−0.05	3.36	−0.06	−0.13	0.95	
	7	0.47	3.09	−0.74	−0.89	4.31	−0.32	−0.28	0.46	
	8	0.78	2.79	−0.21	−0.24	4.35	−0.12	−0.17	0.51	
	9	0.47	2.30	−0.27	−0.05	3.45	−0.15	−0.22	0.63	
	10	0.74	2.47	−0.39	−0.42	4.18	−0.28	−0.39	0.62	
	11	0.28	2.53	−0.42	−0.54	3.76	−0.22	−0.37	0.59	
Am	1	0.81	1.53	0.58	1.19	2.56	0.15	0.05	0.85	lp
	2	0.70	1.54	0.34	0.89	2.76	0.07	0.01	0.81	lp
	3	0.86	2.02	−0.26	0.33	3.23	0.11	0.00	0.57	lp
	4	1.17	1.84	0.42	1.48	2.92	0.10	0.13	0.74	lp
	5	1.96	1.24	1.47	2.33	2.30	0.16	0.33	0.53	lp
	6	0.40	1.58	−0.20	0.06	2.69	−0.13	−0.14	0.80	lp
	7	0.39	1.48	0.21	0.44	2.84	0.02	0.24	0.85	lp
	8	0.67	1.67	−0.07	0.70	3.00	0.01	0.11	0.79	lp
	9	0.74	1.62	0.02	0.56	2.74	−0.07	0.08	0.88	lp
	10	0.66	1.86	0.11	0.90	3.17	0.08	0.14	0.63	lp
	11	1.20	1.78	0.51	1.98	2.83	0.27	0.27	0.85	lp
	12	1.41	1.61	0.40	1.87	2.39	0.19	0.19	0.97	lp
	13	1.80	1.88	0.08	1.95	1.71	0.09	0.73	0.71	lp
	14	1.17	1.35	0.35	1.66	2.68	0.18	0.30	0.94	lp
	15	1.20	1.45	0.39	1.69	2.24	0.22	0.50	1.09	lp
	16	3.60	1.63	0.52	4.33	2.45	0.30	0.64	0.69	lp
	17	0.18	2.07	−0.36	−0.29	3.36	0.14	0.02	0.72	up
	18	0.70	2.17	−0.15	0.30	3.67	−0.12	0.01	0.68	up
	19	0.79	1.77	0.12	0.70	3.48	−0.03	0.01	0.75	up
	20	0.13	2.25	−0.58	−0.70	3.30	−0.25	0.02	0.72	up
	21	0.33	1.20	−0.28	−0.05	3.29	−0.11	0.16	0.87	up
	22	0.67	1.38	0.20	0.88	2.25	0.09	0.14	1.44	up
	23	0.75	1.26	−0.02	0.44	2.19	−0.14	−0.19	0.75	up
	24	0.52	2.07	−0.41	−0.01	3.06	−0.17	−0.15	0.66	Oiwake-fl
	25	−1.30	2.74	−0.13	−1.26	3.59	0.01	0.20	0.49	Oiwake-fl
	26	−0.48	2.87	−0.44	−1.17	3.94	−0.17	−0.12	0.57	Oiwake-fl
	27	−3.00	3.19	0.32	−2.31	4.03	0.17	0.26	0.39	Oiwake-fl
	28	−1.85	3.28	0.19	−2.05	4.30	−0.05	−0.02	0.87	Oiwake-fl
	29	0.10	2.66	−0.71	−1.06	3.62	−0.31	−0.33	0.47	Oiwake-fl
	30	2.77	1.13	−0.04	2.81	1.71	0.02	0.03	0.61	Oiwake-fl
	31	0.40	2.71	−0.68	−1.74	5.24	0.41	−0.16	0.25	Agatsuma-fl
	32	0.15	2.32	−0.29	−0.75	5.29	−0.26	−0.22	0.92	Agatsuma-fl
	33	0.46	1.89	−0.12	−0.45	3.15	0.00	−0.85	1.04	Agatsuma-fl
	34	0.30	2.07	−0.42	−0.26	3.46	−0.16	0.00	0.60	(Kambara-na)
	35	0.13	2.41	−0.80	−0.96	3.46	−0.32	−0.21	0.43	Shiraito-fl
	36	1.63	1.34	0.04	1.72	2.02	0.04	0.11	0.68	1958-XI-10-fl
	37	1.33	1.21	−0.20	1.05	2.33	−0.12	−0.01	0.66	1958-XI-10-fl
	38	0.26	1.66	−0.24	−0.01	3.45	−0.08	0.02	0.14	1958-XI-10-fl
Hn	1	0.52	1.76	−0.07	0.40	3.09	−0.02	0.20	0.84	p
	2	0.83	1.55	0.11	1.04	2.57	0.08	0.33	0.94	p
	3	0.24	1.12	0.02	0.24	1.69	0.00	0.44	1.08	p
	4	0.60	1.90	0.29	1.15	2.88	0.19	0.51	0.72	p

Table 7. (Continued)

Sp.	no.	$Md\phi$	Q'	Q''	$M\phi$	$\sigma\phi$	$\alpha\phi$	$\alpha_{2\phi}$	$\beta\phi$	Remark
Hn	5	0.62	1.37	0.07	0.67	2.08	0.02	0.62	1.14	p
	6	0.46	1.98	−0.09	0.57	3.13	0.02	0.34	1.76	p
	7	0.07	1.78	−0.41	−0.38	2.71	−0.16	0.38	1.06	p
	8	0.10	2.50	−0.38	−0.10	3.97	−0.05	0.16	0.63	s
	9	0.21	1.90	0.01	0.27	2.81	0.02	0.13	0.41	s
	10	−0.28	2.98	0.20	0.44	3.81	0.19	0.48	0.70	s
	11	−2.12	3.25	−0.65	−3.28	4.22	−0.27	−0.20	0.43	cc
	12	−1.93	3.00	−0.38	−2.74	4.36	−0.19	−0.10	0.44	cc
	13	−0.53	2.34	−0.40	−1.29	3.59	−0.21	−0.27	0.65	cc
KF	1	−1.42	3.50	−0.18	−1.71	4.76	−0.06	0.24	0.48	
	2	−1.25	3.48	−0.16	−1.64	4.39	−0.09	0.06	0.36	
	3	−2.36	2.88	0.39	−1.70	3.93	0.17	0.24	0.52	
	4	−1.03	1.75	0.00	0.15	2.79	0.32	0.62	0.77	
	5	−1.11	0.95	0.35	−0.84	3.57	0.21	0.12	0.52	
	6	−1.33	3.07	0.02	−1.11	4.16	0.05	0.20	0.46	
	7	−0.24	3.36	−0.27	−0.30	4.57	−0.01	0.16	0.50	
	8	−1.47	2.79	0.04	−1.09	3.93	0.10	0.22	0.53	
	9	−0.67	2.42	−0.29	−1.09	3.24	−0.13	0.01	0.35	
	10	−2.73	2.66	0.56	−1.76	3.47	0.28	0.55	0.37	
As	1	3.92	1.93	−0.16	3.77	2.85	−0.03	0.23	0.91	
	2	3.68	1.59	0.11	3.70	2.48	−0.01	0.49	1.55	
Ai	1	1.67	1.79	−0.02	1.52	2.88	−0.05	0.29	1.30	m
	2	0.98	2.30	−0.24	0.55	3.32	−0.13	0.17	0.81	m
	3	−0.57	1.85	−0.23	−0.78	2.60	−0.08	−0.21	0.76	
	4	3.77	1.70	−0.08	3.72	2.62	−0.02	0.15	1.14	
	5	1.52	1.75	0.26	1.97	2.54	0.18	0.33	0.81	u
	6	1.13	2.02	−0.11	0.60	3.30	−0.16	−0.02	0.75	m
	7	1.20	2.04	−0.16	0.56	3.39	−0.19	−0.15	0.59	m
	8	2.57	1.72	0.44	3.50	2.82	0.33	0.89	0.92	l
	9	1.67	2.71	−0.60	0.85	3.73	−0.21	0.09	0.66	l
	10	2.29	1.32	0.15	2.37	2.04	0.04	0.25	0.98	l
	11	1.62	1.47	−0.11	1.44	2.19	−0.08	−0.22	1.23	m
	12	1.77	1.66	0.05	1.58	2.65	−0.07	−0.36	1.00	m
	13	1.63	1.70	0.00	1.27	2.87	−0.13	−0.09	1.00	m

value of α_ϕ is zero. On the other hand, in a skewed distribution, the mean departs from the median. If the size distribution is skewed towards smaller phi values (coarser diameters), the skewness measure α_ϕ is positive, and conversely α_ϕ is negative for the size distribution skewed towards higher phi values (finer diameters), and the larger the values the stronger the degree of asymmetry. The measure of primary skewness α_ϕ is related to the moment skewness α_3 of statistics by the approximate relationship, $\alpha_3=6\alpha_\phi$. The secondary skewness $\alpha_{2\phi}$ is another measure of the departure of the curve from normal distribution. It is most sensitive to skew properties within the tails of the size distribution of the deposit, and also serves as a check on the continuity of the skew properties of the size distribution. The measure of kurtosis β_ϕ is that of the degree of peakness. For a normal distribution β_ϕ has a values

Table 8. Ranges of parameter values in a single unit of pyroclastic flows.

Volc.	Md_ϕ	M_ϕ	σ_ϕ	α_ϕ	$\alpha_{2\phi}$	β_ϕ	
Kc	1.77~ 3.37	2.27~ 3.31	1.99~2.61	−0.13~ 0.20	0.04~ 0.25	0.64~1.06	m
Kc	0.19~ 1.85	0.04~ 2.06	2.38~3.75	−0.05~ 0.30	−0.33~ 0.28	0.45~0.74	u
Ms	0.56~ 2.02	0.99~ 2.05	2.86~3.38	0.01~ 0.15	−0.05~ 0.41	0.70~0.74	
Ak	1.46~ 1.98	1.70~ 2.11	2.30~2.48	0.05~ 0.10	−0.08~ 0.05	0.71~0.76	
Ak	0.01~ 1.09	−0.40~ 0.51	2.39~3.12	−0.25~−0.13	−0.56~ 0.10	0.61~0.76	cc
D	1.91~ 2.28	−0.78~ 0.09	3.35~3.87	−0.27~−0.13	−0.23~−0.30	0.73~0.74	
TkW	1.97	1.88	2.22	−0.04	−0.05	0.84	
Tk	−0.98~ 0.16	−1.51~−0.90	3.11~3.50	−0.43~−0.16	−0.59~ 0.16	0.47~0.73	p
Tk	−0.10~ 0.61	−1.74~−0.34	3.24~4.37	−0.37~−0.18	−0.53~ 0.18	0.47~0.78	s
S	0.72~ 2.46	1.08~ 2.58	2.64~4.71	−0.15~ 0.18	−0.17~ 0.22	0.13~0.77	
Kt	0.83~ 0.96	0.65~ 2.35	2.82~2.90	−0.07~ 0.48	0.08~ 0.18	0.88~0.98	
Ty	0.27	0.64	2.61	0.14	0.39	0.84	o
Ty	2.27~ 3.27	2.06~ 3.20	2.03~3.14	−0.09~ 0.08	−0.01~ 0.22	0.51~0.89	l
Ty	0.04~ 1.15	−0.02~ 1.15	2.39~3.85	−0.02~ 0.18	0.25~ 0.58	0.46~1.35	u
Km	−0.30~ 0.47	−2.06~−0.36	2.88~3.99	−0.44~−0.29	−0.21~ 0.33	0.53~1.17	
Km	0.20~ 0.50	−0.83~−0.23	3.06~3.64	−0.37~−0.20	−0.20~ 0.05	0.74~1.21	o
Tw	−1.83~ 1.18	−1.17~ 1.18	2.69~3.65	0.00~ 0.21	−0.13~ 0.52	0.43~0.96	o
Tw	−0.11~ 3.08	−1.70~ 3.36	2.63~4.36	−0.16~ 0.18	−0.16~ 0.22	0.46~1.18	
Os	1.57	2.08	2.80	0.18	0.11	0.79	
Hd	0.66	3.50	3.69	0.77	0.74	1.06	
Tz	1.37	2.34	2.71	0.40	0.58	0.82	
On	1.18~ 2.97	1.20~ 3.58	3.05~4.24	−0.39~ 0.41	−0.45~ 0.35	0.41~0.76	
Hj	0.66~ 0.84	0.29~ 0.56	2.19~2.81	−0.17~−0.10	−0.17~ 0.18	0.67~0.83	
Nm	0.07	−0.94	3.91	−0.26	−0.26	0.63	
Nn	−1.46	−0.32	5.02	0.23	0.54	0.47	s
Nn	−0.05~ 1.43	−0.82~ 2.03	2.55~4.38	−0.19~ 0.43	−0.20~ 0.33	0.47~0.69	p
Th	2.25	2.34	2.16	0.05	0.32	1.26	
Hr	−0.67 −0.53	−1.03~−0.88	3.00~3.09	−0.11	−0.03	0.58~0.59	l
Hr	0.92	0.52	2.86	−0.16	0.51	0.80	u
KS	0.22~ 1.58	−0.38~ 1.01	2.86~4.61	−0.14~−0.10	0.01~ 0.77	0.55~1.62	
My	−0.98~ 0.78	−1.05~ 0.24	3.36~4.35	−0.32~−0.06	−0.42~−0.13	0.46~0.95	
Am	0.39~ 1.96	0.33~ 2.33	1.71~3.17	−0.13~ 0.27	−0.14~ 0.73	0.53~1.09	l
Am	0.13~ 0.79	−0.70~ 0.88	2.19~3.67	−0.25~ 0.14	−0.19~ 0.16	0.68~1.44	u
Am	−3.00~ 0.52	−2.31~−0.01	3.06~4.30	−0.31~ 0.17	−0.33~ 0.26	0.39~0.87	O
Am	0.13	−0.96	3.46	−0.32	−0.21	0.43	S
Am	0.15~ 0.46	−1.74~−0.26	3.15~5.24	−0.26~ 0.41	−0.85~ 0.00	0.25~1.04	A
Am	0.26~ 1.63	−0.01~ 1.72	2.02~3.45	−0.12~ 0.04	−0.01~ 0.11	0.14~0.68	
Hn	0.07~ 0.83	−0.38~ 1.15	1.69~3.13	−0.16~ 0.19	0.20~ 0.62	0.72~1.76	p
Hn	−0.28~ 0.21	−0.10~ 0.44	2.81~3.97	−0.05~ 0.19	0.13~ 0.48	0.03~0.70	s
Hn	−2.12~−0.53	−3.28~−1.29	3.59~4.36	−0.27~−0.19	−0.27~−0.10	0.43~0.65	cc
KF	−2.73~−0.24	−1.76~ 0.15	2.79~4.76	−0.13~ 0.32	0.01~ 0.62	0.35~0.77	
As	3.68~ 3.92	3.70~ 3.77	2.48~2.85	−0.03~−0.01	0.23~ 0.49	0.91~1.55	
Ai	1.67~ 2.57	0.85~ 3.50	2.04~3.73	−0.21~ 0.33	0.09~ 0.89	0.66~0.98	l
Ai	1.13~ 1.77	0.55~ 1.97	2.19~3.39	−0.19~ 0.18	−0.36~ 0.33	0.59~1.30	m

of 0.65, and if the distribution is less peaked than normal, β_ϕ is greater than this value. Conversely, values of β_ϕ less than 0.65 indicate that the distribution is more peaked than normal.

Summary of Results

The results of mechanical analyses of the pyroclastic flow deposits are summarized as follows.

Table 9. Data of parameters of the particle size distribution of pyroclastic fall deposits

Sp.	no.	$Md\phi$	Q'	Q''	$M\phi$	$\sigma\phi$	$\alpha\phi$	$\alpha_2\phi$	$\beta\phi$	Remark
Kc	11	1.14	0.75	0.11	1.28	1.21	0.11	0.72	0.46	
	12	3.32	0.75	0.26	3.50	1.22	0.15	0.91	0.29	
	13	−1.98	1.36	0.24	−1.70	2.03	0.14	0.69	0.94	
Ms	4	−2.23	1.83	0.33	−1.81	2.41	0.15	0.17	0.35	
Ak	5	4.20	1.40	0.39	4.78	1.91	0.30	0.28	0.20	1959-X-3-fa
D	3	−1.08	1.06	0.20	−0.96	1.48	0.08	0.25	0.95	
	4	−2.06	1.71	0.46	−1.59	2.29	0.21	0.51	0.63	
S	12	−1.73	1.05	0.23	−1.49	1.54	0.16	0.36	0.54	
	13	2.57	0.82	−0.17	2.48	1.20	−0.08	0.40	1.22	
	14	−1.83	1.03	0.07	−1.75	1.43	0.07	0.22	0.45	
	15	−2.94	1.44	0.54	−2.22	2.18	0.33	0.41	0.27	
	16	−1.78	1.18	0.13	−1.64	1.68	0.09	0.43	0.81	
Ty	11	0.10	0.92	−0.80	−0.47	1.29	−0.44	−0.64	0.55	
	12	0.32	1.08	−0.87	−0.33	1.54	−0.42	−0.33	0.56	
Km	11	−4.73	0.53	−0.10	−4.73	0.73	0.00	0.89	1.23	1929-fa
	12	−4.32	0.87	0.59	−3.70	1.47	0.42	1.12	0.85	
Tw	23	−1.61	1.61	0.02	−1.45	2.22	0.07	0.53	0.89	
	24	−4.21	0.86	0.67	−3.65	1.25	0.45	1.15	0.80	
	25	−1.19	1.05	0.02	−1.22	1.51	−0.02	0.10	0.54	
	26	−1.74	1.40	−0.05	−1.78	1.96	−0.20	−0.09	0.44	
Nn	7	−2.98	0.80	0.38	−2.61	1.28	0.30	0.74	0.69	
Hr	5	−3.70	0.95	0.25	−3.37	1.42	0.24	0.87	0.83	u-fa
KS	5	−0.05	0.69	−0.57	−0.44	1.04	−0.42	−0.63	0.78	
Am	39	−4.25	1.27	0.96	−2.31	2.86	0.68	1.12	0.54	
	40	−3.29	1.03	0.39	−1.75	2.75	0.56	1.13	0.74	
	41	−1.34	1.38	0.25	−0.96	1.96	0.19	1.40	1.49	1783-fa
	42	−3.15	1.18	0.30	−2.80	2.02	0.17	0.25	0.48	1783-fa
	43	−2.73	1.41	0.52	−2.19	1.92	0.28	0.28	0.43	1783-fa
	44	−2.99	0.85	0.41	−2.60	1.37	0.29	0.52	0.79	1783-fa
	45	−3.95	0.44	−0.05	−3.94	0.71	0.01	0.44	1.68	1783-fa
	46	−1.16	1.20	−1.03	−1.16	0.96	0.00	−0.08	1.33	1958-XI-10-fa
	47	2.42	0.47	0.28	2.58	0.73	0.21	0.79	1.43	1958-XI-11-fa
KF	11	−2.23	0.72	0.32	−1.79	1.29	0.34	2.13	2.11	
F	1	−2.80	0.50	0.28	−2.62	0.84	0.21	1.07	1.52	
	2	−1.35	1.63	0.49	−0.56	2.48	0.32	0.89	0.87	
	3	−0.73	0.77	−0.17	−0.85	1.13	−0.11	0.16	0.52	
	4	−1.89	0.76	−0.08	−1.91	1.09	−0.02	0.13	0.51	
	5	−0.32	0.66	−0.39	−0.58	1.00	−0.26	−0.48	0.59	
	6	−2.42	0.74	0.43	−2.07	1.14	0.32	0.89	0.76	

1) Lack of sorting: Size characteristics of the pyroclastic flow deposits are quite particular, and make a distinct contrast with those of the pyroclastic fall deposits. The lack of sorting or ill-sorting of the pyroclastic flow deposits has been emphasized as a characteristic feature and a criterion for the recognition of them, contrasting with the well-sorted character of the pyroclastic fall deposits. This is clearly indicated

Table 10. Data of parameters of the particle size distribution of foreign pyroclastic flow deposits.

Sp. no.		$Md\phi$	Q'	Q''	$M\phi$	$\sigma\phi$	$\alpha\phi$	$\alpha_2\phi$	$\beta\phi$
SV	1	0.72	1.55	0.23	0.42	2.26	−0.14	−0.20	0.60
	2	−3.50	4.29	−0.19					
	3	−0.05	2.25	0.42	−0.62	3.25	−0.17	0.20	0.57
P	1	−4.75	4.74	0.92					
SS	1	2.65	1.74	0.13	2.74	2.67	0.03	0.00	0.64
CL	1	0.62	2.46	−0.39	−0.03	3.66	−0.18		
	2	0.38	3.31	−0.31	−0.67	4.24	−0.25		
	3	2.65	2.01	−0.01	2.04	3.04	−0.20		
	4	3.28	1.77	−0.17	2.98	2.57	−0.12		
NZA	1	3.50	1.15	−0.26	3.30	1.75	−0.11		
	2	3.25	1.58	−0.29	2.65	2.45	−0.25		
VTTS	1	2.80	1.90	−0.42	1.88	2.93	−0.32		

Table 11. Data of parameters of the particle size distribution of dry mud-flow deposits.

Sp. no.		$Md\phi$	Q'	Q''	$M\phi$	$\sigma\phi$	$\alpha\phi$	$\alpha_2\phi$	$\beta\phi$	Remark
Tk	9	0.73	1.81	−0.14	0.25	3.07	−0.16	−0.17	1.56	1926-mfl
	10	0.16	3.01	−0.43	−0.80	4.66	−0.21	−0.07	0.82	1926-mfl
	11	1.23	3.72	0.20	2.20	5.43	0.18	0.27	0.54	1926-mfl
	12	0.20	2.24	0.19	0.76	3.07	0.18	0.54	0.96	1926-mfl
	13	−3.82	2.12	0.63	−2.92	3.56	0.31	0.54	0.79	1926-mfl
Km	13	−0.37	2.10	−0.06	−1.30	3.28	−0.30	−0.31	0.73	
	14	0.15	2.72	−0.05	−0.76	3.99	−0.23	−0.21	0.62	
	15	−1.53	3.96	0.09	−1.09	4.29	0.10	0.21	0.58	
Z	1	−0.90	2.23	−0.21	−1.01	3.28	0.37	0.34	0.78	Sukawa-mfl
	2	−0.80	3.57	0.45	0.72	5.15	−0.30	0.43	0.37	Sukawa-mfl
G	1	−1.80	2.95	0.39	−0.64	4.37	0.27	0.36	0.40	Sasagawa-mfl
B	1	−0.38	3.45	−0.47	−1.36	4.59	−0.21	−0.19	0.44	1888-mfl
	2	−1.33	3.02	−0.08	−1.54	4.07	−0.05	−0.21	0.67	1888-mfl
	3	−3.75	4.41	0.17	−2.62	6·22	0.18	0.27	0.38	1888-mfl
Hn	14	−6.68	3.29	0.44	−5.27	4.51	0.31	0.64	0.45	

Table 12. Data of parameters of the particle size distribution of auto-brecciated lava flows

Sp. no.		$Md\phi$	Q'	Q''	$M\phi$	$\sigma\phi$	$\alpha\phi$	$\alpha_2\phi$	$\beta\phi$	Remark
Ak	5	−3.60	2.11	0.63	−2.60	3.04	0.33	0.54	0.21	cc-1 fl
Km	16	−1.14	3.84	−0.91	−2.34	4.94	−0.24	−0.13	0.31	
Z	3	−3.79	1.57	0.79	−2.57	2.52	0.46	0.45	1.21	Kanno-lfl
Nn	8	−3.60	3.08	−0.25	−3.53	4.26	0.02	0.06	0.44	Osawa-lfl
F	7	−3.01	1.93	0.61	−2.73	3.16	0.09	0.28	0.68	

in values of σ_ϕ, the parameter of standard deviation. Those of the pyroclastic flow deposits are generally larger than 2, while those of the

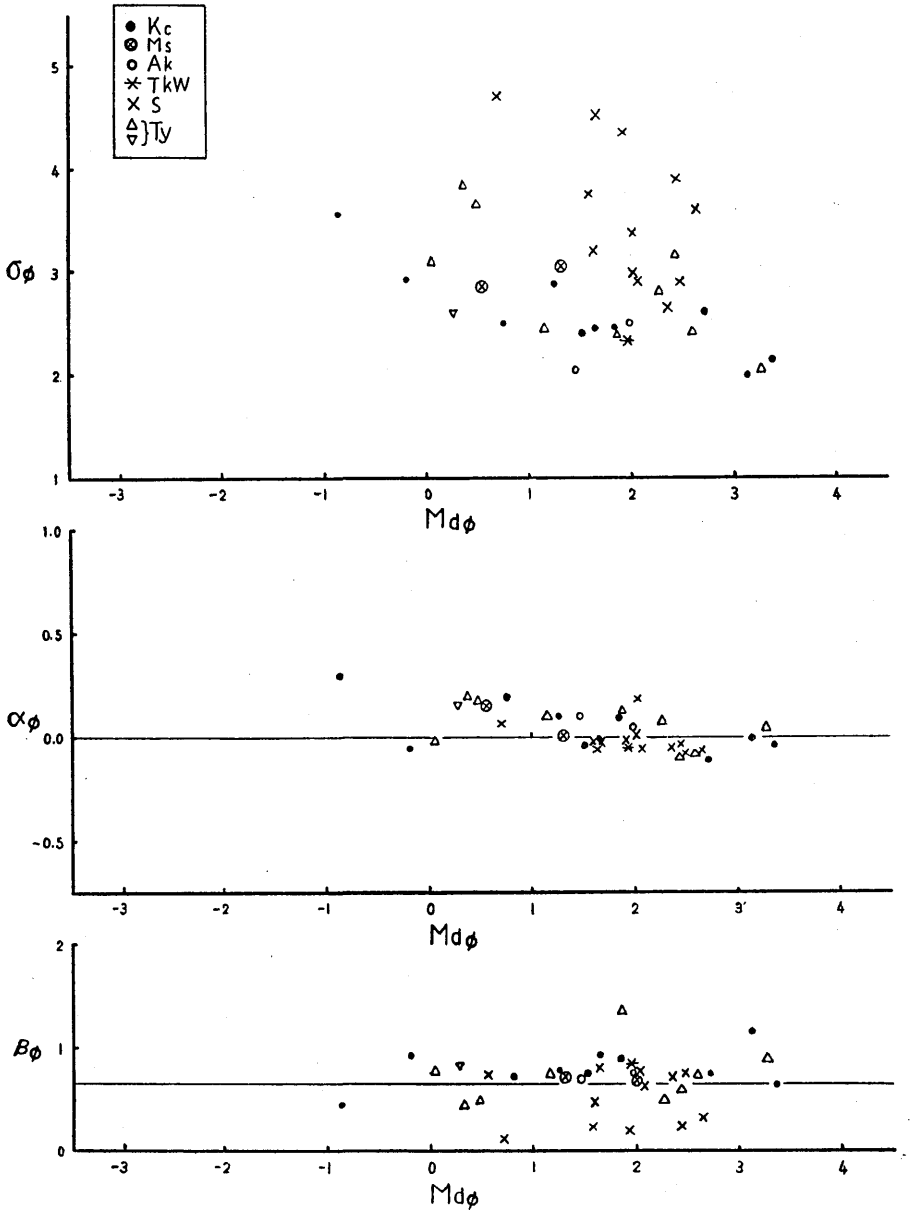

Fig. 6. Relation of values of $\sigma\phi$, $\alpha\phi$, and $\beta\phi$ to values of $Md\phi$.
Fig. 6a. The Krakatoa type ash-flows.

pyroclastic fall deposits are usually less than 2 (see Figs. 6a–6f).

The shape of the size distribution curve is quite different between these two types of pyroclastic deposits. The most distinct feature of

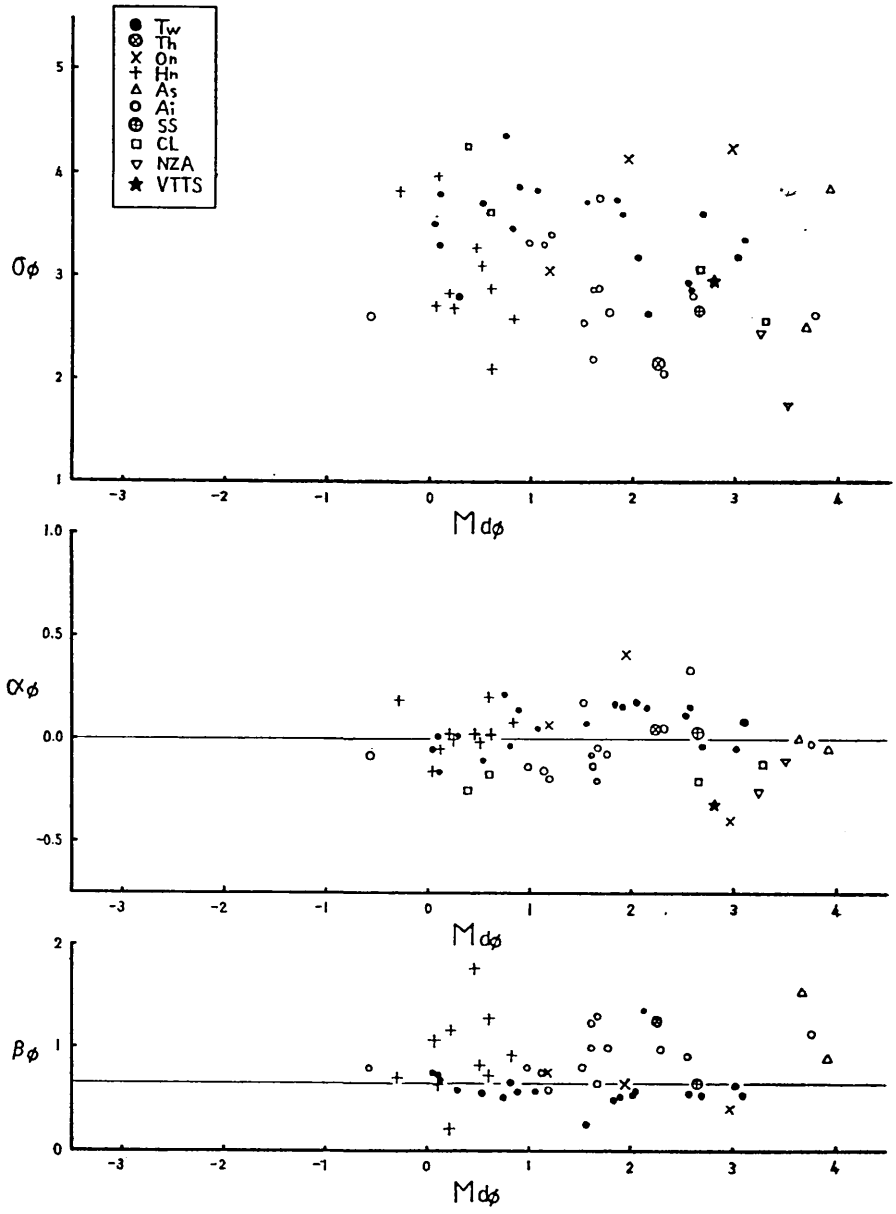

Fig. 6b. The Krakatoa type ash-flows.

the particle size distribution of the pyroclastic fall deposits is a pronounced modal peak and asymmetrical property skewed towards coarser

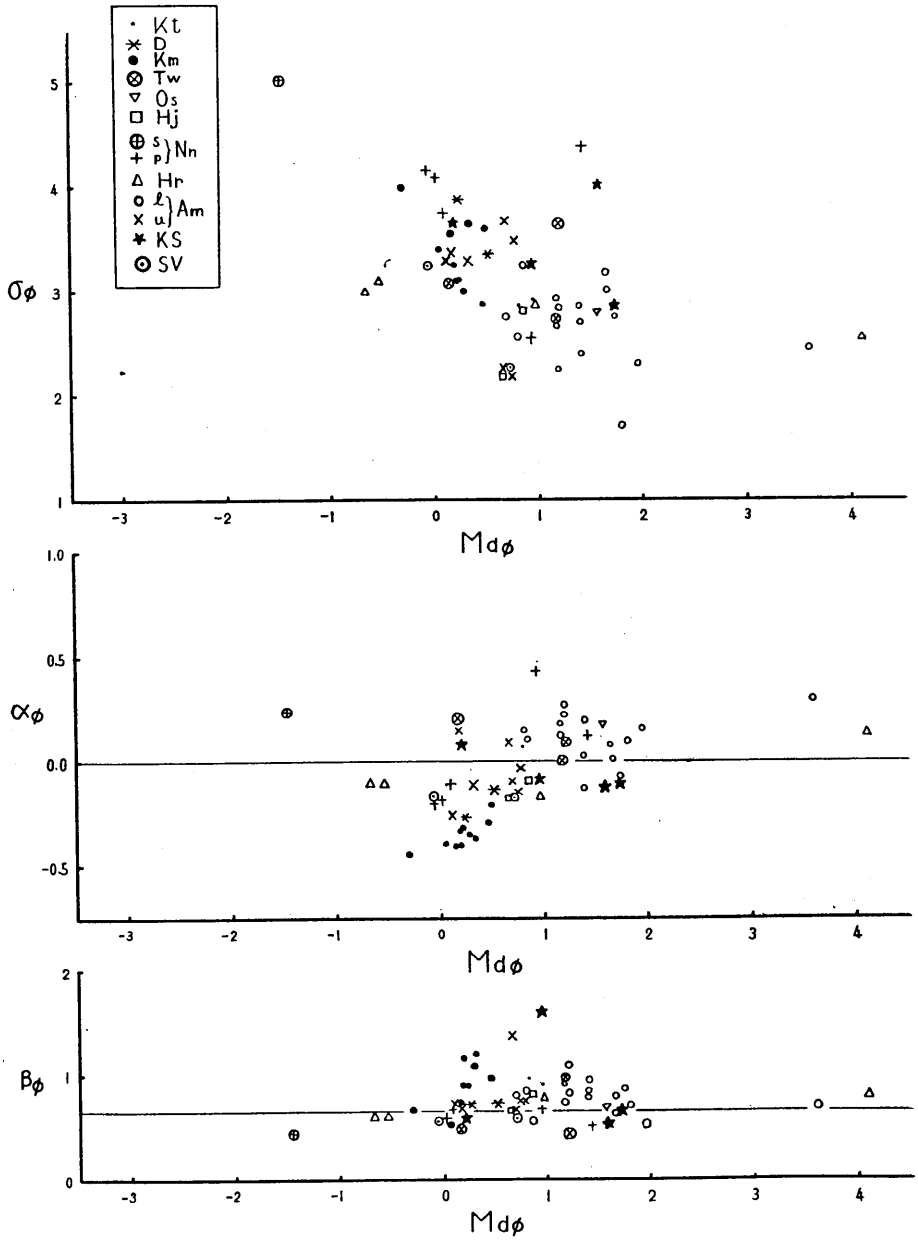

Fig. 6c. The St. Vincent type ash-flows.

diameters, being cut the tail in the coarser fractions, while the distribution curve of the pyroclastic flow deposits shows a gentle mode and

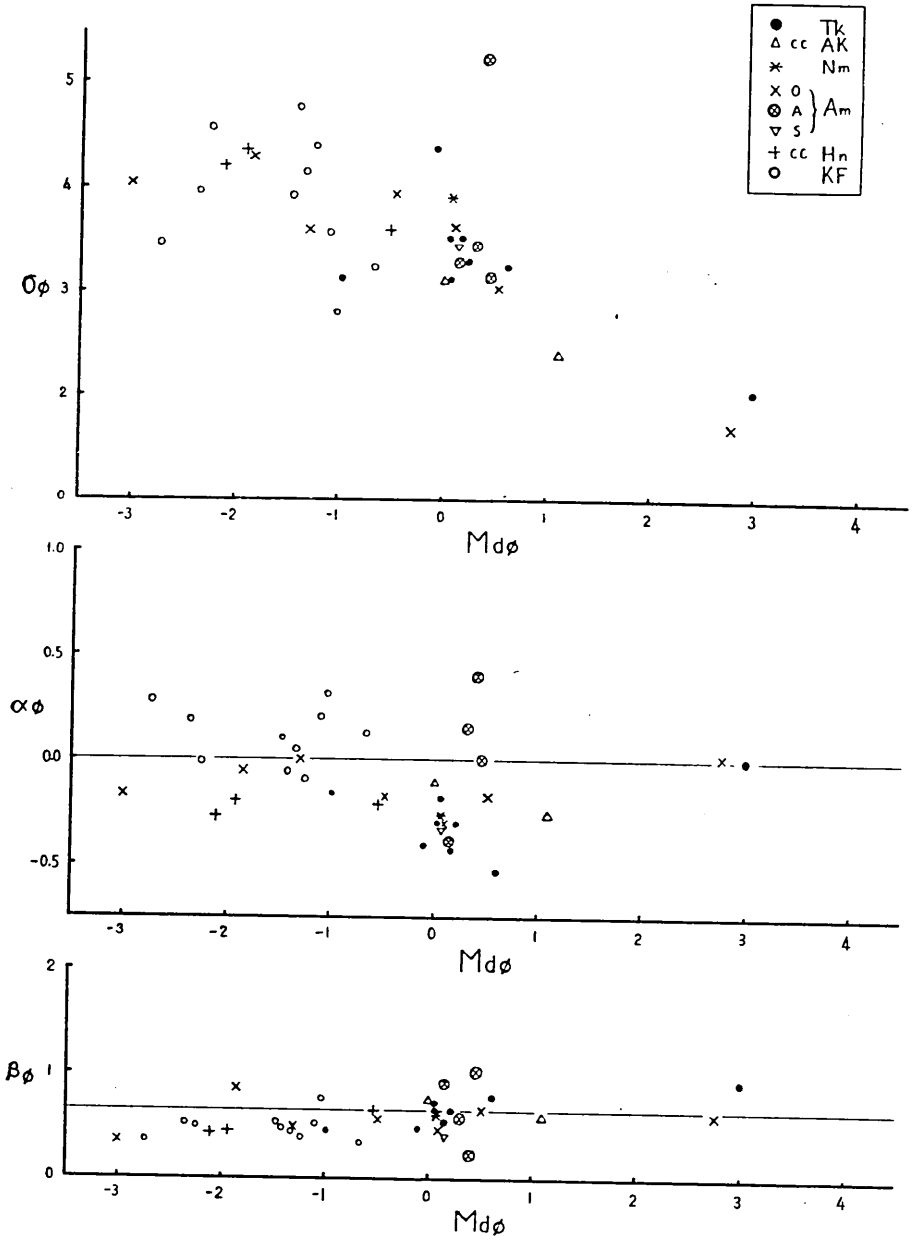

Fig. 6d. The Intermediate type pyroclastic flows.

marked tails at both ends of the curve. Consequently, the values of α_ϕ and $\alpha_{2\phi}$, the parameters of skewness, of the pyroclastic fall deposits tend to fall into a positive range, while those of the pyroclastic flow

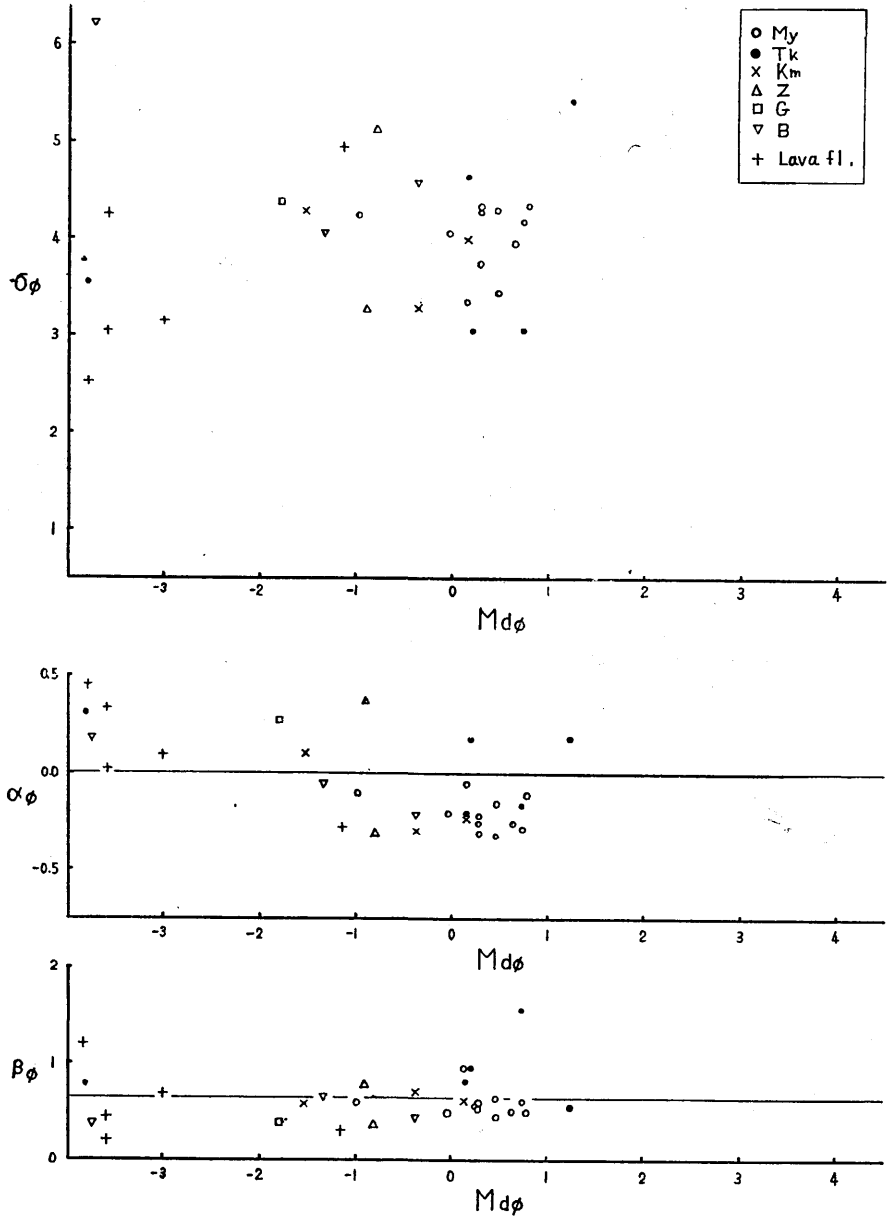

Fig. 6e. The nuées ardentes, dry mud-flows, and auto-brecciated lava flows.

deposits scatter in both possitive and negative ranges (see Figs. 6a–6f). The weight per cent of the modal fraction in histograms of the size distribution of the pyroclastic fall deposits in one size unit in phi scale always exceeds 20 per cent and sometimes reaches 35 per cent. On the other hand, the mode of size distribution of pyroclastic flow deposits is usually not so peaked, and the weight per cent of the modal fraction on one size unit in phi scale is mostly less than 20 per cent, although

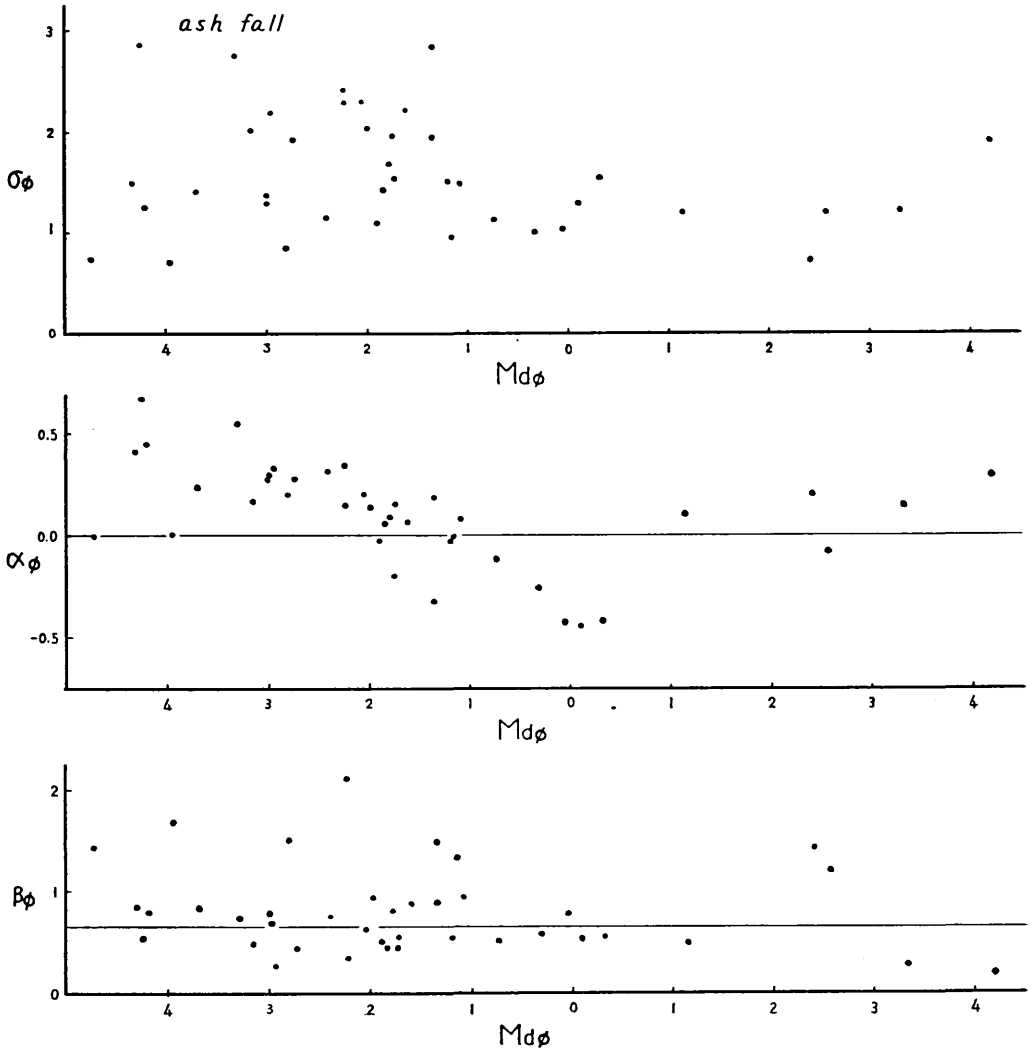

Fig. 6f. Pyroclastic falls.

there are a few exceptional cases having a mode that exceeds 20 per cent or 25 per cent (see Tables 4 and 5, and Figs. 11a–11c).

Ill-sorted size characteristics as mentioned here are always recognized in the pyroclastic flow deposits, whether closest to or far from the source. It is generally believed that they are caused by emplacement *en masse* from a turbulent flow or avalanche rather than by air fall. Most of the pyroclastic flow deposits, especially those near distal ends or in the uppermost layers of the flows, however, actually show some degree of sorting as well as some flowage features such as pumice swarms, rafted pumice and inclusion trains as mentioned by Kuno (1941) and Taneda (1954 and 1957). It may be presumed that the movement of the flows slows down before coming to rest. Sorting and flowage features are generally considered to be related directly to flowage of the laminar flow.

Some air-fall deposits in the vicinity of eruptive vents may show ill-sorted size characteristics, and are occasionally indistinguishable from the pyroclastic flow deposits. The regular grading of coarseness in both lateral and vertical sections is surely recognized in the air-fall deposits, however. Such grading of coarseness with distance from the source cannot be found in the pyroclastic flow deposits. Samples collected from thinly laminated air-fall pyroclastic deposits may also exhibit poorly sorted particle size distribution, which is due to the mixing of thin laminae of different coarseness. Such deposits may be readily distinguished from the pyroclastic flow deposits by other sedimentary features. Besides, ill-sorted features, several criteria of the pyroclastic flow deposits are recognized, e.g. topographic restriction on the distribution of deposits to valleys or other lows, the nearly level upper surfaces of deposits, some flowage features, retention of heat for long periods of time resulting in fumarolic activity, scorching of buried materials, welding and crystallization, flowage deformation, and incoration of surface debris by erosional agency of flows, as summarized by Smith (1960).

2) Homogeneity: Size characteristics of pyroclastic flow deposits are quite homogeneous. There is little variation among the size characteristics of every sample collected from a single unit of pyroclastic flow deposits. Consequently, values for every sort of parameter of particle size distribution remain a narrow range (see Table 8). Morever, similar homogeneity in the size characteristics is frequently found among various units of pyroclastic flow deposits discharged in different ages from a certain volcano. For instance, the ash-flow of the 1929 eruption and those of the previous eruptions of the Komagatake Volcano in Hokkaido

have the same size characteristics (see Fig. 3c). This indicates that similar eruptions of pyroclastic flows took place repeatedly on the Komagatake Volcano.

Homogeneity in size characteristics within a single unit of pyroclastic flow deposits always exists, irrespective of the magnitude of the unit. In ash-flow deposits of huge magnitude such as those surrounding the Krakatoa type calderas, usually comprising several units which represent various periods in eruptions separated by some time intervals, a tendency toward homogeneity in their size characteristics is found throughout the whole mass of the deposits. For example, in the ash-flow deposits of the Kutcharo, Toya, Towada, and Aira Volcanoes, such homogeneity in size characteristics is found (see Figs. 3a–u, 3c–m, 3d–u, and 3k–m). The deposits caused by repeated eruptions of pyroclastic flows of small magnitude, such as nuées ardentes of the Pelée type, usually consist of layers separated from each other by block accumulations, beds of ash, materials reworked by wind and water or minor erosional disconformities. In such deposits, homogeneity in size characteristics also exists. For example, every sample of the pyroclastic flow deposits of the Myoko Volcano shows the same size characteristics with each other (see Fig. 3g–l). Moreover, size characteristics of pyroclastic flow deposits in adjoining volcanoes exhibit some resemblance to each other. For example, among the deposits of ash-flows of the Asama, Haruna, Akagi and Nantai Volcanoes (see Figs. 3f–m, 3g–u, 3h–u and 3h–m), and between those of the Kutcharo and Akan Volcanoes, resemblance in size characteristics is found (see Figs. 3a–u and 3a–l).

3) Median diameters: Phi values of median diameters, Md_ϕ, vary within a wide range. Most of them, however, fall within a range of -2 to 4. This indicates that most of the pyroclastic flow deposits belong to the category of "ash flow deposits" defined by Smith (1960), which consist of 50 per cent or more in weight of ash and fine ash in terms of the Wentworth and Williams' size scale. Moreover, it may be possible to group Md_ϕ values in accordance with the subdivisions of types of pyroclastic flows. Md_ϕ values of the Krakatoa type ash-flow deposits, and perhaps those of the fissure eruption type ash-flow deposits, are generally within a range of 0 to 4 (see Figs. 6a and 6b), those of the St. Vincent type ash-flow deposits are within a range of 0 to 2 (see Fig. 6c), and those of the intermediate type pyroclastic flow deposits and the nuée ardente deposits are smaller than 1 (see Figs. 6d and 6e).

The regular variation of Md_ϕ values with distance from a source

can not be found. Values of Md_ϕ are almost constant throughout a single unit of pyroclastic flow deposits (see Figs. 7a, 7b and 7c). Whereas,

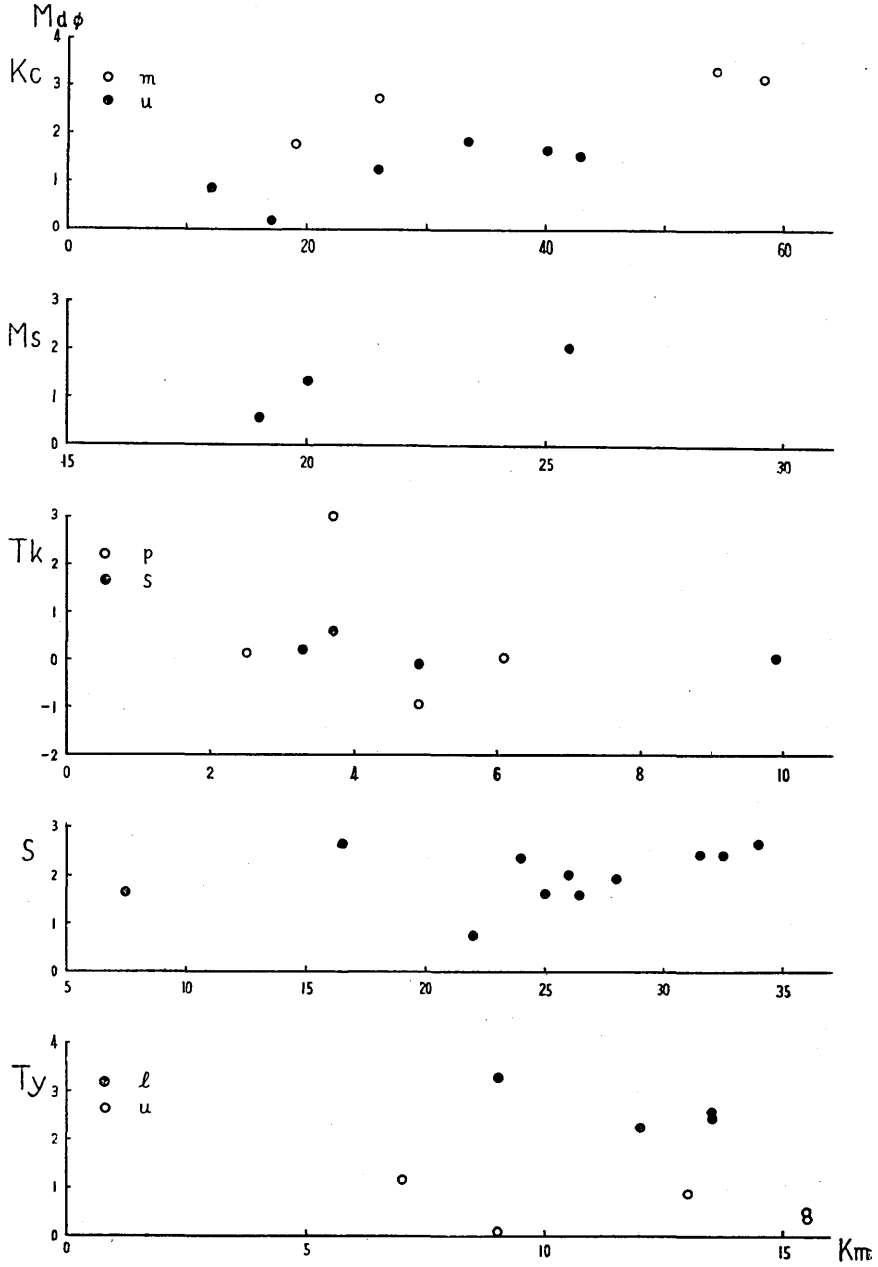

Fig. 7a. Relation of values of Md_ϕ and distances from the source.

other features, such as the roundness of particles and the proportions of lithic fragments or vesicular dust to the whole of the deposits, may vary within a single unit of pyroclastic flow deposits. For instance, it has

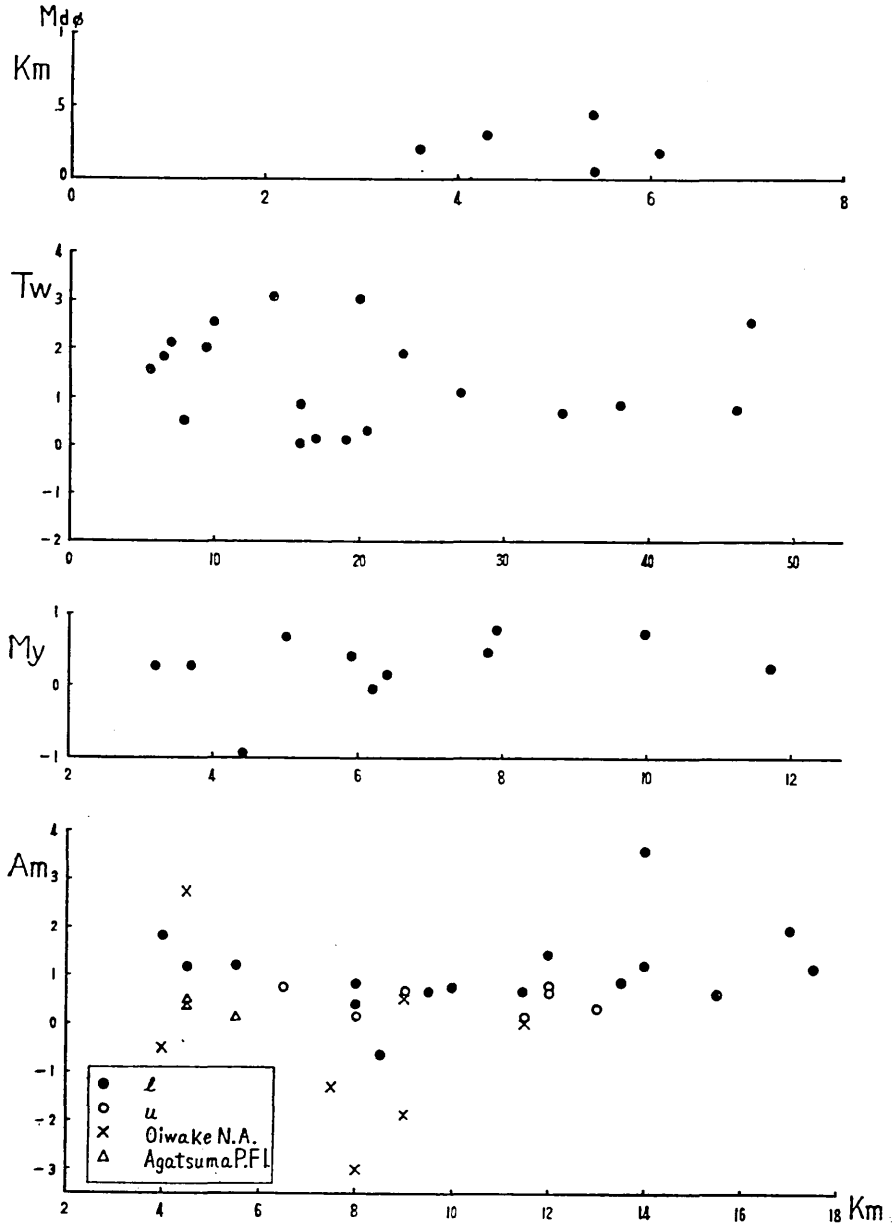

Fig. 7b. Relation of values of $Md\phi$ and distances from the source.

been clarified that fine dust in the Pelean deposits tends to increase in amount away from the parent dome. Detailed discussions on these respects are presented in the later chapters.

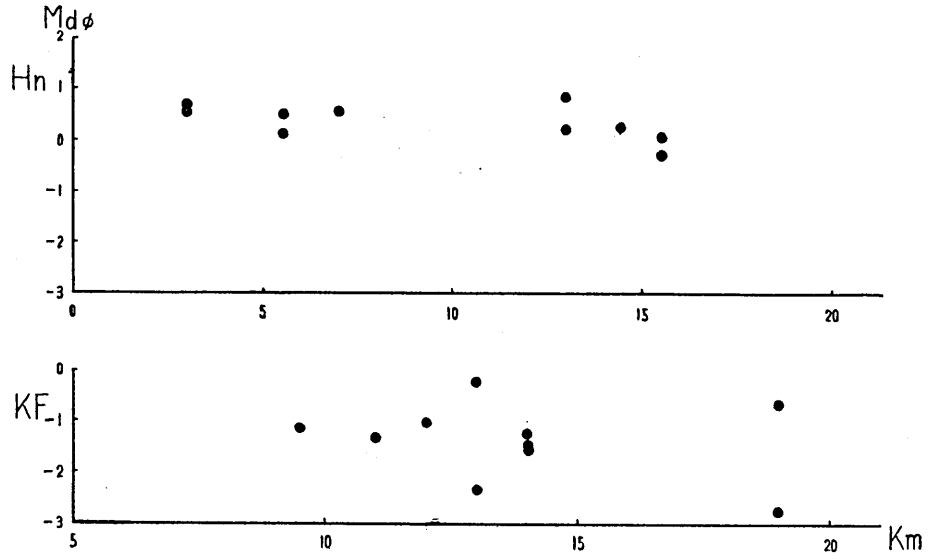

Fig. 7c. Relation of values of $Md\phi$ and distances from the source.

4) Shape of particle size distribution: The shape of the particle size distribution of every kind of pyroclastic flow deposit shows the resemblance to one another as a whole as clearly indicated in the diagrams of cumulative curves (see Figs. 3a–3k). Every curve has tailingout parts of both, in coarser and finer fractions, and a gentle mode in medium fractions. There is, however, a considerable range of variation within the framework of the cumulative curves. Values of Md_ϕ vary within a wide range as mentioned above, and values of σ_ϕ also vary considerably, being within a range of 2 to 5 in general (see Figs 6a–6e). Large values of σ_ϕ are usually due to the increase of the amount of coarse materials. Pyroclastic flow deposits consisting of a mixture of coarse blocks and fine ash usually show bimodal particle size distributions. The cumulative curves of particle size distribution of the pyroclastic flow deposits plotted on normal probability paper often show undulatory lines having two crests in the medium and coarse fractions, instead of smooth lines (see Fig. 8). A distinct sub-mode is found in the tailingout part of coarser fractions in the size distribution on histogram (see Figs. 11a–11c). Such a bimodal character is most conspicuous in

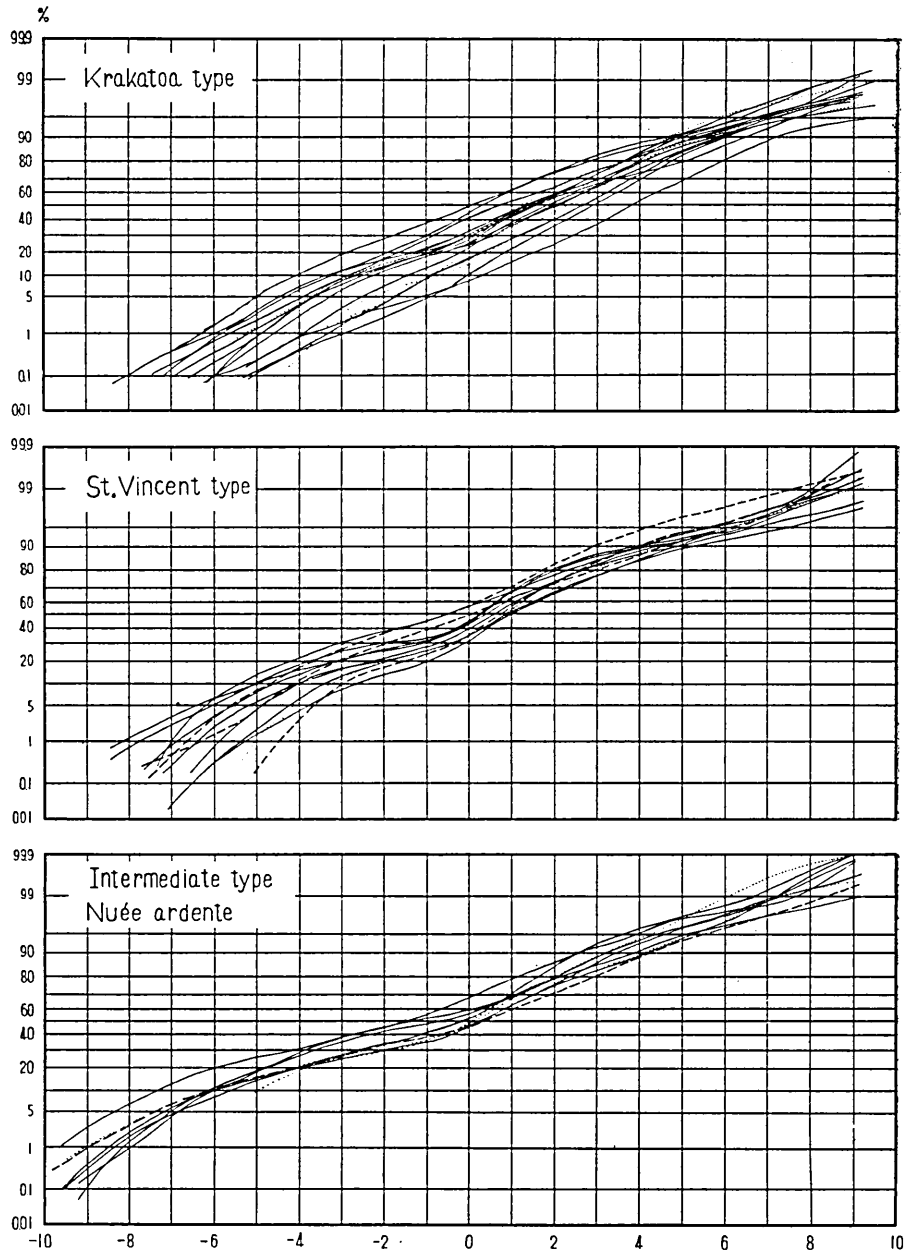

Fig. 8. Cumulative curves of the pyroclastic flow deposits plotted on normal probability paper. Solid lines are average curves of samples in a single unit of pyroclastic flow. Dotted lines are curves of one sample. Each curve represents one unit of flow. Broken lines in the middle figure represent the variety having an intermediate nature between the St. Vincent type ash-flows and dry mud-flows. A broken line in the lower figure is a curve of a nuée ardente.

the nuée ardente deposits and also in the intermediate type pyroclastic flow deposits. Moreover, a similar tendency towards bimodal size distribution is found in most deposits of the various types of pyroclastic flows, although the degree of the bimodal tendency may vary greatly. Values of σ_ϕ become large in proportion to the increase in bimodal tendency. Fine-grained ash-flow deposits, such as those of the fine-grained Krakatoa type ash-flows, the V.T.T.S. type ash-flows, and those settled from overriding clouds of expanding gas and dust of pyroclastic flows, generally show unimodal size distributions.

The skewness of the size distribution curves of all kinds of pyroclastic flow deposits varies in two senses, and values of α_ϕ and $\alpha_{2\phi}$ are scattered both in negative and positive ranges (see Figs. 6a–6e, and Table 8). In general, the pyroclastic flow deposits containing a large amounts of coarse materials such as those of the nuées ardentes and the intermediate type pyroclastic flows tend to show size distribution curves skewed towards finer diameters. The values of their skewness measures tend to fall within a negative range. For example,the pyroclastic flow deposits of the Myoko Volcano and those of the 1929 eruption of the Tokachi-dake Volcano have negative values for the skewness measures. Size distribution curves of every kind of pyroclastic flow deposit tend to be less peaked than the normal distribution curve. Values of β_ϕ in general tend to bear larger values than 0.65, although actually they scatter widely around the value 0.65 of normal (see Figs. 6a-e, and Table 8).

The main mode of medium fractions in size distribution curves of pyroclastic flow deposits is generally not peaked as sharply as that of air-fall deposits as already mentioned. The weight per cent of a modal fraction of one size unit in phi scale is usually less than 20 per cent (see Table 4). In some pyroclastic flow deposits, however, it attains to or exceedes 25 per cent. For example, in the ash-flow deposits of the Komagatake Volcano, it ranges from 19.0 to 27.8 per cent. In general, size distribution curves of the St. Vincent type ash-flow deposits exhibit such peaked main modes, in spite of their ill-sorting as indicated by large values of σ_ϕ. In the size distribution curves of the Krakatoa type ash-flow deposits, which show a general tendency toward a unimodal character, the mode is not peaked as sharply as in those of the St. Vincent type ash-flow deposits. The size distribution curves of the nuée ardente deposits and the intermediate type pyroclastic flow deposits show a dull main mode, contrasting with the peaked main mode of the St. Vincent type ash-flow deposits.

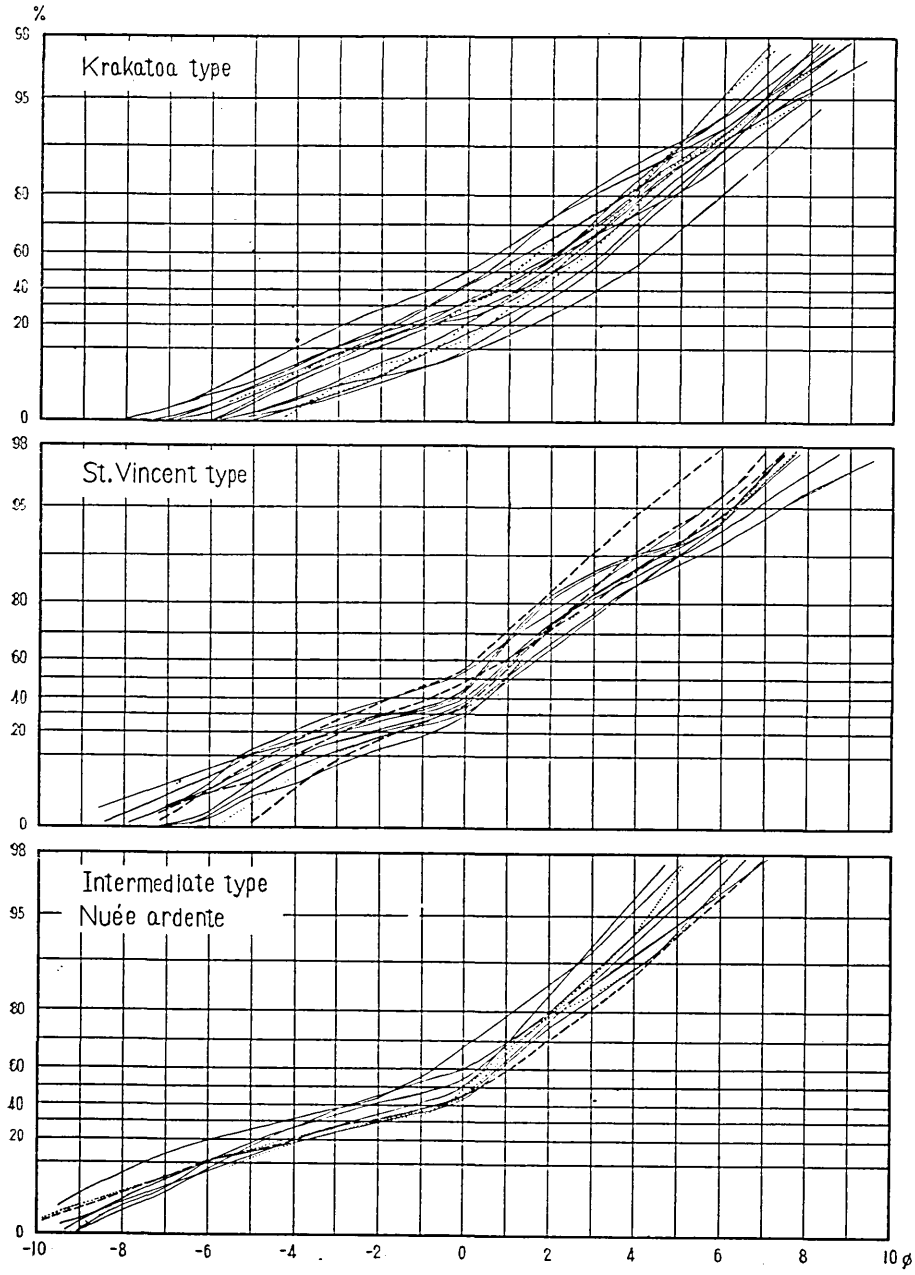

Fig. 9. Cumulative curves of the pyroclastic flow deposits plotted on Rosin law paper. The explanation of the curves is the same as in Fig. 8.

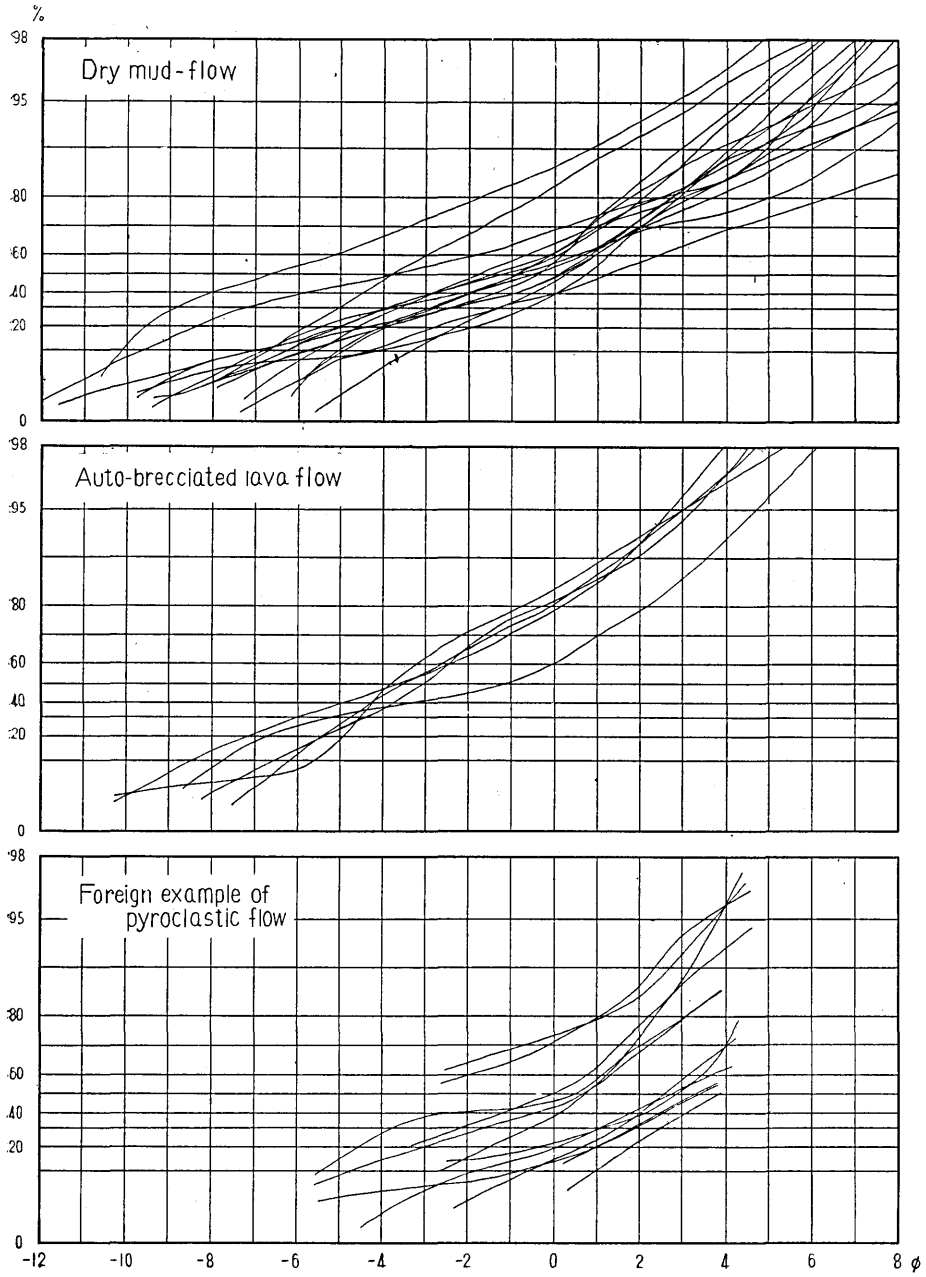

Fig. 10. Cumulative curves plotted on Rosin law paper. Upper: dry mud-flows, middle: auto-brecciated lava flows, lower: foreign examples of pyroclastic flows. Every line represents a curve of each individual sample.

Krumbein and Tisdel (1940) showed that the size distribution of the pumice flow deposits of the Crater Lake region conform to Rosin's law. Rosin's law was introduced by Rosin and Rammler in 1934, and reviewed by Bennett taking into consideration the degree of probability in 1936. It is expressed as $R=100\,e^{-(x/k)^n}$, where R is the weight per cent retained on a sieve of mesh x, e is the number 2.7188, and k and n are constants for any given material; k represents an average size and n represents a reciprocal for a measure of the spread of the curve. If any size distribution plotted in cumulative fashion forms a straight line on the special graph paper devised by Geer and Yancy (1938), that distribution conforms to Rosin's law. Rosin's law has been found to fit artificially crushed products of many kinds and sizes, although most of the available data are on coal. Krumbein and Tisdel believed that some materials, notably the products of weathering and certain peculiar sediments, such as boulder clay or till and nuée ardente (pyroclastic flow) deposits follow Rosin's law[26].

In reality, however, the cumulative curves of every kind of pyroclastic flow deposit plotted on Rosin law paper tend to show bent lines instead of straight ones (see Fig. 9). They exhibit three types of curves in accordance with the classification of pyroclastic flows. The Krakatoa type ash-flow deposits show gently concave curves, the St. Vincent type ash-flow deposits show wavy curves, and the intermediate type pyroclastic flow deposits and the nuée ardente deposits show curves broken into two nearly straight parts. The irregular shapes of the latter two types of curves are due to the bimodal characteristic of the size distributions as mentioned above. Undulatory curves of the St. Vincent type deposits have two crests in the lower and middle parts, which represent two distinct modes in coarse and medium fractions respectively on histograms or size frequency curves (see Fig. 11b). Curves of the intermediate type pyroclastic flow deposits and the nuée ardente deposits consist of two parts; the gently sloping lower part represents a sub-mode in coarse fractions and the steeply sloping upper part represents a main mode in medium fractions (see Fig. 11c). It may be expected that crushing

26) W. C. KRUMBEIN and F. W. TISDEL, "Size distribution of source rocks of sediments," *Am. Jour. Sci.*, **238** (1940), 296-305.

P. O. ROSIN and E. RAMMLER, "Die Kornzusammensetzung des Mahlgutes im Lichte der Wahrscheinlichkeitslehre," *Kolloid Zeits.*, **67** (1934), 16-26.

J. G. BENNETT, "Broken coal," *Jour. Inst. Fuel*, **10** (1936), 22-39.

M. R. GEER and H. F. YANCEY, "Expression and interpretation of the size composition of coal," *Am. Inst. Min. Met. Eng., Tech. Pub.*, **948** (1938).

processes, such as explosive disintegration and attrition during the ascent of frothing magma and during the flowage of discharged materials,

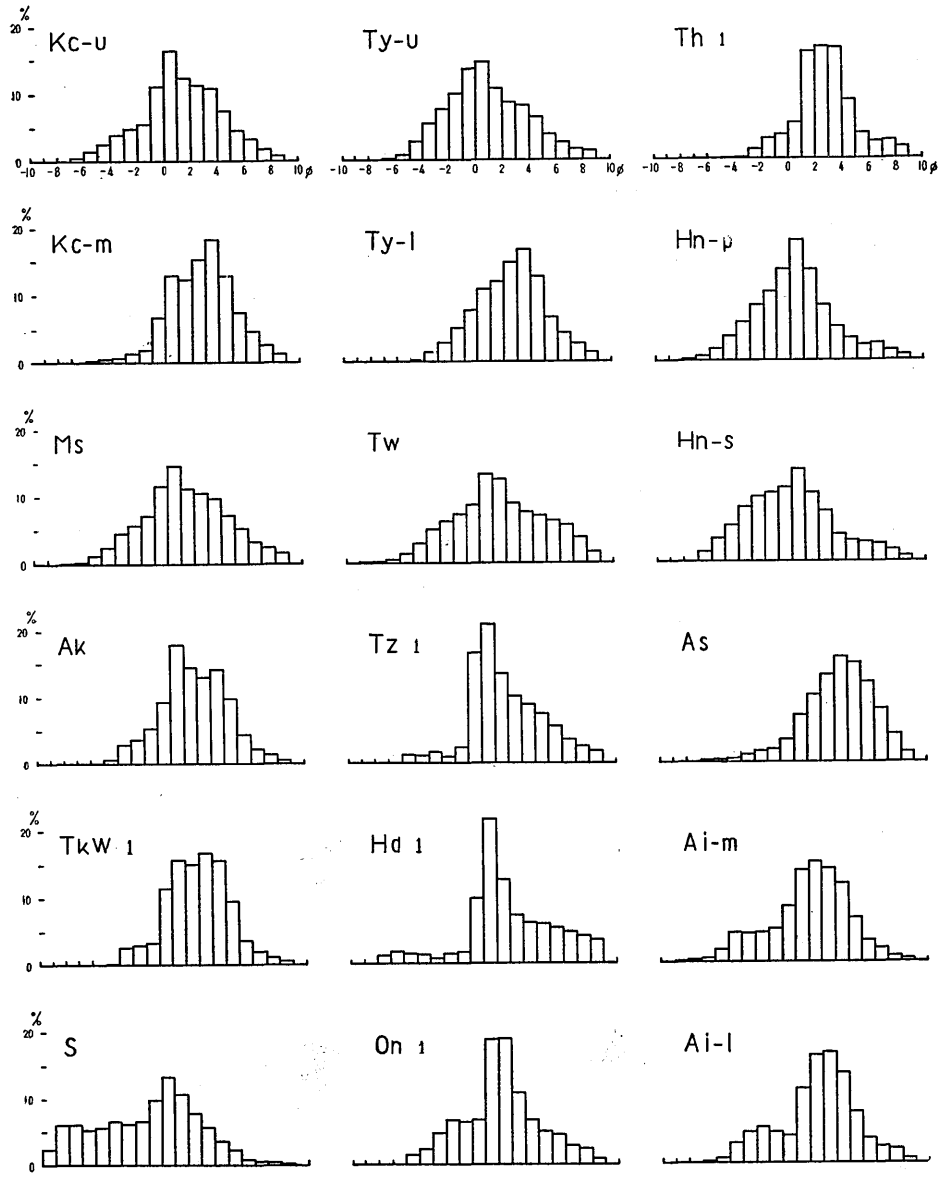

Fig. 11. Histograms of particle size distribution of the pyroclastic flow deposits. One which represents the individual result of only one sample is noted by its sample number. The others represent the average results of several samples.

Fig. 11a. Histograms of the Krakatoa type ash-flow deposits.

may produce size characteristics of pyroclastic flow deposits fitting to Rosin's law. Consequently, those size distributions uncompatible with Rosin's law may suggest the effectiveness of a sorting agency in the emplacement of pyroclastic flow deposits. Moreover, such variations in size distribution curves among various types of pyroclastic flow deposits as mentioned here may be due to differences in the mode of origin and

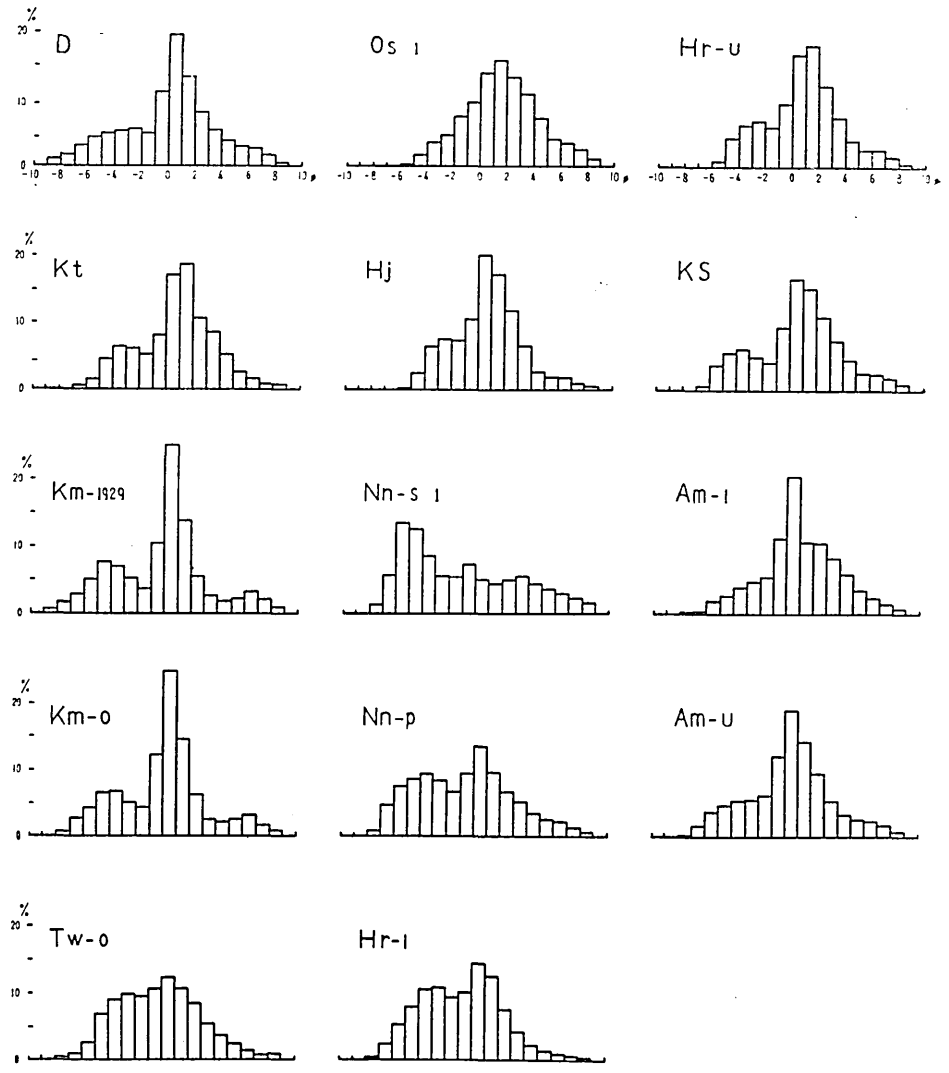

Fig. 11b. Histograms of the St. Vincent type ash-flow deposits and the deposits having an intermediate nature between pyroclastic flows and dry mud-flows.

mechanism of pyroclastic flows. Detailed discussions are presented in the later chapters.

5) Subdivisions of pyroclastic flow deposits based upon size characteristics: As mentioned above, the size distribution curves of the pyroclastic flow deposits exhibit characteristic forms in accordance with the types of flows. The size characteristics of the deposit produced by each type of pyroclastic flow are summarized as follows:

a) Fine-grained Krakatoa type ash-flow deposits and V.T.T.S. type ash-flow deposits: They consist exclusively of fine vesicular materials and show poorly sorted unimodal size distribution whose shape approaches the normal distribution curve. Cumulative curves of particle

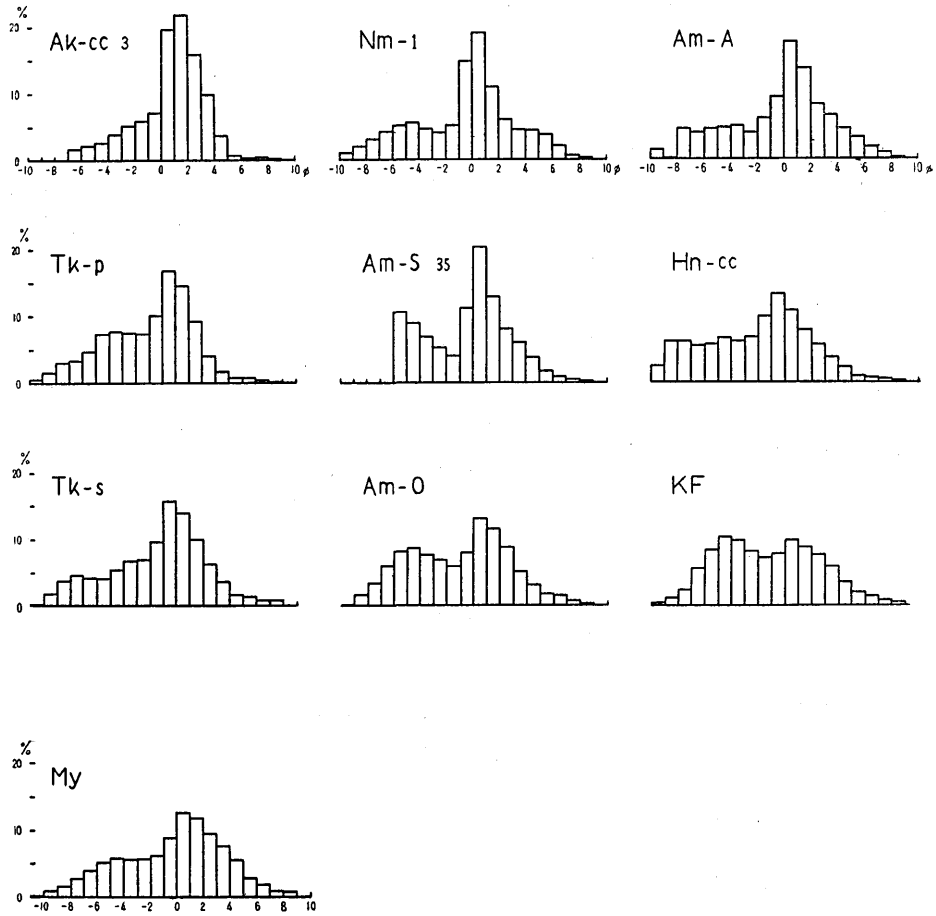

Fig. 11c. Histograms of the intermediate type pyroclastic flow deposits and the nuée ardente deposits.

size distribution plotted on normal probability paper form nearly straight lines (see Fig. 8-u). Cumulative curves plotted on Rosin law paper show gentle concave lines (see Fig. 9-u). A mode appears usually in the fraction of 1 to 2 or 2 to 3 in phi scale. Md_ϕ values are mostly within a range of 2 to 4. Values of skewness measures scatter in both positive and negative ranges. Values σ_ϕ are mostly within a range of 2 to 4.5. (See Figs. 6a, 6b and 11a.)

b) Medium-grained Krakatoa type ash-flow deposits: Md_ϕ values are usually larger than those of the former subdivision, being within a range of 0 to 2. Values of σ_ϕ are also mostly within a range of 2 to 4.5 as with those of the former subdivision. Values of skewness measures also scatter in both positive and negative ranges. Size distribution curves are similar to those of the former subdivision, but show a slight tendency towards bimodal characteristics. A main mode appears usually in the fraction of 0 to 1 or 1 to 2 in phi scale. A sub-mode in coarse fractions is quite feeble, differing in size distributions from those of the St. Vincent type ash-flow deposits and the intermediate type pyroclastic flow deposits. (See Figs. 6a, 6b, 8-u, 9-u and 11a.)

c) St. Vincent type ash-flow deposits: They show characteristic bimodal size distribution having a pronounced main mode in medium fractions and a sub-mode in coarse fractions. The main mode appears usually in the fraction of 0 to 1 in phi scale. Values of skewness measures tend to fall within a negative range, although they scatter actually in both positive and negative ranges. Md_ϕ values are within a range of 0 to 2, with a few exceptions. Values of σ_ϕ are within a range of 2 to 4.5 as in those of the former two subdivisions. Cumulative curves plotted both on normal probability paper and on Rosin law paper show wavy lines, indicating the characteristic bimodal property of size distribution. (See Figs. 6c, 8-m, 9-m, and 11b).

d) Intermediate type pyroclastic flow deposits: Size distribution curves always show a bimodal property. Main modes are not so sharply peaked as those of the St. Vincent type ash-flow deposits. They appear usually in the fraction of -1 to 0 or 0 to 1. A sub-mode appears in coarse fractions, and form a high percentage in weight to the whole of the size distribution. Md_ϕ values vary widely within a range of -3 to 1. Values of σ_ϕ are within a range of 3 to 5. Values of skewness measures tend to fall within a negative range, although they scatter around zero. There exists a minor variation in the size distribution curves among samples collected from a single unit of the flows, which

is due to the differences in the amount of coarse materials in the deposits. Cumulative curves plotted on normal probability paper show gently undulating lines. Those plotted on Rosin law paper show lines broken into two straight parts. (See Figs. 6d, 8-l, 9-l and 11c).

e) Nuée ardente deposits: The chaotic mingling of fragments of all sizes, graduating from large blocks to fine dust, is the most pronounced feature of the nuée ardente deposits. It is considered that they have similar size characteristics to those of the intermediate type pyroclastic flow deposits, although the writer could not obtain various examples of the nuée ardente deposits. The coarseness of the nuée ardente deposits may be remarkably large, and M_ϕ values may be sometimes less than -3, judging from the data on size characteristics of the deposits at Mt. Pelée and of the ancient deposits at St. Vincent (Hay, 1959), although those of the nuée ardente deposits of the Myoko Volcano remain exclusively within a range of 0 to 1.

6) Comparison of the size characteristics of dry mud-flow deposits and auto-brecciated lava flows: It is considered that the size characteristics of dry mud-flow deposits and laharic deposits are similar to those of pyroclastic flow deposits, but perhaps generally of coarser grain. There exist, however, some differences between these two types of deposits. In dry mud-flow deposits, homogeneity in size characteristics is rather unrecognizable. Size distribution curves are unstable and show large disparities with one another whithin a single unit of dry mud-flow deposits. They show a very flat shape having a dull mode in medium fractions and tailingout parts both in the coarser and finer fractions. Values of Md_ϕ vary greatly from sample to sample. Sorting is generally worse than in pyroclastic flow deposits. Values of σ_ϕ are within a range of 3 to 5. Bimodal property in size distribution is also found at times, but not as distinct as in pyroclastic flow deposits. It is possible to distinguish dry mud-flow deposits from pyroclastic flow deposits by other criteria. For instance, the former consist of various lithic fragments caused by the disintegration of pre-existing rock formations, while the latter consist mainly of porous essential fragments produced from frothing magma. The upper surface of dry mud-flow deposits is mostly undulating and shows a characteristic topography of flowed-mounds, contrasting with a nearly level surface of pyroclastic flow deposits.

The size characteristics of auto-brecciated parts of lava flows are also similar to those of pyroclastic flow deposits. In auto-brecciated lava flows, however, transition to solid parts of lava flows may be easily

discovered by a careful field survey. The homogeneity of size characteristics cannot be maintained even in a small portion of the bulk body. Size distribution curves are unstable and show large variations from sample to sample.

It may be possible to consider that both dry mud-flow deposits and auto-brecciated lava flows follow Rosin's law of crushing, for they are caused by the disintegration of solid or plastic materials. Their cumulative curves plotted on Rosin law paper appear to form roughly straight lines in general, although some of them tend to show irregular lines (see Fig. 10). Some dry mud-flow deposits show cumulative curves broken into two straight parts on Rosin law paper, suggesting some effectiveness in sorting during flowage. The writer considers that further detailed studies on the size characteristics of dry mud-flow deposits and auto-brecciated lava flows may reveal a closer conformity of their distribution curves to Rosin's law.

Roundness of Particles

It is well known that there is no regular variation in the coarseness of pyroclastic flow deposits with the distance from the source, as mentioned repeatedly. Some data, however, suggest an increase in the amount of fine vesicular materials in the deposits from the source to the distal ends of the flows. Some volcanologists have considered the agency of attrition during flowage to be responsible for the high proportion of fine ash in pyroclastic flow deposits. Williams (1957) stated that the size of pumice lumps bears no relation to the distance from the source although they are generally more rounded at the distal ends. The writer thinks that studies on the roundness of particles in pyroclastic flow deposits should supply important data in estimating the agency of attrition, which may take place on the way of ascent of effervescing magma, at the time of effusion, and during flowage of the flows. They offer some clues denoting the mechanism of the initiation and flowage of pyroclastic flows.

The writer conducted measurements of the roundness of particles on samples of pyroclastic flow deposits and also on those of preliminary pyroclastic falls which preceded the discharge of flows. The roundness of a particle is a measure of the curvature of the corners and edges expressed as a ratio to the average curvature of the particle as a whole. Actually it is more convenient to work with a two-dimensional figure rather than the three-dimensional object itself. In this case roundness is defined as the average radius of the curvature of the corners of a

particle image divided by the radius of the maximum inscribed circle drawn in a projection of the particle in a plane. Thus, roundness is expressed as $P=\sum(r_i/R)/N$, where r_i are the individual radii of the corners, N is the number of corners, and R is the radius of the maximum inscribed circle (Wadell, 1932)[27]. Wadell's method for measuring the roundness of a particle requires drawing an image of the particle at a standard magnification and determining the radii of the inscribed circle and of the edges and corners of the image, and from these data the value of roundness P is calculated. This method is fairly laborious and takes very much time. Therefore, the writer adopted Krumbein's rapid method (1941)[28]. The particle is compared with standard images of known roundness, redrawn from particles which were measured by Wadell's method. Scores or a hundred particles are measured, and the average value of roundness (PK) is calculated from these data. Statistical studies have shown that the average values (PK) agree well with Wadell's values (P). Particles are divided into size classes and the average roundness for each class size is determined separately. It has been already clarified that there is a marked correlation between the roundness and the particle size in natural clastic deposits, especially in those which have undergone considerable abrasion. The larger sizes of clastic materials are in general more rounded than the smaller grades[29]. Consequently, a comparison of roundness from sample to sample must be carried out in terms of a restricted range in size. The writer determined the average roundness in every kind of particle contained in pyroclastic flow deposits and preliminary air-fall deposits in the three size classes of 32–16 mm, 16–8 mm, and 8–4 mm in diameters. The values of average roundness (PK) are listed in Table 13 with the numbers of measured particles (N), the confidence ranges of average values with 95 per cent confidence coefficient (CR), and values of standard deviation (σ). Summary of the results are as follows :

1) It has been considered that particles in pyroclastic flow deposits,

27) Hakon WADELL, "Volume, shape, and roundness of rock particles," *Jour. Geol.*, **40** (1932), 443-451.

28) W. C. KRUMBEIN, "Measurement and geologic significance of shape, and roundness of sedimentary particles," *Jour. Sed. Petrol.*, **11** (1941), 64-72.

29) E. J. PETTIJOHN and A. C. LUNDHL, "Shape and roundness of Lake Erie beach sands," *Jour. Sed. Petrol.*, **13** (1943), 69-78.

R. D. RUSSELL and R. E. TAYLOR, "Roundness and shape of Mississippi River sands," *Jour. Geol.*, **45** (1937), 225-267.

Hakon WADELL, "Volume, shape and roundness of quartz particles," *Jour. Geol.*, **43** (1935), 250-280.

Table 13. Data on average values of roundness.

Sp. no.			32–16mm				16–8mm				8–4mm			
			PK	CR	N	σ	PK	CR	N	σ	PK	CR	N	σ
Kc	2	p	0.419	±0.122	8	0.137	0.433	±0.026	36	0.075	0.445	±0.019	92	0.093
		l	0.325	0.152	4	0.083	0.344	0.018	18	0.102	0.363	0.018	89	0.095
Kc	5	p									0.502	0.004	65	0.018
		l									0.432	0.017	19	0.033
Kc	6	p	0.456	0.020	9	0.024	0.466	0.011	94	0.053	0.436	0.012	114	0.065
		l					0.375	0.152	4	0.083	0.424	0.023	34	0.064
Kc	9	p									0.487	0.016	43	0.051
Ms	2	p	0.383	0.079	6	0.069	0.341	0.015	70	0.064	0.328	0.012	106	0.064
		l					0.300	0.020	8	0.071	0.311	0.016	96	0.076
Ak	1	p	0.375	0.073	8	0.083	0.453	0.017	45	0.053	0.373	0.017	132	0.098
		l					0.367	0.143	6	0.125	0.410	0.019	100	0.093
Ak	3	p	0.400	0.065	4	0.035	0.377	0.027	30	0.072	0.368	0.020	65	0.081
		s					0.325	0.036	16	0.065	0.333	0.016	104	0.083
		l									0.348	0.023	46	0.077
Ak	4	p	0.440	0.068	5	0.048	0.378	0.048	9	0.058	0.377	0.015	99	0.076
		s	0.364	0.044	7	0.044	0.358	0.018	33	0.049	0.347	0.012	101	0.062
		l	0.288	0.027	8	0.086	0.302	0.017	42	0.060	0.322	0.027	54	0.098
D	4	p	0.423	0.038	11	0.054	0.400	0.022	39	0.068	0.397	0.023	59	0.086
		se									0.387	0.023	38	0.070
		l					0.400	0.066	6	0.058	0.372	0.018	58	0.069
TkW	1	p					0.390	0.023	49	0.079	0.387	0.017	133	0.096
		l									0.380	0.088	10	0.117
Tk	1	p	0.425	0.080	4	0.043	0.400	0.025	31	0.067	0.368	0.016	90	0.076
		se	0.417	0.043	6	0.036	0.400	0.038	9	0.046	0.360	0.020	72	0.084
		l					0.325	0.057	16	0.103	0.338	0.012	114	0.065
Tk	4	p									0.308	0.034	24	0.081
		se									0.300	0.051	14	0.085
		l									0.357	0.105	7	0.105
Tk	6	s					0.304	0.030	25	0.072	0.260	0.016	84	0.073
		ds	0.260	0.067	5	0.049	0.297	0.021	32	0.059	0.308	0.014	120	0.079
		l					0.311	0.063	10	0.083	0.335	0.013	126	0.074
S	1	p					0.485	0.013	24	0.097	0.428	0.011	104	0.056
		l									0.350	0.037	34	0.104
S	6	p	0.450	0.124	5	0.089	0.488	0.024	56	0.087	0.476	0.009	173	0.060
Kt	1	p	0.413	0.054	8	0.060	0.431	0.020	74	0.085	0.378	0.018	93	0.087
		l	0.320	0.104	5	0.075	0.314	0.017	44	0.092	0.336	0.018	67	0.073
Ty	7	p					0.406	0.020	33	0.055	0.370	0.013	138	0.078
		l					0.340	0.035	30	0.092	0.332	0.016	96	0.071
Ty	8	p									0.378	0.032	18	0.063
		l									0.330	0.048	10	0.203
Ty	10	p					0.356	0.039	18	0.076	0.384	0.012	111	0.064
		l					0.367	0.050	15	0.087	0.344	0.012	115	0.062
Km	3	p	0.421	0.037	28	0.098	0.398	0.030	44	0.099	0.403	0.024	71	0.100
		se					0.390	0.097	10	0.013	0.389	0.011	28	0.086
		l					0.383	0.123	6	0.107	0.323	0.033	35	0.099
Km	4	p	0.457	0.037	23	0.083	0.437	0.026	46	0.087	0.404	0.011	115	0.061
		se					0.433	0.086	6	0.075	0.405	0.047	21	0.100
		l									0.417	0.079	6	0.069
Km	7	p	0.421	0.037	24	0.085	0.434	0.019	59	0.074	0.402	0.016	93	0.095
		se	0.280	0.056	5	0.040	0.360	0.046	15	0.080	0.398	0.020	82	0.091
		l					0.343	0.105	7	0.105	0.379	0.020	56	0.077
Km	8	p	0.435	0.044	17	0.084	0.394	0.018	72	0.076	0.391	0.020	56	0.071
		se									0.367	0.041	24	0.094
		l									0.380	0.040	25	0.094
Tw	15	p	0.500	0.130	4	0.071	0.522	0.020	58	0.079	0.445	0.019	86	0.090
		l	0.329	0.070	7	0.070	0.381	0.034	36	0.100	0.360	0.061	82	0.087

Table 13. (Continued)

Sp. no.			32−26mm				16−8mm				8−4mm			
			PK	CR	N	σ	PK	CR	N	σ	PK	CR	N	σ
Tw	16	p					0.453	±0.018	18	0.034	0.438	±0.011	81	0.049
		l									0.350	0.033	23	0.077
Tw	17	p	0.456	±0.040	9	0.048	0.435	0.015	60	0.060	0.433	0.014	85	0.064
		l					0.330	0.083	10	0.110	0.394	0.017	70	0.074
Tw	21	p					0.408	0.025	26	0.062	0.399	0.014	94	0.068
		se					0.333	0.054	6	0.046	0.326	0.022	62	0.086
		l					0.380	0.080	10	0.105	0.373	0.024	49	0.083
Os	1	p					0.442	0.035	26	0.084	0.421	0.011	126	0.063
		l					0.384	0.037	19	0.074	0.398	0.023	80	0.102
Hj	2	p	0.441	0.047	11	0.067	0.453	0.017	44	0.057	0.443	0.014	87	0.064
		dp					0.408	0.107	6	0.093	0.402	0.024	42	0.076
		l					0.347	0.031	30	0.083	0.391	0.022	80	0.099
On	2	p	0.384	0.033	19	0.067	0.420	0.018	66	0.072	0.385	0.013	128	0.075
Nm	1	p	0.394	0.038	17	0.073	0.412	0.018	59	0.069	0.405	0.012	147	0.074
		se					0.360	0.111	5	0.080	0.360	0.055	15	0.095
		c					0.325	0.019	8	0.066	0.357	0.022	56	0.082
		l					0.317	0.079	6	0.069	0.335	0.026	34	0.072
Nn	1	p					0.422	0.045	23	0.102	0.398	0.026	61	0.100
		c									0.292	0.050	12	0.076
		l	0.333	0.077	9	0.094	0.377	0.035	26	0.085	0.384	0.019	75	0.083
Nn	6	p	0.429	0.029	21	0.063	0.379	0.020	53	0.071	0.348	0.013	103	0.065
		l									0.339	0.046	13	0.074
Th	1	p					0.426	0.035	23	0.079	0.400	0.018	120	0.099
		l									0.323	0.056	13	0.089
Hr	2	p	0.400	0.039	14	0.066	0.432	0.017	66	0.070	0.374	0.017	105	0.088
		c					0.358	0.046	19	0.094	0.358	0.016	89	0.075
		l	0.390	0.063	10	0.083	0.338	0.022	42	0.069	0.354	0.017	119	0.092
Hr	4	p	0.458	0.028	24	0.064	0.433	0.019	51	0.068	0.420	0.009	137	0.053
		l					0.300	0.088	5	0.063	0.342	0.011	150	0.070
KS	3	p									0.463	0.043	16	0.078
		l					0.309	0.036	22	0.079	0.321	0.013	116	0.073
My	1	p	0.322	0.064	9	0.079	0.330	0.031	20	0.064	0.340	0.017	81	0.075
		c	0.333	0.144	3	0.047	0.343	0.090	7	0.090	0.314	0.021	42	0.068
Am	1	p	0.416	0.029	19	0.059	0.404	0.023	50	0·080	0.374	0.017	97	0.082
		se									0.390	0.041	10	0.054
		l					0.346	0.040	13	0.063	0.351	0.016	89	0.077
Am	6	p	0.400	0.130	4	0.071	0.436	0.026	31	0.070	0.376	0.018	82	0.081
		l					0.282	0.033	17	0.062	0.333	0.020	60	0.077
Am	17	p	0.458	0.050	12	0.076	0.400	0.020	67	0.081	0.397	0.014	102	0.071
		se	0.368	0.014	8	0.047	0.372	0.044	18	0.087	0.346	0.016	93	0.077
		l					0.318	0.034	22	0.078	0.327	0.017	71	0.073
Am	20	p	0.415	0.054	13	0.086	0.422	0.015	85	0.068	0.378	0.016	100	0.078
		se									0.370	0.021	60	0.082
		l					0.378	0.045	23	0.102	0.357	0.019	72	0.080
Am	24	s	0.375	0.019	8	0.066	0.367	0.022	46	0.072	0.362	0.012	109	0.060
		l					0.300	0.019	46	0.063	0.320	0.013	115	0.070
Am	27	s	0.388	0.017	8	0.059	0.379	0.022	38	0.066	0.343	0.015	63	0.058
		ds					0.365	0.054	17	0.102	0.308	0.013	97	0.064
		l					0.300	0.054	9	0.067	0.346	0.017	68	0.072
Am	31	s	0.424	0.034	17	0.064	0.360	0.018	68	0.075	0.340	0.014	114	0.077
		ds	0.375	0.019	8	0.066	0.332	0.021	22	0.047	0.323	0.014	86	0.066
Am	35	ds	0.344	0.041	9	0.050	0.347	0.023	38	0.068	0.332	0.012	112	0.063
Hn	1	p	0.394	0.032	18	0.062	0.402	0.018	62	0.042	0.401	0.015	90	0.072
		l					0.315	0.025	26	0.060	0.375	0.018	76	0.080
Hn	8	p					0.411	0.059	9	0.074	0.378	0.019	45	0.063
		s	0.367	0.038	9	0.047	0.372	0.024	50	0.085	0.362	0.019	65	0.078

Table 13. (Continued)

Sp. no.			32–16mm				16–8mm				8–4mm			
			PK	CR	N	σ	PK	CR	N	σ	PK	CR	N	σ
Hn	8	l									0.326	±0.025	38	0.075
Hn	12	s					0.242	±0.050	12	0.076	0.252	0.029	23	0.065
		ds									0.309	0.017	53	0.062
		l									0.369	0.032	16	0.058
KF	1	ds					0.395	0.021	37	0.061	0.342	0.019	64	0.075
As	1	s									0.546	0.008	75	0.036
		l									0.470	0.056	5	0.040
Ai	1	p	0.533	±0.144	3	0.046	0.511	0.011	32	0.030	0.384	0.015	70	0.062
		l					0.325	0.080	4	0.043	0.338	0.032	29	0.081
Ai	4	p					0.492	0.012	6	0.019	0.506	0.008	50	0.029
Ai	10	p	0.483	0.017	3	0.024	0.514	0.022	11	0.031	0.515	0.008	60	0.031
		l									0.485	0.023	13	0.036
D	3	p	0.400	0.123	3	0.129	0.407	0.023	44	0.074	0.405	0.014	77	0.062
		l					0.376	0.021	49	0.072	0.406	0.016	48	0.056
S	12	p	0.300	0.094	6	0.082	0.364	0.021	68	0.081	0.343	0.012	168	0.078
		l									0.319	0.047	18	0.092
Ty	11	p					0.443	0.010	15	0.017	0.402	0.013	83	0.060
Km	11	p	0.384	0.019	64	0.075	0.342	0.017	71	0.073	0.333	0.018	88	0.086
Tw	23	p	0.362	0.019	46	0.064	0.370	0.013	86	0.082	0.386	0.073	162	0.083
		l					0.375	0.073	8	0.083	0.383	0.016	78	0.068
Nn	7	p	0.328	0.029	46	0.096	0.351	0.025	57	0.094	0.348	0.013	138	0.077
		l					0.262	0.021	21	0.044	0.263	0.012	136	0.072
Hr	5	p	0.404	0.014	10	0.049	0.378	0.014	78	0.063	0.367	0.015	125	0.084
		dp	0.370	0.048	10	0.064	0.370	0.033	23	0.074	0.373	0.019	71	0.080
		l	0.257	0.049	7	0.049	0.291	0.022	23	0.090	0.326	0.015	122	0.082
Am	39	p	0.328	0.015	54	0.056	0.322	0.016	83	0.071	0.229	0.013	93	0.061
		l									0.390	0.092	10	0.122

PK: value of average roundness, CR: confidence range with 95% confidence coefficient, N: number of measured particles, σ: standard deviation.

p: pumice, s: scoria, ds: dense scoria, se: basic segregation, l: lithic fragment.

especially at the distal ends of flows, may be rounded remarkably by attrition during flowage. Porous essential fragments in pyroclastic flow deposits, however, are actually not as remarkably rounded as have been expected in general. Values of the average roundness of porous essential particles in the ash-flow deposits are usually within a range of 0.3 to 0.5 on the size classes concerned with here, and belong to the roundness grade, "subrounded" defined by Russell and Taylor (1937)[30]. They are generally larger than values of solid lithic fragments in the same ash-flow deposits, but the difference between these two kinds of constituent particles is no more than about 0.1. No remarkable variation in roundness values with the distance from the source can be found, although data are insufficient for detailed discussion. These facts may

30) R. D. RUSSELL and R. E. TAYLOR, "Roundness and shape of sedimentary rock particles," *Rept. Comm. Sedimentation 1936-1937, Nat. Res. Council*, (1937), 225-267.

suggest that emitted gas may act as a lubricant during the flowage of ash-flows, reducing the effect of attrition. Particles may be transported in suspension in expanding gas. The rounding of particles due to attrition during flowage may proceed to some degree, but may be canceled with the reducing effect of breaking due to collision.

2) Eruptions of pyroclastic flow and pyroclastic fall often occur together in a single phase in eruption. Most of the Krakatoa type ash-flow deposits are underlain by deposits of preliminary pyroclastic falls. The discharge of St. Vincent type ash-flows usually succeeds the violent ejection of pumice and ash. Roundness values of particles in the preliminary air-fall deposits are generally smaller than those in the following pyroclastic flow deposits, but the difference between these two types of deposits is no more than about 0.1 in every case. This indicates that the rounding of particles due to attrition during the flowage of pyroclastic flows proceeds to a certain degree, but not as remarkably as has been generally considered. It may be possible to infer that particles of pyroclastic falls and also those of succeeding pyroclastic flows, especially ash-flows, may have been partly rounded on the way of ascent through the vent. Part of the ascending magma may have already been disintegrated into frothing clots of pumice within the vent, and some proportion of porous essential fragments may have already been rounded to some degree by attrition within the vent before the discharge from the crater-rim. This may be true especially in eruptions of the Krakatoa type, St. Vincent type, and V.T.T.S. type ash-flows.

3) In eruptions of the intermediate type pyroclastic flows and nuées ardentes, matters are somewhat different from in eruptions of the ash-flows. Porous essential fragments in their deposits are fairly angular, and the average values of roundness are mostly within a range of 0.25 to 0.4 in the three size classes concerned with here, which belong to the Russell and Taylor roundness grades of "subangular" and "subrounded". These values are relatively small in comparison with those of ash-flow deposits. Roundness values of lithic fragments in the same deposits are generally within the same range of 0.25 to 0.4 as are those of essential fragments. In some deposits, roundness values of porous essential fragments are conversely smaller than those of dense essential fragments, cognate lithic fragments and accessory and accidental lithic fragments. For example, in the pyroclastic flow deposits of the 1929 eruption of Tokachidake and of the central cone of the Hakone Volcano, the average roundness of porous essential fragments shows smaller values than those

of the other constituent fragments. This may indicate the auto-explosive property of pyroclastic flows during flowage, which has been discussed by many volcanologists (Fenner, 1923; Perret, 1935). It may be possible to infer that a greater part of ascending magma may have remained as effervescing melt at the crater-rim, and most of the gas-emission may have occurred after the flow had been initiated. Angular essential fragments characterized by a high degree of porosity may have been produced by explosive vesiculation during flowage.

Types of Vesicular Shards and Pumice

Essential fragments in pyroclastic flow deposits are typified by their high degree of vesiculation. It is considered that the movement of pyroclastic flows is controlled both by gravitational force and by the upward force of expanding gas. The unexpectedly high mobility of pyroclastic flows, especially over low gradients, as having been reported by many volcanologists, may be partly attributed to the lubricating action of expanding gas. Vesiculation of ascending magma may occur in several different ways. In some cases most vesiculation may take place during the flowage of pyroclastic flows, and in other case total vesiculation may occur before the discharge of magma from the crater-rim. The release of gas by vesiculation during flowage has been discussed by Fenner (1923, p. 74) and Perret (1935, p. 22–24) as a self-explosive or auto-explosive property. It may be possible to infer that such differences in the gas-emission process may be responsible for the existence of various types in the mode of eruption of pyroclastic flows and in the nature of discharged materials. In order to clear up fully the nature of the gas-emission process, quantitative studies on the types of glass shards and porous essential fragments in pyroclastic flow deposits should be most effective, together with studies on the roundness of constituent particles. They may offer important clues in deciphering the origin and mechanism of pyroclastic flows.

Some ash-flow deposits contain quantities of pumice crowded with stretched vesicles. It is considered that such pumice may have been formed by vesiculation within the vent, conduit, or magma chamber. On the way of the ascent of the magma, the shape of the vesicles in frothing clots of pumice may have been deformed into the characteristic fine tubular shape. The writer examined the rough proportion of such a type of pumice and of glass shards to the whole of the deposits, in

some samples of both pyroclastic flow and preceding fall deposits. The results are shown in Table 14, with figures of 5 to 0 in the order of

Table 14. Data on types of pumice and glass shards.

Kc-m	K	4	Km-1929	S	0	Hr-u-fa		1
Kc-u	K	3	Km-1929-fa		0	KS	S	0
Ms	K	3	Km-o	S	0	My	P-N	0
Ak	K	3	Tw-o	S*	0	Am-lp	S	1
Ak-cc	I	0	Tw	K	2	Am-up	S	1
D	S	1	Tw-fa		2	Am-up-fa		1
D-fa		1	Os	S*	0	Am-O	I	0
Tkw	K	2	On	K	3	Am-S	I	0
Tk-1926-p	I	0	Hj	S*	0	Am-A	I	0
Tk-1926-p	I	0	Nm	I	0	Hn-p	K	2
S	K	5	Nn-s	S	0	Hn-s	K	0
S-fa		5	Nn-p	S	1	Hn-cc	I	0
Kt	S	2	Nn-p-fa		0	KF	I	0
Ty-o	S	2	Th	K or V	3	As	K	4
Ty-l	K	4	Hr-l	S*	0	Ai-m	K	4
Ty-u	K	3	Hr-u	S	0	Ai-l	K	4

Figures represent the degree of abundance of pumice and glass shards crowded with fine tubular vesicles. K, etc. represent the types of pyroclastic flows.

abundance of such a type of pumice and shards.

Deposits of the Krakatoa type ash-flows, especially fine-grained deposits, are characterized by a large quantity of pumice and shards crowded with fine tubular vesicles. For example, the deposits of the lower layer of the ash-flows on the Toya, the middle layer of the ash-flows on the Kutcharo, the ash-flows on the Aso, and the ash-flows on the Aira Volcanoes contain abundant quantities of such a type of pumice and of shards. On the contrary, deposits of the intermediate type pyroclastic flows and the nuées ardentes are always lacking such essential fragments with stretched tubular vesicles. Almost the entirety of the essential fragments in these deposits shows irregular or spherical vesicles. Deposits of the St. Vincent type ash-flows have a paucity or lack of pumice and shards with stretched vesicles.

These facts may indicate the actual condition of the gas-emission process of pyroclastic flows. In eruptions of the nuées ardentes and intermediate type pyroclastic flows, most of the vesiculation may take place after the discharge of the flows. On the contrary, in eruptions of the Krakatoa type ash-flows and perhaps the V.T.T.S. type ash-

Table 15. Constituents of coarse fractions of lappili size in samples of pyroclastic flow deposits and preceding fall deposits.

Sp.	no.	Remark	Type of fl.	p	s	de	se	l	c	etc
Kc	2	u	K	87.9				11.3		0.8
Kc	5	u	K	73.5				26.5		
Kc	6	u	K	83.3				13.5		3.2
Ms	2		K		49.7			50.3		
Ak	1		K	66.9				32.3		
Ak	3	cc	I	39.4	55.6			5.0		
Ak	4	cc	I	14.7	30.2			55.1		
D	2		S	83.1			5.0	11.9		
D	3	fa		87.8				12.2		
D	4	fa		91.2			2.4	6.4		
Tkw	1		K or V	94.4				5.6		
Tk	1	p	I	34.7	30.9			34.4		
Tk	4	p(f)	I	36.5	49.3			14.2		
Tk	6	s	I		25.3	53.9		20.8		
S	1	u	K	82.8				17.2		
S	6	u	K	97.4				2.6		
S	12	fa		97.9				2.1		
Kt	1	u	S	61.0				37.8		
Ty	3	l	K	35.0				59.6		
Ty	7	u	K	29.8				64.1		
Ty	8	l	K	38.3				61.7		
Ty	10	o	S	33.2				57.0		
Ty	11	fa		100.0						
Km	3	1929	S	90.0			4.5	5.5		
Km	4	1929	S	91.8			7.2	1.0		
Km	7	K-fl	S	79.4			13.4	7.2		
Km	8	H-fl	S	88.1			2.6	9.3		
Km	11	1929-fa		96.7			2.3	1.0		
Tw	6		K	72.6				27.4		
Tw	14		K	49.2				50.8		
Tw	15		K	24.6				75.4		
Tw	16		K	87.9				12.1		
Tw	17		K	69.3				30.7		
Tw	21	o	S*		5.0			93.7		1.3
Tw	23	fa		91.3				8.7		
Os	1		S*	28.2				71.8		
On	2		K	99.8				0.2		
Hj	2		S*	47.2			1.9	42.0	8.9	
Nm	1		I	77.6			2.9	11.2	8.3	
Nn	1	s	S		44.9			50.2	4.9	
Nn	3	p	S	70.6	(11.1)		10.2	8.1		
Nn	6	p	S	98.4				1.4		0.2
Nn	7	p-fa		73.2			11.8		15.0	
Th	1		K or V	93.0				7.0		
Hr	2	l	S*	40.0				46.3	12.8	
Hr	4	u	S	80.7				16.7		2.6
Hr	5	u-fa		85.7				14.3		
KS	3	l	S*	11.9				36.9	51.2	
My	1		N-P	75.1				1.8	33.2	
My	10		N-P	64.9				1.9	33.2	
Am	1	lp	S	72.8			5.3	21.9		
Am	6	lp	S	33.8			2.6	63.6		
Am	17	up	S	43.6			23.0	33.4		
Am	20	up	S	59.5			6.3	33.0		1.2
Am	24	O-fl	I		8.2	34.7		57.1		
Am	27	O-fl	I		69.7	16.0		14.3		
Am	31	A-fl	I		52.4	43.7		1.8		2.1

Table 15. (Continued)

Sp. no.		Remark	Type of fl.	p	s	de	se	l	c	etc
Am	34	K-na	N-S		72.3	25.3		0.3		2.1
Am	35	S-fl	I			96.4		3.6		
Am	36	up-fa		99.6				0.4		
Hn	1	p	K	48.2			3.7	48.1		
Hn	7	p	K	16.8	29.7		2.6	50.9		
Hn	8	s	K	10.6	84.0			5.4		
Hn	12	cc	I		63.5	27.6		8.9		
As	1		K		89.2			10.8		
Ai	1	m	K	69.7	89.2			30.3		
Ai	4		K	99.3				0.7		
Ai	10	l	K	88.1				11.9		

p: pumice, s: scoria, de: dense essential fragment, se: basic segregation, l: accessory and accidental lithic fragment, c: cognate lithic fragment.

flows, total vesiculation may occur before the discharge of the flows, although the release of gas may continue during flowage, partly caused by the rupture of vesicles that contain gas or by diffusion from pumice clots and shards. In eruptions of the St. Vincent type ash-flows, vesiculation may occur explosively at the time of effusion. Detailed discussions are presented in the later chapters.

Constituent Characteristics

Pyroclastic flow deposits consist of several different constituents; the materials in the coarser fractions consist dominantly of porous essential fragments and non-vesicular lithic fragments; the materials in the medium fractions consist of crystals, porous essential fragments, and lithic fragments in order of abundance; and the materials in the finer fractions consist mainly of crystals and vesicular glass shards. Their constituent features vary greatly perhaps according to the difference in the type of the pyroclastic flows. The chief differences among the deposits seem to be in the relative proportions of essential and accessory or accidental lithic fragments, and the relative proportions of crystals and vitreous materials. It may be possible to consider that the nature of each type of pyroclastic flow is precisely reflected in the constituent characteristics of the deposits. In general, the composition in the coarser fractions of pyroclastic flow deposits may supply some information about the conditions of the initiation of the flows. On the other hand, the composition in finer fractions may represent the effectiveness of the sorting agency. The writer measured the percentage weight of every element in the composition of coarser fractions of some samples of

pyroclastic flow deposits and their preceding air-fall deposits. Measurement was carried out mainly on the size fractions of lapilli, e.g. 32 mm to 4 mm in the diameter of the particles, for convenience. Results are listed in Table 15. They show clearly the different constituent characteristics of the deposits according to the difference in the type of the pyroclastic flows.

1) Nuée ardente deposits: As Williams (1957) stated, the Pelean deposits show the distinct textural characteristics of chaotic mingling of fragments of all sizes and various porosity. They contain both cognate lithic fragments torn from the already solidified crust of the dome and vesicular essential fragments derived from the interior of the dome. For example, the pyroclastic flow deposits of the Myoko Volcano show such features. Cognate lithic fragments tend to bear angular and faceted shapes and also tend to be dense and non-vesicular, while essential fragments tend to be more vesicular and even pumiceous. Breadcrust bombs or ovoid bombs are very rare. Accidental lithic fragments torn from the basement beneath the volcano are quite scarce and usually lacking. Accessory lithic fragments torn from rocks around the vent are found, although they amount to a very small percentage.

Judging from accounts of the nuée ardente deposits by many geologists, fragments in the Merapi type deposits are generally less vesicular, while those in the Pelée type deposits are generally more vesicular. In general the deposits of the former contain a small quantity of fine material, while those of the latter contain a large quantity of vesicular ash and dust, in general. Most of the essential fragments in these deposits tend to bear poorly rounded shapes which suggest the auto-explosive property of effused materials during flowage.

Deposits of the Sakurajima type nuée ardente contain huge essential blocks typified by the characteristic shape and internal structure of which make appearance very much like breadcrust bombs. It is clear that these blocks were popped by internal expansion during emplacement or even after settlement. For example, those of the Kambara Nuée Ardente of the Asama Volcano in 1783 and those of the 1939 nuée ardente of the Sakurajima Volcano show such features[31]. The deposits of the Kambara Nuée Ardente contain a small amount of fine material and show a rugged surface due to huge blocks exceeding sometimes

31) Shigeo ARAMAKI, *op. cit.*, (1956),
Hiromichi TSUYA and Takeshi MINAKAMI, "Minor activity of Volcano Sakurazima in October, 1939," *Bull. Earthq. Res. Inst., Tokyo Univ.*, **18** (1940), 318-339. (Japanese with English abstract.)

several meters in diameter. It showed strong erosive power to produce a deep ditch along its lower course on the gentle slope of the volcano. Consequently, the deposits in the distal ends contain a great quantity of surface debris. At the foot of the volcano, it entered flowed into for surface water and produced secondary hot mud-flows.

2) Intermediate type pyroclastic flow deposits: The composition of intermediate type pyroclastic flow deposits resembles that of the Sakurajima type nuée ardente deposits, although the former contain a larger amount of fine materials than the latter. The deposits also show the distinct textural characteristics of the chaotic mingling of fragments of all sizes and of varying porosity. Most of the large blocks found in them are characterized by fairly high degrees of porosity and show an appearance very like breadcrust bombs which indicate that they were derived from bits of plastic magma torn apart at the time of effusion. The degree of porosity of the essential fragments varies within a wide range. As already mentioned, well-vesiculated fragments show in general an angular shape, which indicates the auto-explosive property during flowage. Lithic fragments of both accessory and accidental origin are found in the deposits, although their quantity is very small. The deposits at the distal ends of the flows, however, sometimes contain an increasing amount of surface debris, indicating the erosive power during flowage. The weight of fine ash materials often amounts to 50 per cent or more of the deposits. They consist of phenocrystic mineral grains and their fragments and minute vesicular glass shards. The deposits are considerably indurated at times, contrasting with the nuée ardente deposits which tend generally to be poorly indurated or incoherent.

3) St. Vincent type ash-flow deposits: Deposits of the St. Vincent type ash-flows vary greatly in composition. This may depend partly upon the degree to which the erupting magma has crystallized immediately before discharge, and partly upon the condition of the initiation of the flows. The distinct feature of the concentration of crystals in medium fractions of the deposits is usually recognized. For instance, the ash-flow deposits of the 1902 eruption of the Soufrière on St. Vincent (Hay, 1959) and those of the 1929 eruption of the Komagatake Volcano show such features. It is considered that crystals may be concentrated by the sorting of both in the vertically rising ash column and in the descending cloud of flows, as explained in detail in the later chapter. Concentration of crystals is found distinctly in the lower parts of the deposits. Coarse fragments of pumice or scoria are also concentrated in the St. Vincent

type ash-flow deposits, especially in their upper and frontal parts, although the degree of concentration varies considerably from part to part within a single unit of the flows. Breadcrust bombs derived from plastic magma make up an insignificant or no fraction of the whole of the deposits. Accessory and accidental lithic fragments torn from the walls of the vent and from the basement are usually small and quite subordinate in amount. Lithic fragments tend to concentrate in the lower part of the deposits. Dark colored fragments of basic segration and banded pumice are usually found in the deposits, and sometimes occupy a fairly large percentage. The deposits are generally incoherent, although some are considerably indurated.

There is another type of pyroclastic flow deposits which have size characteristics similar to those of the St. Vincent type ash-flow deposits but which show dissimilar features in their constituent characteristics. They have intermediate characteristics between dry mud-flow deposits and pyroclastic flow deposits, being described sometimes as the products of mud-flows and sometimes as those of pyroclastic flows. Such deposits contain large quantities of lithic fragments of mostly accessory origin. They also contain considerable amounts of lithic fragments of cognate origin derived from a solidified body at the apex of the magma column. It is considered that they may have been originated from violent explosions attended by the discharge of juvenile materials. Perhaps part of a volcanic cone may have been destroyed by a destructive explosion, and the disintegrated materials flowed down *en masse* along the mountain-slope in company with a large amount of juvenile materials discharged simultaneously. For instance, the Lower Ash-flow of the Haruna Volcano and the Ash-flow of the Osoreyama Volcano may belong to such types of flows each having an intermediate nature between pyroclastic flows and dry mud-flows. The bottom layers of the St. Vincent type ash-flow deposits sometimes show such an intermediate nature. For example, the bottom layer of the Ash-flow of the Kusatsu-Shirane Volcano shows such a nature. In these intermediate cases the deposits near the source contain large amounts of lithic fragments sometimes surpassing the amounts of essential fragments, while those far from the source contain increasing amounts of essential fragments as well as decreasing amounts of lithic fragments. The concentration of crystals in medium fractions of the deposits is recognized, but generally not as conspicuous as in the deposits of the St. Vincent type ash-flows, and the degree varies greatly. Strictly speaking, the deposits having such an intermediate nature be-

tween pyroclastic flows and dry mud-flows as mentioned here must be distinguished clearly from the pure pyroclastic flow deposits. In reality, however, they often accompany deposits of the St. Vincent ash-flows, showing some resemblances between them in size characteristics and in the nature of the discharged juvenile materials, and it may be convenient to deal with them as a variety of the St. Vincent type ash-flows.

4) Krakatoa type ash-flow deposits: The composition of the Krakatoa type ash-flow deposits resembles that of the St. Vincent type ash-flow deposits, although the former usually contain a larger amount of vesicular dust than the latter. The concentration of crystals in medium fractions is also generally recognized, but not as distinct as in the St. Vincent type ash-flow deposits, and its degree varies widely. Essential fragments are characterized by an extremely high degree of porosity and finely stretched vesicles. Deposits of the Krakatoa type ash-flows contain lithic fragments, both accessory and accidental, in fairly abundant amounts. Accidental fragments are derived from the deeper walls of the conduit and the chamber. During the ascent of frothing magma a large quantity of lithic fragments may be brought to the surface. The abundance of lithic fragments, especially of accidental origin, in deposits of the Krakatoa type ash-flows contrast strikingly with the paucity of them in deposits of the St. Vincent type ash-flows. Intense vesiculation arising within the conduit or even in the chamber may be responsible for such an abundance of lithic fragments. The deposits contain a small amount of surface debris, suggesting the lack of erosive power during flowage. They exhibit strong welding at times.

5) Valley of Ten Thousand Smokes type ash-flow deposits: There is another type of ash-flow deposit produced by fissure eruptions. This was first recognized from the study of tuff deposits emplaced in the Valley of Ten Thousand Smokes. They often form extensive ash-sheets whose volume sometimes exceeds 1,000 km^3. Many examples of this type of ash-flow deposits have been discovered in many regions of the world. Few examples have been discovered in Japan, but other many ones will be recognized in detailed studies in the near future. Such deposits may show fine-grained size characteristics which may resemble those of the fine-grained Krakatoa type ash-flow deposits. They may contain less amounts of lithic fragments than the Krakatoa type deposits.

Bulk Density of Essential Fragments

The mode of eruption of pyroclastic flows may be closely related to the content of volatiles in the eruping magma, and the difference in the volatile content in magma may be reflected in the degree of vesiculation of essential fragments. Aramaki's classification of pyroclastic flows (1957) is based upon the viscosity of discharged materials, which is inferred from the nature of the deposits, especially from the porosity of essential fragments. Accurate measurement of the porosity, however, is actually quite difficult. Therefore, the writer caried out measuremets of the bulk density instead of the porosity. Measurements were carried out on the essential fragments larger in diameter than lapilli size. Although values of the bulk density of essential fragments in samples collected from a single unit of pyroclastic flow deposits vary within a wide range, they tend to concentrate around a certain central value. An average values computed from a large number of individual measurements may offer a certain significant value which represents the degree of vesiculation of the erupting magma. The average values of bulk density of essential fragments ($\bar{d}_B$) both in pyroclastic flow deposits and the preceding pyroclastic fall deposits are listed in Table 16.

In general, values of the Krakatoa type ash-flows are within a range of 0.5 to 0.7, those of the St. Vincent type ash-flows are within a range of 0.7 to 1.2, and those of the intermediate type pyroclastic flows and of the nuées ardentes are large than 1.2. In the deposits of the intermediate type pyroclastic flows, and of nuées ardentes, the individual value of bulk density of each sample in a single unit of flow varies more remarkably than in the deposits of the ash-flows.

Average values of the bulk density of ovoid bombs ejected in eruptions of the Strombolian type are generally within a range of 1.5 to 2.0. Those of pumice and breadcrust bombs ejected in explosive eruptions of the Vulcanian type are usually within a range of 0.8 to 1.5. Those of pumice fragments in the Krakatoa type ash-flow deposits are remarkably small, compared with these values. On the other hand, those of essential fragments in the St. Vincent type ash-flow deposits are of the same order as those of pumice in the Vulcanian eruptions.

As already mentioned, eruptions of pyroclastic flows usually follow preliminary eruptions of pyroclastic falls. An average value of the bulk density of essential fragments in the succeeding pyroclastic flow deposits tends to be larger than those in the preceding pyroclastic fall deposits,

although the data are insufficient to discuss in detail. This relation is recognized between the preliminary pyroclastic falls and the succeeding flows of the Daisetsu, Shikotsu (Katsui, 1959), Komagatake, Towada, Nantai, Haruna, and Asama Volcanoes. Perhaps a preceding explosive

Table 16. Average values of the bulk density of essential fragments of pyroclastic flows and preceding falls.

	$\bar{d}_B$	No. of loc.	No. of sp.		$\bar{d}_B$	No. of loc.	No. of sp.
Kc-m	0.57	2	7	Hj	1.17	1	10
Kc-u	0.55	6	49	Nm	1.03	1	12
Ms	0.46	3	17	Nn-s	1.29	1	6
Ak	0.56	2	20	Nn-p	0.99	5	49
Ak-cc-p	1.08	2	19	Nn-p-fa	0.65	1	8
Ak-cc-s	1.55	1	9	Th	0.45	1	14
D	0.97	2	15	Hr-l	1.12	1	11
D-fa	0.90	2	20	Hr-u	0.87	1	12
Tkw	0.65	1	5	Hr-u-fa	0.69	1	11
Tk-1926-p	1.27	3	31	KS	1.25	2	8
Tk-1926-s	1.73	4	38	My	2.04	11	10
S	0.54	10	58	Am-lp	0.68	13	117
S-fa	0.53	1	9	Am-up	0.83	7	57
Kt	0.75	2	15	Am-up-fa	0.71	1	8
Ty-l	0.78	3	11	Am-O	1.41	5	40
Ty-u	0.74	5	37	Am-S	2.24	1	11
Km-1929	0.94	6	64	Am-A	1.13	3	27
Km-1929-fa	0.84	1	13	Hn-p	0.64	4	43
Km-K	1.09	1	11	Hn-p	0.84	2	17
Km-H	1.05	3	24	Hn-cc	1.78	3	26
Tw-o	1.03	2	14	KF	2.18	10	122
Tw	0.50	20	151	As	0.74	2	11
Tw-fa	0.47	1	12	Ai-l	0.59	2	22
Os	0.83	1	4	Ai-m	0.59	6	61
On	0.52	2	17	Ai-u	0.47	1	4

eruption which produces violent pyroclastic falls may be caused by intense vesiculation of gas-rich magma in the uppermost level of the magma column, and the rather fluent discharge of magma having a decreasing content of gas in the lower level of the magma column succeeds, forming flows of frothing materials. Such a succession of eruptive events is discussed in the following chapter.

Succession of Eruptive Events

The eruption of pyroclastic fall, pyroclastic flow and effusion of lava often occur together in a single phase of volcanic activity. Among these events a certain order of succession may be maintained in almost every case as Yamasaki (1959) and Kennedy (1955) pointed out[32]. The eruption of pyroclastic flows usually follows the preliminary eruption of pyroclastic falls. In the 1883 eruption of the Krakatoa Volcano, a voluminous discharge of pumice and ash in the form of ash-flows followed the preliminary eruptions of pumice falls. The eruption of the ash-flows in the Crater Lake region succeeded the eruption of pumice falls (Williams, 1942). A similar succession has been recognized in many cases of Japanese ash-flow deposits. In the 1929 eruption of the Komagatake Volcano the discharge of ash-flows followed the early powerful explosion which caused heavy pumice falls (Tsuya, 1930; and Kozu, 1934). The ash-flows of the Mashu, Daisetsu, Shikotsu, Tarumai, Towada, Nantai, Haruna, Akagi, Asama, Hakone and Aira Volcanoes are underlain by preliminary pyroclastic falls. In the eruption of the Asama Volcano in 1783, a systematic succession of eruptions of pumice fall, scoria flow, intermediate type pyroclastic flow, nuée ardente and lava flow took place. Throughout the whole of the eruptive events in this 1783 activity, the chemical composition and petrological character of the effused materials showed no significant variation, while the gas content of magma which was inferred from the porosity of the discharged materials decreased gradually (Aramaki, 1956 and 1957). A similar systematic succession of pyroclastic fall, flow and effusion of lava has been recognized in the 1739 eruption of the Tarumai Volcano (Katsui, 1958) and in the prehistoric eruptions of the Nantai (Yamasaki, 1957) and Haruna Volcanoes.

In the prehistoric eruption of the Shikotsu Volcano, an explosive eruption of rhyolitic magma which caused heavy pumice falls occurred in the initiation of the culminant phase of the eruptive activity. Katsui (1959) considered that this eruption originated from the apex of the magma column which was rich in volatiles and alkalies, and then followed the discharge of a tremendous amount of dacitic magma in a state of

32) Masao YAMASAKI, "Role of water in volcanic eruption," *Bull. Volcanol. Soc. Jap., 2nd Series*, **3** (1959), 95-106. (Japanese with English abstract.)
G. C. KENNEDY, "Some aspects of the role of water in rock melts," *Crust of the earth, Geol. Soc. Am. Special Paper*, **68** (1955), 489-503.

ash-flow, which originated from the lower level of the magma column[33]. Such a change of the composition of the effused materials, from more silicic to less silicic, or from felsic to mafic, has been recognized in other eruptions. In the prehistoric eruption of the Mashu Volcano, a succession of felsic pumice fall, mafic pumice fall and flow has been recognized (Katsui, 1955). During the culminating eruptions of ash-flows from Mt. Mazama in the Crater Lake region, a transition from dacite pumice whose silica content ranges from 66.4 to 68.9 per cent to basic scoria whose silica content rang as from 53.9 to 56.9 per cent occurred suddenly without a detectable time break[34]. In the eruption of the ash-flows from the Hakone Volcano, a similar transition from pumice to scoria was also recognized. Some volcanologists consider that these facts may suggest a role of water in the magma, where the water tended to concentrate at the top of the magma column, bringing together alkalies and silica (Kennedy, 1955; and Katsui, 1960).

The systematic succession of the pyroclastic fall and flow and effusion of lava as mentioned here, may suggest the important role of volatiles in erupting magma as noticed by Yamasaki (1959) and Kennedy (1955). At the initiation of a single phase of volcanic activity, an explosive eruption occurs suddenly. An intense vesiculation of erupting magma hurls up ash and pumice high above the crater, causing pyroclastic falls. The magma represents the higher level of the magma column, in which the gas content may be greater than in the lower level. This high content of gas, as well as the heavy confining load of solidified crust at the apex of the column, may be attributed to the violent explosion in the initial stage of eruptive activity. The gas content of magma decreases with the preceding violent explosion. In the following stage, because of the decreasing content of gas as well as the removal of the confining load of solidified crust at the top of the vent, magma discharges without powerful explosion, and may form pyroclastic flows at times. The magma in this stage represents the lower level of the magma column, containing relatively lesser amount of gas than in the preceding stage. The eruption of pyroclastic flows

33) Yoshio KATSUI, "On the Shikotsu pumice-fall deposit," *Bull. Volcanol. Soc. Jap., 2nd Series,* **4** (1959), 33-48. (Japanese with English abstract.)

Yoshio KATSUI and Tsutomu MURASE, "Some considerations on the activity of the Shikotsu Volcano," *Jour. Geol. Soc. Jap.*, **66** (1960), 631-638. (Japanese with English abstract.)

34) Howel WILLIAMS, "The geology of Crater Lake National Park, Gregon, with a reconnaissance of the Cascade Range southward to Mount Shasta," *Carnegie Inst., Washington Pub.* **540** (1942), 162.

may be generated by a less intense vesiculation than the preceding pyroclastic fall eruption. In the later stage of eruptive activity, magma does not contain a large amount of gas. The gas content of magma becomes poor partly because of the escape of volatiles during the earlier stages, and a calm extrusion of lava may occur.

Chemical Properties of Pyroclastic Flow Deposits

There exist wide variations in the chemical properties among various types of pyroclastic flow deposits. The deposits contain almost all the rock types from basalts to rhyolites, although basalts are exceedingly rare. Many chemical analyses of rocks recognized to be of pyroclastic flow origin have been published. They record compositions ranging from basalts to rhyolites and trachytes, but in general, silicic rocks predominate. Values of the silica content vary widely, mostly falling within a range of 55 to 75 per cent. Those of the nuées ardentes, the intermediate type pyroclastic flows and the St. Vincent type ash-flows are relatively less silicic and range from 55 to 65 per cent, while those of the Krakatoa type ash-flows and the Valley of Ten Thousand Smokes type ash-flows are more silicic and range from 60 to 75 per cent or more. Color indices (the percentage of normative ferromagnesian minerals) usually take values less than 20. There are no notable differences in the chemical properties between pyroclastic flow deposits and normal lava flows. Essential fragments of pyroclastic flow deposits are typified by a high degree of porosity, and consist of phenocrystic mineral grains and vesiculated amorphous groundmass. Consequently it is impossible to determine whether they belong to the pigeonitic rock series or the hypersthenic rock series of Kuno (1950 and 1953) in almost every case.[35] Bulk chemical compositions of all types of pyroclastic flow deposits, however, tend to show the chemical properties of the hypersthenic rock series. The ratio of $(FeO+Fe_2O_3) : MgO : (Na_2O+K_2O)$ plotted on the triangular diagram tends to fall in the region of the hypersthenic rock series and also shows a trend of variation almost coinciding with that of Daly's averages of igneous rocks (1941), except for a very few cases (see Fig. 12). Variation diagrams of oxides plotted against solidification indices (S. I.) of Kuno (1954 and 1959) generally manifest the general features of rocks of the calc-alkali rock series and of the hyper-

35) Hisashi KUNO, "Petrology of Hakone volcano and adjacent areas, Japan," *Bull. Geol. Soc. Am.*, **61** (1950), 957-1020.
Hisashi KUNO, *op. cit.*, (1953).

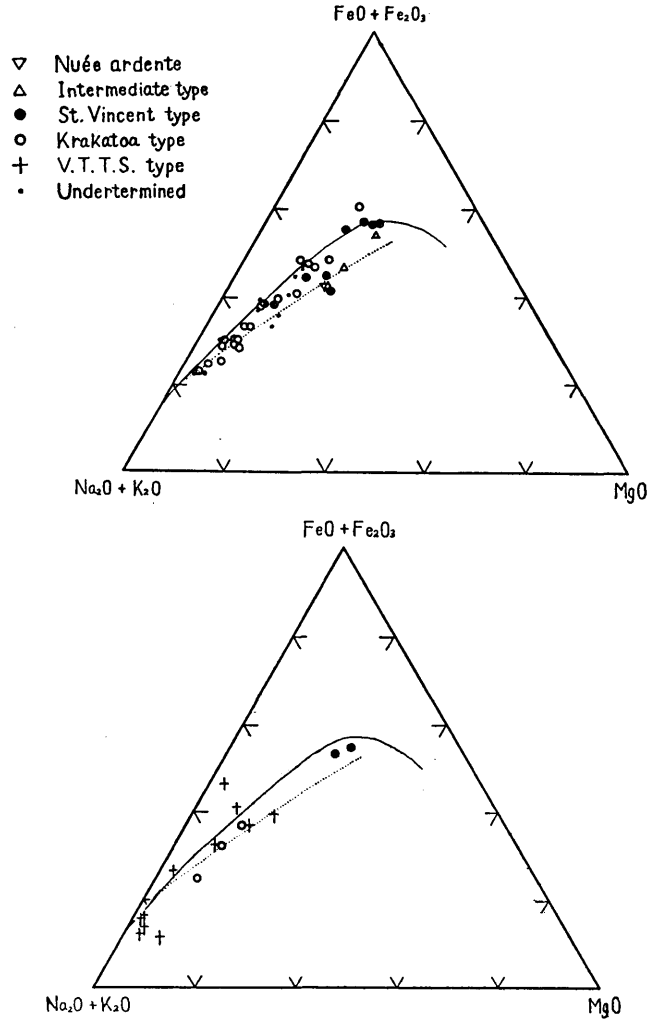

Fig. 12. MgO: $FeO+Fe_2O_3$: Na_2O+K_2O triangular diagram. Upper: Japanese examples, lower: foreign examples. The solid line is the border between the pigeonitic rock series and the hypersthenic rock series drawn by Kuno (1953). The dotted line represents the variation line of Daly's averages on volcanic rocks of the World (1941).

sthenic rock series (see Fig. 13). (S. I.) are values of $MgO\times100/(MgO+FeO+Fe_2O_3+Na_2O+K_2O)$, which are adopted as measures of magmatic differentiation.[36] Every point on the diagram tends to center around a

36) Hisashi KUNO, "Volcanoes and volcanic rocks," *Iwanami and Co., Tokyo* (1954), 255. (Japanese)

Hisashi KUNO, "Origin of Cenozoic petrographic provinces of Japan and surrounding areas," *Bull. Volcanol., ser.* **ii**, **20** (1959), 37-76.

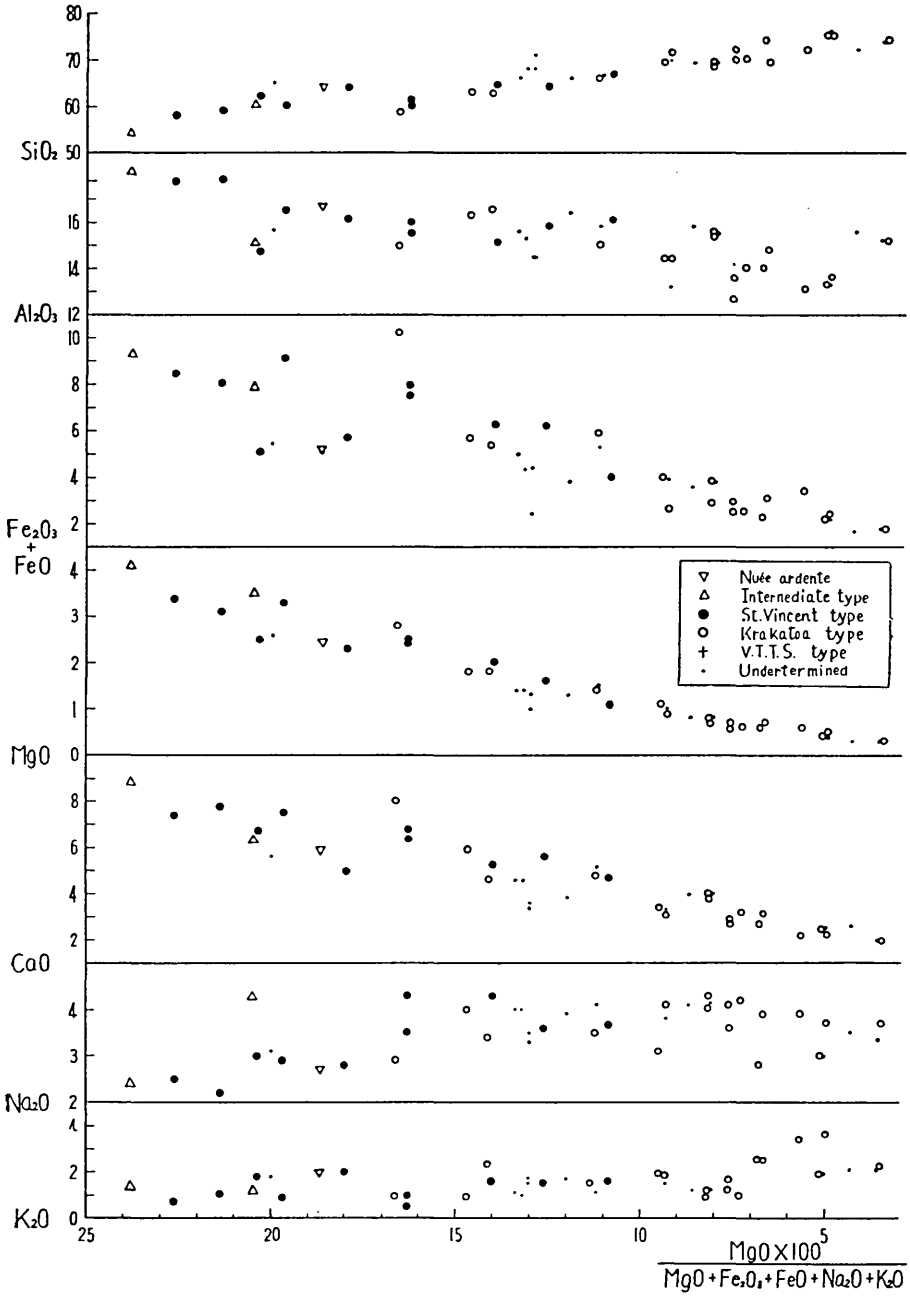

Fig. 13a. Variation diagrams of oxides, Japanese examples.

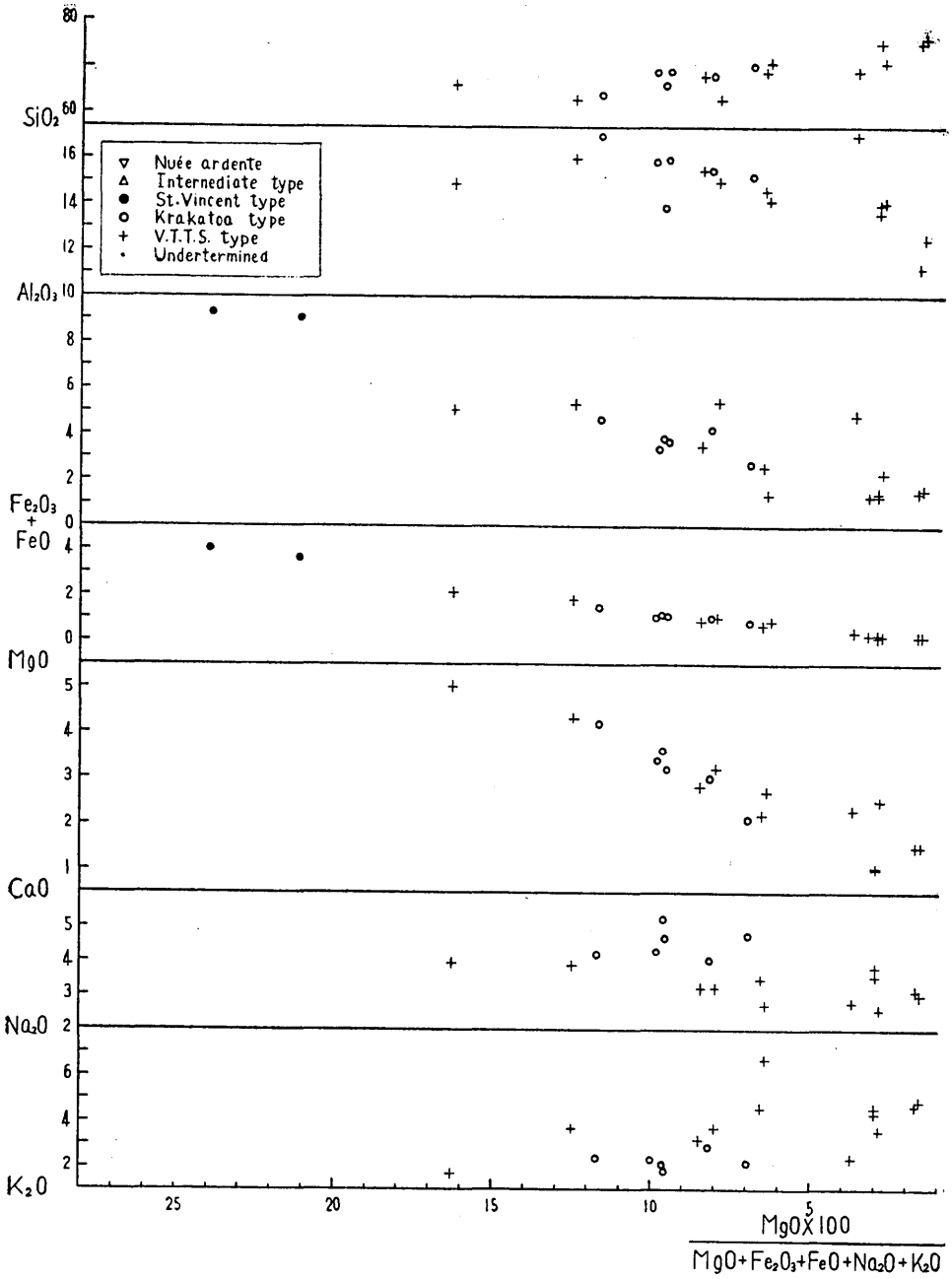

Fig. 13b. Variation diagrams of oxides, foreign examples.

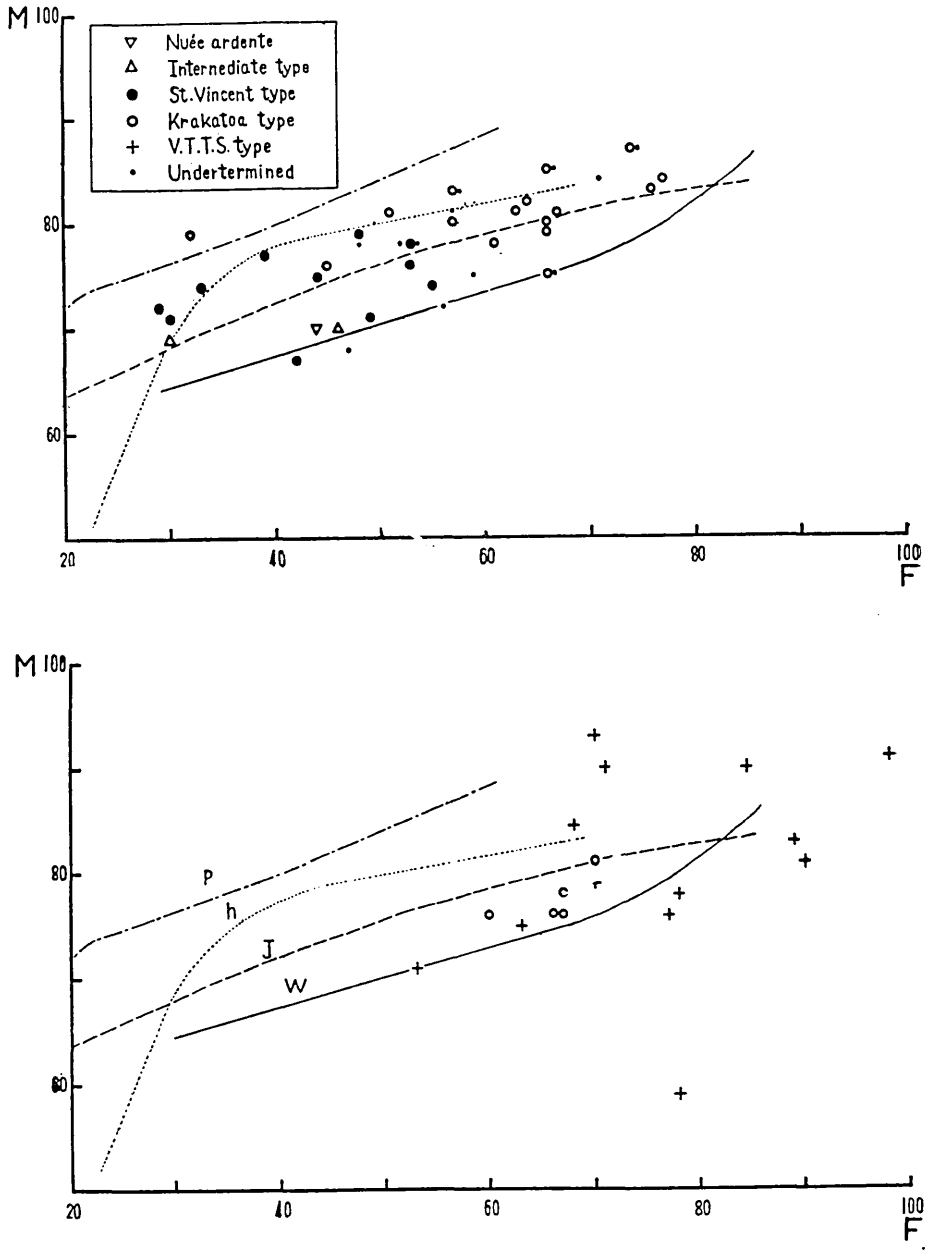

Fig. 14. F-M diagrams. Upper: Japanese examples, lower: foreign examples, p: pigeonitic rock series of Izu-Hakone district, h: hypersthenic rock series of Izu-Hakone district, J: the average of Japanese volcanic rocks (Iwasaki, 1948), W: average of volcanic rocks of the World (Daly, 1941).

certain nearly straight line of variation, indicating the differentiation process of contaminated magma. Data of various pyroclastic flow deposits plotted on M-F diagrams of Simpson (1954), in which (F) are values of $(Na_2+K_2O)\times 100/(CaO+Na_2O+K_2O)$, and (M) are value of $(FeO+Fe_2O_3)\times 100/(MgO+FeO+Fe_2O_3)$, also show the general tendency of rocks of the hypersthenic rock series. (see Fig. 14)[37]. Kuno (1950) considered that the hypersthenic rock series are formed by the contamination of primary

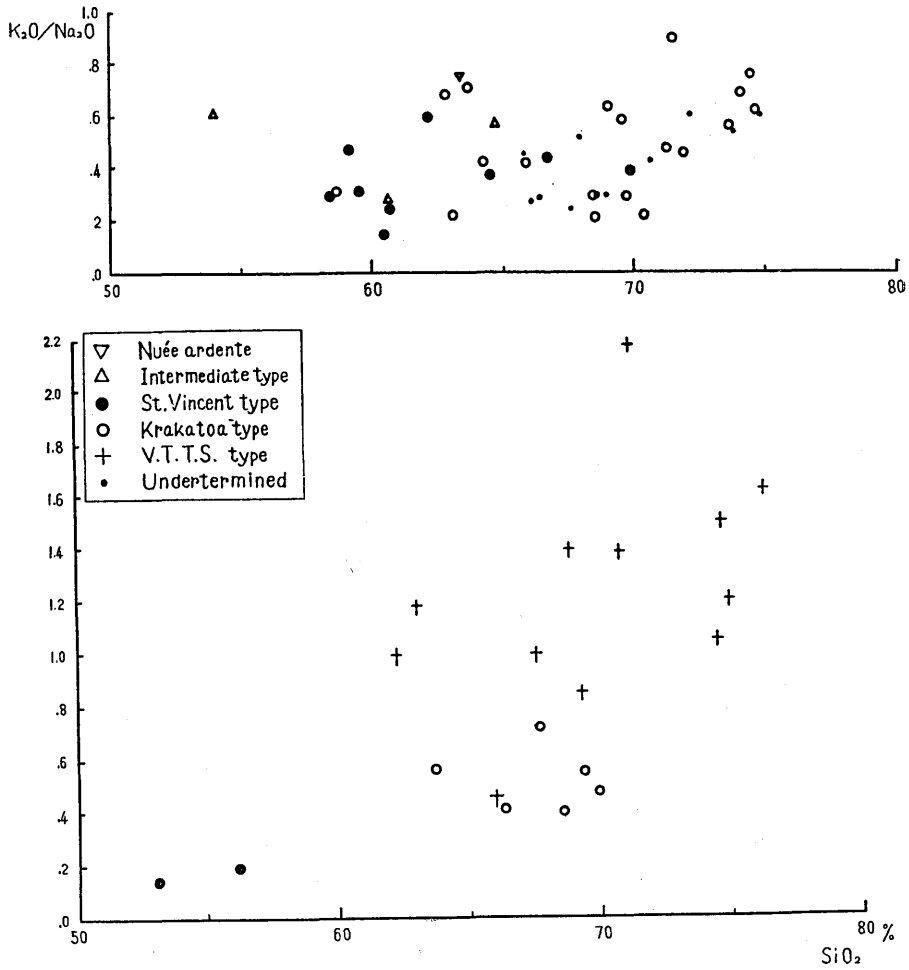

Fig. 15. K_2O/Na_2O-SiO_2 diagram. Upper: Japanese examples, lower: foreign examples.

37) E. S. SIMPSON, "On the graphic representation of differentiation trends in igneous rocks," *Geol. Mag.*, **91** (1954), 238-244.

magma with granitic materials. Volatiles dissolved in the primary magma may concentrate into the contaminated part and lower the temperature of crystallization, resulting in the growth of rhombic pyroxene in the groundmass. Magmas that cause the eruptions of pyroclastic flows may be formed by such contamination, which may be attributed to the high degree of concentration of volatiles in magmas. Chemical analyses of the deposits sometimes show a high content of $H_2O(+)$. Other proofs of the contamination are recognized in general. For example, some pyroclastic flow deposits contain relic crystals which are considered to be derived from felsic igneous rocks, or crystals of cordierite. The ratio of K_2O to Na_2O of the pyroclastic flow deposits shows the general tendency of the hypersthenic rock series and tends to bear a considerably higher value in comparison with that of the pigeonitic rock series, indicating the influence of the contamination (see Fig. 15). Katsui (1955) also pointed out that the pumice ejected from the pre-Mashu caldera and the Towada double caldera belong to the hypersthenic rock series and are considered to be of contaminated origin.

The magmas which produce the Krakatoa type ash-flow and V.T.T.S. type ash-flow may represent the later stages of crystallization differentiation of the hypersthenic rock resies, while the magmas of the nuée ardente and the intermediate type pyroclastic flow may represent the earlier stages, and those of the St. Vincent type ash-flow represent the middle stages, as seen in the diagrams on their chemical properties.

Discussions on the Mode of Origin and Mechanism of Pyroclastic Flows

Gas-emission Process

It may be possible to consider that the formation of pyroclastic flows is closely related to the high content of gas in erupting magmas and the condition of the release of gas from magmas. Herein lies a problem to be solved, that is, the actual condition of the gas-emission process in different types of pyroclastic flows must be cleared up. As mentioned in the preceding chapters, quantitative analyses of pumice and shards types and measurements of the roundness of different constituent particles in pyroclastic flow deposits may offer some important clues to help to solve this problem. Judging from the results of such examinations, together with the results of inspections of other characteristics

of the deposits, it may be possible to infer the actual condition of the gas-emission process in every type of pyroclastic flow as follows.

In eruptions of the Krakatoa type ash-flows, vesiculation commences within the conduit or even in the magma chamber, and most of the gas-emission takes place before the discharge of ash-flows. A large proportion of ascending magma may be disintegrated into frothing clots of pumice within the conduit, shattered to fine pieces and shards crowded with stretched fine tubular vesicles. Pumice clots are shattered and stretched by attrition along the way of ascent through the conduit. Essential fragments of the Krakatoa type ash-flows are typified by an extremely high degree of porosity as well as peculiar fine tubular vesicles. After the preliminary explosive eruption which causes heavy pyroclastic falls and removes the confining load of solidified crust at the top of the conduit, tremendous commingling mass of pumice clots, crystals and their fragments, fine vesicular ash and the dust of vitreous materials, lithic fragments torn from the walls of the conduit or magma chamber, and emitted gases, is discharged without a violent explosive emission of gas. Almost the entirety of the discharged materials pours out rather fluently and flows down *en masse* in the state of ash-flows without being hurled up high into the air.

The deposits of the Krakatoa type ash-flows are characterized by their huge volumes usually exceeding 10 km^3, contrasting with the St. Vincent type ash-flow deposits whose volumes are mostly less than 10 km^3. The magnitude of the former is mostly oder 5 or 6 in Smith's oders of magnitude (1960), while that of the later is generally oder 4 or 3. The Krakatoa type ash-flow deposits are almost always distributed in the surrounding area around the characteristic topography of depressions, especially calderas, which are formed by collapse following the eruption of a tremendous amount of ash-flows. Kuno (1953) indicated that most of the Japanese calderas belong to those of the Krakatoa type classified by Williams (1941). For example, the caldera lakes of Shikotsu and Toya in Hokkaido, those of Towada and Tazawa and the caldera of Onikobe in northern Honshu, the younger caldera of Hakone, and the four calderas in Kyushu, belong to the Krakatoa type calderas. Many of the Krakatoa type ash-flow deposits surrounding the Krakatoa type calderas are underlain with preliminary pyroclastic fall deposits as repeatedly mentioned. In every case, the volume of the ash-flow deposits is far larger than that of the preceding pyroclastic fall deposits. At the paroxysmal phase of the 1883 eruption of the Krakatoa Volcano, a tremendous volume of pumice and ash, amounting to more than 90 per

cent of all the effused materials of the 1883 eruption, was discharged in a short time, and fell virtually *en masse* as an avalanche and was accumulated close to the source as an unstratified pile up to 60 meters thick. Only the finer particles of vesicular fragments were thrown out high into the air, and drifted away for long distances (Williams, 1941). Perhaps, the mode of eruption in every case of Krakatoa type ash-flows may be similar to the paroxysmal phase of the 1883 eruption of the Krakatoa Volcano. Erupting magmas of the Krakatoa type ash-flows may have an extremely high content of volatile substances, judging from a distinct feature of fully-vesiculated essential fragments in the deposits. Such a high concentration of volatiles may be attributed to the eruptions of high magnitude which cause the effusion of a tremendous amount of ash-flows of the order of 5 or 6 (its volume is more than 10 km^3 or 100 km^3) and the following collapse of the apical part of the volcano.

It may be inferred that eruptions which produce the fine-grained Krakatoa type ash-flow deposits may somewhat resemble to those of the V.T.T.S. type ash-flows. Pyroclastic materials may effuse from fissures developed on the volcanic cone rather from a central crater, the writer considers.

In eruptions of the intermediate type pyroclastic flows and the Sakurajima type nuées ardentes, most of the vesiculation occurs after the discharge of the flows. Magmas ascend to the crater-rim in a state of effervescing melt. The intermediate type pyroclastic flows are generally formed without explosive eruption, and effervescing magmas discharge rather fluently over the crater-rim and rush down the mountain-slope. The rising of a lofty column of ash and steam which causes heavy pyroclastic fall, as in eruptions of the St. Vincent type ash-flows, may not occur in general. Almost the entirety of the discharged materials descend *en masse*, forming flows of frothing fragments.

In eruptions of the Pelée type nuées ardentes which are initiated by lateral propulsion due to powerful explosions, intense vesiculation occurs at the time of initiation and continues during flowage. On the other hand, in eruptions of the Merapi type nuées ardentes of Escher's classification (1933), initiated by feeble explosions or without explosion, the total vesiculation takes place during flowage. Such a process of gas-emission which occurs during flowage gives rise to the so-called "auto-explosive property" discussed by Perret (1935) and Fenner (1923).

In eruptions of the St. Vincent type ash-flows, matters are otherwise. Vesiculation begins partly within the vent, and occurs mostly at the time of the effusion of the magma. Gases are released explosively from

the erupting magma at the crater-rim. The erupting magma may no longer be an effervescing melt but have already been disintegrated into frothing clots of pumice and droplets of liquid at the time of effusion. The discharge of ash-flow follows the preliminary explosion. The gas content of the magma may be fairly high, but the initial velocity of the emitting gas at the crater-rim is lower than in the case of a major explosion of the Vulcanian type eruption, and in the preceding explosion. Most of the effused materials are ejected into the height in the ash column, and phenocrystic mineral grains and pumice blocks are sorted and concentrated in the slowly rising outer part of the ash column, and then form an ash-flow descending down the mountain-slope under the influence of graviational force (Hay, 1959). The release of gas may continue during flowage of the flows, although most of the vesiculation occurs before the discharge of the flows. Some vesiculation may continue even after the discharge of the flows. Gas may be also released by rupture of vesicles during flowage.

In eruptions of the Valley of Ten Thousand Smokes type ash-flows, the gas-emission process may be similar as in eruptions of the Krakatoa type ash-flows, although the writer has no available datum based upon sure examples.

There exist wide variations in the actual condition of the gas-emission process among different types of pyroclastic flow eruptions as explained here, and such variations may be due to the differences in the degrees of concentration of volatiles in the erupting magmas. Magmas which produce eruptions of the Krakatoa type ash-flows and the Valley of Ten Thousand Smokes type ash-flows are generally dacitic or rhyolitic, containing extremely high amounts of silica. Such magmas represent the later stages of crystallization differentiation and may contain high amounts of volatiles, and such a high concentration of volatiles may be attributed to the eruptions of high magnitude and the vesiculation of a tremendous mass of magma within the conduit or chamber. On the other hand, magmas which produce eruptions of the other types of pyroclastic flows of lower magnitude are generally less silicic and may contain lesser amounts of volatiles than the former two types of higher magnitude. Especially, magmas of the nuées ardentes and the intermediate type pyroclastic flows generally represent the earlier stages of crystallization differentiation and may contain the least amounts of volatiles, although they may show a considerably high content of volatiles in comparison with normal lava flows. The lesser concentration of volatiles in erupting magmas may be responsible for the delayed vesiculation that

takes place after the discharge of flows of these two types. Magmas which produce eruptions of the St. Vincent type ash-flows generally represent the middle stages of crystallization differentiation and may contain fairly large amounts of volatiles. Consequently, vesiculation takes place explosively, partly within the vent and mostly at the crater-rim, and the discharge of flows usually accompanies a violent effusion of the vertical column of ash and steam.

Dual Character of Pyroclastic Flows

Judging from descriptions of many observers on eruptions of pyroclastic flows, it appears that they consist of two parts, namely, a basal avalanche and an overriding spectacularly expanding cloud of gas and dust. Such a separation of the basal avalanche and the overriding cloud in pyroclastic flows may occur at any time, although a distinction between these two parts may not always be sharply drawn. This dual character of pyroclastic flows may be recognized most distinctly in eruptions of the nuées ardentes and the intermediate type pyroclastic flows in which most of the vesiculation takes place during flowage. During the eruption of May 8th, 1902, at Mt. Pelée, it was the overriding cloud that swept away St. Pierre. Deposits of ash and lapilli a few feet thick settled from the cloud. On the other hand, the basal avalanche from which the devastating cloud was derived flowed down in the confined area of the valley of the Rivière Blanche, on the south-west of the parent dome. Deposits characterized by the chaotic mingling of fragments of all sizes settled from the basal avalanche (Lacroix, 1904 and 1908). During the eruption of May 7th, 1902, at the Soufrière, a "great black cloud" descended from the crater, and the upper part of the cloud spread outward as a "hot blast" over the eastern and western slopes of the Soufrière, causing the death and devastation of the settlement, and deposited a few inches of ash. The lower, denser part of the cloud flowed down mostly in the valleys of the Rabaka and Wallibu Rivers on the east and west respectively. The deposits which settled from the lower avalanche are typical of this type of ash-flow scores or a hundred feet thick (Anderson and Flett, 1903).

It is possible to infer that the deposits which settled from the overriding cloud are very fine-grained and abundant in vesicular dust, showing a great disparity from those of the basal avalanche in size characteristics and constituents, judging from actual examples of these pyroclastic flow deposits. Such deposits which settled from the

Table 17. Localities of samples.

Sp. no.	Locality
Kc 1-13, Ms 1-4, Ak 1-6	See Fig. 2a.
D 1-4	Ôbako, Kamikawa-machi
TkW 1	Shimizuyama, Furano-machi
Tk 1-13	See Fig. 2c.
S 1-16, Kt 1-2, Ty 1-12	See Fig. 2b.
Km 1-16	See Fig. 2d.
Tw 1-26, Hd 1	See Fig. 2e.
Os 1	Futamata, Mutsu-machi
Tz 1	Funaba, Obonai-machi
On 1	Uehara, Narugo-machi
2	Haguro, Furukawa-shi
3	Tsuidate-machi
Z 1	Zaô hot spring, Yamagata-shi
2	Matsusan, Yamagatashi
4	Yamanokami, Yamagata-shi
Hj 1	Komatsukura, Ôkura-mura
2	Hikagekura, Ôkura-mura
G 1	Tôge, Haguro-machi
B 1	Goshiki-numa
2	South side of Hibara-ko
3	South side of Onogawa-ko
Nm 1	Nakanosawa, Inawashiro-machi
Nn 1-7	See Fig. 2f.
Th 1	Hariu, Yaita-machi
Hr 1	Ikaho hot spring
2-5	Kurosawa, Shibukawa-shi
KS 1-5, Am 1-47	See Fig. 2g.
My 1-11	See Fig. 2h.
Hn 1-14	See Fig. 2i.
KF 1-10	See Fig. 2j.
11	Hôei-zan
F 1-3	Subashiri-mura
4	Ôsaka, Gotenba-shi
5-6	Uchiyama, Yamakita-machi
As 1	Usuki-shi
2	Hitoyoshi-shi
Ai 1-13	See Fig. 2k.

overriding cloud are usually very thin, and easily worn away. Sometimes, however, deposits showing great disparities in their size

characteristics and constituents from those of the main deposits in a single unit of pyroclastic flow are found. They are distributed along the borders and distal ends of the flows, or form the uppermost layer of the deposits. For example, Sp. no. Tk 4 of the 1926 eruption of the Tokachidake Volcano, Sp. no. Hr 3 of the Lower Ash-flow of the Haruna Volcano, Sp. no. Am 16 of the Lower Ash-flow, and Sp. no. Am 30 of the Oiwake Pyroclastic Flow and Sp. no. Am 16 of the Lower Ash-flow of the Asama Volcano are deposits of more finely-grained and more abundant vesicular dust, compared with the bulk deposits of the flows. These deposits afford positive proof of the dual character of pyroclastic flows.

The dual character of pyroclastic flows is considered to be due to the release of gas during flowage. The conspicuous separation of cloud and avalanche may caused by delayed vesiculation and usually occurs in eruptions of the nuées ardentes and the intermediate type pyroclastic flows. It also occurs in eruptions of the St. Vincent type-flows, for the release of gas may continue after the discharge of the flows. In eruptions of the Krakatoa type ash-flows and the Valley of Ten Thousand Smokes type ash-flows, the dual character of the flows may be rather ambiguous, for most of the vesiculation may take place within the conduit.

Sorting Agency

As mentioned in the former chapter, particle size distribution curves of pyroclastic flow deposits do not in general conform to Rosin's law of crushing. This may indicate some efficiency in the sorting agency in the emplacement of deposits. The degree of disparity with Rosin's law is most remarkable in deposits of the St. Vincent type ash-flows. Cumulative curves of the St. Vincent type ash-flow deposits plotted on Rosin law paper show a distinct undulating shape which represents the pronounced bimodal property of size distribution. The deposits usually show a remarkable concentration of crystals in medium fractions as well as the concentration of pumice blocks in coarse fractions. Such size characteristics of the St. Vincent type ash-flow deposits which are different from those of the other types of pyroclastic flow deposits may be attributable to the strong efficacy of sorting in the vertically rising ash column as well as in the descending cloud of flows. Most of the deposits of the St. Vincent type ash-flows are underlain by preceding air-fall deposits, and their volumes are generally much less than those of the preceding air-fall deposits. The volume of the ash-fall is calculated as

0.35 km^3, while that of the ash-flow is 0.025 km^3, in the 1902 eruption of St. Vincent (Hay, 1959). In the 1929 eruption of the Komagatake Volcano, the volume of the air-fall is calculated as 0.4 km^3 or more, while that of the ash-flow is 0.15 km^3. This fact may suggest the subordinate origin of the St. Vincent type ash-flows from the vertically rising ash column.

In the eruptions of St. Vincent in 1902 and of the Komagatake Volcano in 1929, crystal-rich andesitic magma having a high content of gas was discharged through an open carter with relatively low initial velocity. At the time of discharge from the crater-rim, the magma was no longer an effervescing melt but had already disintegrated into frothing clots of pumice and droplets of liquid disrupted into crystals and finely comminuted shards of vesicular glass. Phenocrystic mineral grains and pumice blocks may have concentrated in the slowly rising outer part of the vertical ash column, settling within the turblent current of gas, while lighter shards of vesicular glass were born into the air in suspension. Consequently the dense outer part of the ash column tended to fall to the ground. When once the ash-flow began to descend, gas trapped in the vesicles of ash and pumice escaped and expanded in company with gas newly released by vesiculation from the liquid magma. Consequently the ash-flows were separated into two parts, and phenocrystic mineral grains and pumice blocks were concentrated in the basal avalanche and fine vitric ash was suspended in the overriding cloud. A concentration of crystals is usually found distinctly in the lower part of the deposits, which settled from the basal avalanche, while a concentration of pumice-blocks is seen in the upper part and especially in the front of the deposits. Fine-grained deposits rich in vesicular glass settled from the overriding cloud along the front and margin of the main deposits from the basal avalanche of the ash-flows.

The efficacy of sorting during the flowage of pyroclastic flows, which may cause the marked concentration of crystals in the deposits of their basal avalanches, is recognized in the intermediate type pyroclastic flows and the nuées ardentes. Cumulative curves of size distributions of their deposits, plotted on Rosin's law paper, show irregular lines broken in two nearly straight parts, as already explained. Such features indicate the fact that fine vesicular materials tend to be borne into the overriding cloud by the upward current of expanding gas emitted by auto-explosion during flowage of pyroclastic flows, being transported in suspension within the cloud. Fine materials are transported far from the source and settle beyond the margin and front of the main deposits from the

basal avalanche. In the eruptions of Mt. Pelée in 1902 and the Tokachidake Volcano in 1926, the deposition of fine materials from the overriding cloud was actually recognized. Such separation of the finer and coarser materials within the expanding cloud is explained in the preceding chapter as the dual character of pyroclastic flows.

In the deposits of the basal avalanche of the intermediate type pyroclastic flows, blocks of porous essential fragments tend to concentrate in the upper and frontal part of the deposits, as seen in the deposits of the St. Vincent type ash-flows. It is considered that at the time of settling the movement of flows slows down and the turbulence ceases gradually, changing into the laminar flow, especially in the lower layer of the basal avalanche. Porous blocks are tossed up with the turbulence and rafted on the upper surface of the basal avalanche, while medium particles consisting mainly of crystals settle down from the lower layer of the avalanche.

In the Krakatoa type ash-flows, and perhaps in the Valley of Ten Thousand Smokes type ash-flows, the efficacy of sorting is not as distinct as in the St. Vincent type ash-flows, as indicated by the size characteristics of their deposits. Size distribution curves plotted on Rosin law paper do not show such undulating lines as those of the St. Vincent type ash-flow deposits nor broken lines as with those of the intermediate type pyroclastic flow deposits and the nuée ardente deposits, but exhibit gentle concave lines, as mentioned in the former chapter. The concentration of crystals in medium fractions of the deposits is recognized, but generally not so conspiquous as in deposits of the St. Vincent type ash-flows, and its degree varies widely. The sorting agency in the vertically rising ash column may be not as effective as in the St. Vincent type ash-flows, and sorting in the descending cloud also may be not as effective as in the intermediate type pyroclastic flows and the nuées ardentes. Some effectiveness of sorting, however, may appear during the travelling of flows for long distances from the source. Deposits at the distal ends of flows usually contain large amounts of fine vesicular materials, suggesting such effectiveness of sorting during flowage.

Intermediate Cases between Pyroclastic Flows and Dry Mud-flows

There is a particular type of pyroclastic flow deposit having an intermediate nature between pyroclastic flow deposits and dry mud-flow deposits. They may have originated through violent explosions attended

by a discharge of juvenile materials, sometimes preceding the eruptions of the St. Vincent type ash-flows. Their size characteristics are roughly similar to those of the St. Vincent type ash-flow deposits, although there are small differences between the types of these two deposits. Their size distribution curves exhibit a bimodal character, but their main modes in medium fractions are usually not as pronounced as in the typical deposits of the St. Vincent type ash-flows. Cumulative curves plotted on Rosin law paper show lines similar to those of the St. Vincent type ash-flow deposits, but the remarkable convex crest in the middle part of the curves of the latter tends to disappear. Judging from such size characteristics the mode of initiation of the flows may be somewhat different from that of the typical St. Vincent type ash-flows. It may be able to be inferred that such pyroclastic flows were not attended by the violent emission of a lofty column of ash and steam. They may have been initiated by powerful explosions that caused the collapse of the apical part of the volcanic cone. Discharged materials derived from erupting magma flowed down *en masse*, accompanied by disintegrated rock fragments. Vesiculation may have taken place mostly at the time of explosion and continued during flowage. An expanding cloud of gas and dust may have risen from the flows. Such a mechanism of the flows may be rather similar to the intermediate type pyroclastic flows. The degree of vesiculation of the essential fragments, however, is of the same order as in the typical St. Vincent type ash-flows.

Concluding Remarks

Results of the study on the textural and constituent characteristics of different types of pyroclastic flow deposits are presented in this paper, with some discussions on the mode of origin and mechanism of pyroclastic flow eruptions. The study of the pyroclastic flows is still in a incipient stage, and a great deal of further study is needed. The writer classifies several subdivisions of pyroclastic flows on the basis of of the nature of the representative eruptions of pyroclastic flows actually investigated by geologists and volcanologists, as well as the nature of their deposits. Every discussion mainly centers on these representative eruptions and their deposits. He carried out the analytical investigations on many examples of the pyroclastic flow deposits produced by prehistorical eruptions, and obtained many consistent results sufficient to discuss on the formation and mechanism of pyroclastic flows. There are, however, rather few examples of occurrences of pyroclastic flows

ever investigated on the spot, and some arguments tend to be more or less inferential. Future studies that supply quantitative data to decipher unsolved problems of the phenomena of pyroclastic flows may eliminate the uncertainty of such inferential arguments. Among the main subdivisions classified by the writer, there are all transitions. Future studies may reveal the precise nature of such transitions. The writer could not obtain sure examples of the last subdivision of pyroclastic flows, namely, the Valley of Ten Thousand Smokes type ash-flow or fissure eruption type ash-flow, and the recognition and study of this type of deposit are necessary in the near future in Japan. He omitted in this paper detailed discussions on the origin of the magmas that produce eruption of pyroclastic flow. Herein lies a important problem to be solved, especially in the origin of the magma that produce vast ash-sheets of extremely high magnitude.

---

7. 火砕流堆積物の組織的性質

地震研究所 村 井 勇

概論 1902 年 Martinique 島の Mt. Pelée で烈しい噴火が起つた．側方向に噴出された物質が，ガスとともに一団となつて熱い黒雲を作り，山腹に沿つて非常な速度で流れ下つた．噴火はその後もつづき，同様な噴火が繰り返えされた．これらの噴火は，従来知られていなかつた型式のもので，これに対して，Lacroix は nuée ardente と命名した．同じ 1902 年，St. Vincent の Soufrière でも，同様な噴火が起つた．nuée ardente 噴火はこの二つの噴火によつて確認され，その研究が開始された．1929～1932 年にも Mt. Pelée は同様の噴火を行なつた．Merapi 火山 (1930～1935)，Mt. Lamington (1951～1952) や Hibok-Hibok 火山 (1948～1952) でも同様の噴火が起り，詳しく調査された．このようにして，nuée ardente 噴火は今世紀に入つて次々に確認され，その性質はしだいに明瞭になつてきた．一方，火山砕屑堆積物の研究から，nuée ardente の産物と認められるものが世界各地の火山地域で発見されるようになり，この型式の噴火が地域的にも時代的にもかなり普遍的に起つていることが明らかになつてきた．Fenner (1920, etc.) は Katmai 地域で起つた 1912 年の噴火による噴出物を詳細に調査し，Valley of Ten Thousand Smokes を埋めた火山灰が同様な噴火によるものであることを明らかにした．Moore (1934) は Crater Lake 地域に分布する軽石質堆積物の研究を行ない，“Older pumice” と呼んだ軽石層が，nuée ardente の産物であると結論した．Marshall (1935) は New-Zealand の Taupo-Rotorua 地方に分布する rhyolite tuff が同様に nuée ardente 噴火によるものであることを明らかにした．さらに，Williams (1941) は caldera の成因について詳しい検討を行ない，Krakatoa 火山の 1883 年の噴火のさいに大量の軽石が nuée ardente となつて噴出し，その結果，カルデラの陥没が起つたことを明らかにした．Katmai 地域，Crater Lake 地域や Krakatoa 火山で見られるこのような nuée ardente 起源の軽石質堆積物は，その後，世界各地の火山地帯で次々と発見されている．日本では，1929 年北海道駒ケ岳の噴火のさいに，軽石流の噴出が起つた．久野 (1941) はこの堆積物の特徴が一般の降下軽石堆積物と全く異な

ることを指摘した．さらに久野 (1954) は日本の数多くのカルデラが Williams の説と同様の機巧で生じたことを指摘した．日本の各地に分布する nuée ardente 起源の火山砕屑堆積物の確認と記載は多くの人々の手によつて進められている．

Nuée ardente 噴火の機巧とその原因については，実際の観察記録や堆積物の研究から，いくつかの推論が加えられている．しかし研究が進むにつれて，nuée ardente と呼んできた一連の噴火には，規模も型式も，噴出物の性質も著しく異なるものが含まれていることが明らかとなり，この現象の詳しい検討と解析とが必要になつてきた．Lacroix (1930), Escher (1933), Fenner (1937), MacGregor (1952, 1955), Williams (1957), 荒牧 (1957) らは，nuée ardente の機巧について解析を試み，その分類を行なつている．このようにして，nuée ardente の研究はすでに多くの成果をあげているが，しかしこの分野の研究をさらに前進させるためには，実際の噴火の観察記録をさらに充実させるとともに，噴出物の性質について綿密な定量的な調査を進めることが必要となつている．従来の研究により，nuée ardente 噴火の原因と機巧は，マグマの粘性，溶存ガス含量およびその放出の条件などに関係しており，その噴火型式と噴出物の組織的性質との間には密接な関係があるということが示唆されている．この事は研究の将来の方向を暗示するものといえる．すなわち，噴出物の化学組成，鉱物組成や岩石学的特徴の研究と並行して，その組織，構造，構成物質についての解析が必要と考えられる．従つて nuée ardente 起源の火山砕屑堆積物を sedimentary petrology の諸方法をもつて研究を進めれることは，多くの成果をもたらすものと期待できる．筆者はそのような観点から，日本の各火山に見られる nuée ardente 起源の火山砕屑堆積物について，その組織的諸性質と構成物質について定量的な調査を行なつて，nuée ardente 噴火の原因と機巧の解明に役立つような資料を見出そうと考えて研究を進めている．

用語 nuée ardente: この語は Lacroix が Pelée の噴火に対して用いたものである．しかしその後，Pelée の噴火と類似の性質を持つた噴火が次々に認められるようになり，そのいずれに対しても同一の語が適用され，その意味はきわめて広く解釈されるようになつた．こうした弊害を避けるためには，nuée ardente (熱雲) という語を，本来の Pelée 火山の噴火型式およびそれにきわめて近い型式のものに限つて用いるべきである．荒牧は広い意味の nuée ardente に代るものとして pyroclastic flow (火砕流) という語を提唱している．筆者もこれに従うことにする．

ash-flow: 火砕流堆積物の最も顕著な性質は，いろいろな粒径の粒子が雑然と混合していることである．しかし，大部分の堆積物は中位粒径が火山灰の粒径 (1/4～4 mm) 付近にあり，大きな比率で細粒物質が含まれている．これに対して，Smith (1960) は“ash flow deposit”(灰流堆積物) という語を提唱し，直径 4 mm 以下の粒子が 50% またはそれ以上の比率を占めるものと定義している．この語は従来用いられてきた tuff flow, volcanic sand flow, pumice flow, ignimbrite, welded tuff 等々の語のほとんど大部分のものを含めて用いることができる．筆者はこの語を，その火砕流の分類に採用している．

mud-flow: 火砕流堆積物と外見の非常によく似た堆積物に泥流堆積物がある．mud-flow (泥流) という語は一般には非常に広い意味で用いられている．実際に泥流堆積物と呼ばれているものを調査すると，いろいろな成因のものが含まれており，その意味はきわめてあいまいとなつている．ここでは筆者は，爆発によつて火山体が崩壊して発生した泥流堆積物のみを特に取りあげて，その組織的性質を論じたいと思う．このようなものをここでは dry mud-flow と呼ぶことにする．

火砕流の分類 火砕流にはいろいろの型式のものがあり，多くの人々によつてその分類が行なわれている．それらの分類のなかで最も基本的なものは Lacroix (1930) と Escher (1933) の分類である．Williams (1957) はさらに詳しい検討を加え，堆積物の特徴を詳述している．いずれも観察された実際の噴火についての研究の結果に基づいて分類が行なわれている．これらの分類に対し，荒牧の分類 (1956) はその基準が火砕流堆積物の性質に置かれている．この二つの分類法は出発点は異なるが，その内容は決して矛盾するものではない．火砕流の機巧は噴出物の性質と密接な関係があり，この両者を切離して考えることはできないからである．筆者は従来の分類に若干の手を加え，次のような scheme を作つてみた．この分類の基準は，実際の噴火の機巧及びその噴出物の性質に置かれている．(第 1 表および第 2 表参照)

熱雲	{Pelée 型, (Merapi 型) {桜島型
中間型火砕流	
灰流	{St. Vincent 型 {Krakatoa 型 {Valley of Ten Thousand Smokes 型

粒度組成 筆者の調査した火山は第1図および第3表に示す通りである．これ以外にも火砕流堆積物および泥流堆積物の例はいくつか知られているが，未だ調査の機会を得ていない．試料を採集して機械分析を行なつたが，その結果を総括して下に列記する．(第4, 5, 6, 7表および第3, 4, 5図参照)

1) 分級の悪さ．火砕流堆積物は分級が悪いことが特徴であり，この性質に基づいてこの種の堆積物の確認が行なわれている．標準偏差のパラメーターである σ_ϕ は2～5の値をとり，一般の降下火砕堆積物がほとんど2以下の値をとるのと全く対称的である．mode の部分の占める比率が降下堆積物では ϕ scale の1区間について30% 以上になる場合が屢々であるが火砕流堆積物では25% 以上になることはほとんどなく，大部分の場合15～20% 程度である．火砕流堆積物では降下堆積物に見られるような火口からの距離に応じた粒度の変化は見られない．

2) 均質性．火砕流堆積物は単一の unit の中ではきわめて均質な性質を示し，試料間のばらつきは少ない．従つて粒度分布曲線はよくそろい，パラメーターの値は狭い範囲内に入る．また同一の火山から噴出した，時代を異にする火砕流堆積物は屢々ほとんど同様の粒度組成を示す．これは同一の火山では同様の火砕流噴火が屢々繰り返えされることを示している．大規模な火砕流では，かならずしも全体が同一時期に噴出したものではない場合が多いが，しかしそれらの全体を通じて粒度組成の特徴は同一の傾向を明瞭に示している．隣接する火山相互の間にも火砕流堆積物が類似の性質を示す傾向が認められることが多い．

3) 中位粒径 $Md\phi$ の値はかなり広い範囲にわたるが，大部分のものは ϕ: −2～4 の範囲に入る．すなわち大分部の火砕流堆積物は粒度組成からいえば Smith (1960) の定義による "ash flow deposit" に属する．火砕流堆積物の分類による各々の型では，$Md\phi$ の値が大体一定の範囲にある，すなわち，中間型火砕流および熱雲では $Md\phi > 1$, St. Vincent 型では，0～2, Krakatoa 型では0～4 である．

4) 粒度分布曲線の形．火砕流堆積物の粒度分布曲線の形はきわめて特徴的なものである．分級は悪く，分布曲線は粗粒部と細粒部に長く尾をひく．これは，降下堆積物の粒度分布曲線が粗粒部の尾が鋭く切られていることと全く対照的である．さらに細部について見れば，火砕流の型の相異に応じて，その堆積物の粒度分布曲線の型も変化している．$Md\phi$ の値は前記の通り広い範囲にわたつて変化する．歪度は正，負両方の場合があり，中間型火砕流では特に負の傾向が大きい．これは降下堆積物の場合正の傾向が大きいのと全く対照的である．尖度のパラメーターである $\beta\phi$ の値を見れば，0.65 (正規分布の場合) を中心にして上下に広く分布する．しかし一般には 0.65 より大きい値をとる傾向が見られる．粒度分布の型は unimodal と bimodal と両方の場合がある．Krakatoa 型灰流には中粒のものと細粒のものとあり，細粒のものはほとんど unimodal, 中粒のものは bimodal の傾向をわずかに示す．St. Vincent 型灰流は bimodal の傾向が著しく，かつ主 mode が卓越する傾向を示す．中間型火砕流および熱雲では bimodal の傾向が特に顕著となり，かつ分布曲線は変動が大きくなる．中粒部の主 mode はむしろ低くなり，全体として分級は非常に悪くなる．Krumbein と Tisdel (1940) によつて指摘されたような火砕流堆積物の粒度分布が Rosin の法則に適合するという事実は，一般には認められない．これは粒度分布の bimodal な性質からもただちに明らかなことである．Rosin の法則に従わないということは，分級作用がある程度有効に働らいていることを示すものと見られる．Rosin 紙に描かれた積算曲線は火砕流の各型にそれぞれ特徴的な形を示す．すなわち，Krakatoa 型灰流はなだらかな凹形，St. Vincent 型灰流は二つの山をもつ波形，中間型火砕流および熱雲は中央で折れた直線形を示す (第9図参照)．

5) 火砕流の各型の堆積物の粗度組成．火砕流の各型の堆積物にはそれぞれ特徴的な粒度組成が認められる．

細粒 Krakatoa 型灰流堆積物および V.T.T.S. 型灰流堆積物：細粒，unimodal, 正規分布に近い型，分級は悪い．

中粒 Krakator 型灰流堆積物：中粒，unimodal であるが，かすかに bimodal の傾向を示す，中粒部の分級は，St. Vincent 型のようにはよくない．

Vt. Vincent 型灰流堆積物：中粒，bimodal, 中粒部の分級はいちじるしくよく，卓越する主 mode を示す．しかし粗粒部に顕著な副 mode があり全体としては $\sigma\phi$ の値は大きくなる．

中間型火砕流堆積物および熱雲堆積物：粗粒ないし中粒，bimodal, 粒度組成の変化は大きい，中粒部の主 mode は St. Vincent 型灰流のように顕著ではない．

6) dry mud-flow および自破砕熔岩流の粒度組成．火砕流堆積物，特に中間型火砕流および熱雲の堆積物は dry mud-flow の堆積物と粒度組成の点できわめてよく類似している．しかし dry mud-flow の堆積物の場合は均質性が乏しく，分布曲線の形の変化が著しく，分級はさらに一段と悪く，細粒部が特に多量となるなどの点で，火砕流堆積物と異なつている．構成物質についていえば，後者が本質破片を含まぬという点で全く異なつている．自破砕熔岩流も火砕流ときわめてよく似た粒度組成を示す．しかし，分布曲線の形の変化は非常に大きく，火砕流堆積物の場合のような均質性が認められない．恐らくこの二つのものの粒度組成は Rosin の法則に従う傾向があると考えられる(第 10 図参照)．

粒子の円磨度　火砕流堆積物を構成する粒子の roundness (円磨度)はその噴出および流動の状態を示す重要な要素と考えられる．筆者はその直径 32～4 mm の粒径のものについて Krumbein (1941) の方法で円磨度を測定した．また，火砕流の直前，あるいは同時に噴出した降下堆積物の試料を採集して，同様に構成粒子の円磨度を測定した(第 13 表参照)．その結果，次のような事実が知れた．

火砕流堆積物の構成粒子は普通に考えられていたように著しく円磨されてはいない．St. Vincent 型灰流と Krakatoa 型灰流では円磨度の値は 16～8 mm の粒子についていえば，一般に 0.3～0.5 の範囲の値を示す．孔隙率の大きい粒子ほど円磨度の値は大きくなる傾向を示すが，しかし石質破片と多孔質本質破片との間の円磨度の差は 0.1 程度にすぎない．同時，あるいは相次いで噴出した火砕流堆積物と降下堆積物とでは，後者の粒子の方が円磨度の値は小さい．しかしその差は 0.1 程度にすぎない．この事実は，粒子の円磨が火道の途中においてすでに始まつていることを示している．火砕流の流下中には，放出されたガスが滑剤として働らくために，粒子の円磨がその間に著しく進行することはないと考えられる．中間型火砕流と熱雲では，粒子はかなり角ばつており，16～8 mm の粒子については円磨度は 0.25～0.4 である．孔隙率の大きい軟かい粒子の方が，密度の大きい硬い粒子や石質破片より角ばつている場合が屢々あり，これは明らかに火砕流の流動中にガスの放出が続いて，多孔質本質破片の粒子が角ばることを示している．熱雲の流動の機巧については，“auto-explosion”の性質が多くの学者により重要視されているが，中間型火砕流についても同様と見られる．これに対し，灰流の場合は“auto-explosion”の性質がその流動の機巧の主要因をなしていると見ることはできない．

本質破片の形状　火砕流堆積物の本質破片は非常に多孔質であることが特徴である．岩漿からのガスの放出の条件が火砕流の形成と流動の機巧において重要な要因となつていると考えられるから．このガス放出の過程を知ることはきわめて重要であるが，それは本質破片の形状に明瞭に反映されている．特に注目すべき点は，長くひき伸ばされた気泡をもつた軽石質破片のあることと，その量である．このような粒子は細粒 Krakatoa 型灰流およびおそらく V.T.T.S. 型灰流に特に著しい．これに対して中間型火砕流および熱雲では気泡は不規則な形をしており，引き伸ばされたあとは見られない．St. Vincent 型灰流ではこの両者の中間の状態を示す．火砕流の各型の間に見られるこのような本質破片の形状の相異は，ガスの放出の過程の相異を明瞭に示すものである．(第 14 表参照)

構成物質　火砕流堆積物はいろいろな種類の粒子によつて構成されている．特に lapilli の粒径以上のものは多孔質の本質破片と各種の石質破片とによつて構成され，その構成の比率は火砕流の各型の特徴をよく表現してるい．これに対して ash の粒径の部分は主として結晶粒によつて構成されている．細粒の部分はガラス片および結晶片よりなる．Krakatoa 型灰流では類質および異質石質破片はかなり高い比率を示す．その岩石は基盤および火道の周囲の岩石と考えられるもので，流下の途中で火山体の表面より取り込まれた岩石はごく少ない．St. Vincent 型灰流では，類質および異質石質破片の比率は一般に低い．しかし，石質破片の比率の極度に高いものもあり，この場合，岩石

は火山を構成していた岩石から由来したと考えられ，また別に火道を埋めていたと見られる結晶度の高い同源石質破片が認められる場合が多い．このような型の灰流はむしろ dry mud-flow との中間の性質を持つたものであり，厳密には，St. Vincent 型灰流とは区別しなければならない．典型的な St. Vincent 型の灰流では石質破片の量は少なく，中粒部に結晶の著しい集中が認められる．すでに Hay (1959) が明らかにしているように，噴出のさいのガス圧力が低いことから，垂直方向の分級が噴火雲の柱中，特に外側の部分で起り，灰流の発生の原因となつたと考えられる．中間型火砕流では本質破片はかなり緻密なものから著しく多孔質なものまで見られるのが特徴である．火山弾の形状を示すものが普通に見られる．多孔質な破片は円磨度の値が非常に小さく，auto-explosion のあとを見せている．類質および異質石質破片は一般に少ない．しかし，流下のさいに火山体の表面より多量の岩片を取り込む場合がある．熱雲のうち Pelée 型の堆積物では円頂丘の皮殻を作つていたと見られる結晶質の同源石質破片が多孔質な本質破片とともに存在する．この同源石質破片は角ばり，多面形を呈する．類質または異質石質破片の量は非常に少ない．火山弾はほとんど見られない．桜島型熱雲では事情は少し異なつている．粗粒の岩塊はすべて本質岩塊で auto-explosion を示す著しく特徴的なパン皮状火山弾の形状を見せている．(第 15 表参照)

本質破片の見かけの比重　火砕流の噴出機巧を支配する最大の要因は magma 中の溶存ガスの量であり，それは本質破片の発泡状態，即ち孔隙率に反映されていると考えられる．本質破片の孔隙率を正確に測定することは非常に困難であるので，筆者は見かけの比重を測定して見た．その値は一般に変動が大きいが，試料数を十分大きくとれば，だいたい一定の平均値を求められる．この平均値について見ると，Krakatoa 型灰流では 0.5～0.7, St. Vincent 型灰流 (dry mud-flow との中間型も含めて) では 0.7～1.2, 中間型火砕流では 1.2 以上となる．中間型火砕流では，特に各粒子についての変動が著しいのが特徴である．(第 16 表参照)

噴火の順序　火砕流の噴出に先行して爆発的な噴火が起り多量の軽石や火山灰を降らせることは屢々認められている．Kennedy (1955), 山崎 (1959), 勝井 (1960) によつて指摘されているように，一般に噴火の初期には magma 柱の上部のガスを多量に含んだ部分の噴出により爆発的噴火が起り，噴火の後期には次第に下部のガスに乏しい部分が上昇して，lava の流出に移行するという傾向が認められ，その推移の途中において火砕流の噴出が起ると考えられる．この間に岩漿の性質が silicic から mafic へと変化したことが確かめられた例も多い．このような事実は，火砕流の形成の主な要因が岩漿中のガスの量およびその放出の条件にあることを明瞭に物語つている．

化学組成　火砕流堆積物は岩石学的にも化学組成の上からも大きな範囲にわたつて変化を示している．玄武岩質の岩漿の噴火によつて生ずる火砕流はほとんど認められないが，安山岩，石英安山岩，流紋岩質の岩漿の噴火では屢々火砕流が認められる．SiO_2 含量は一般には，55% より 75% の範囲に入る．熱雲，中間型火砕流および St. Vincent 型灰流では SiO_2 % が 55～65% の範囲に入るものが多い．これに対して Krakatoa 型灰流では 65～75% の場合が多い．V.T.T.S. 型灰流では Krakatoa 型の場合とほぼ同程度であるが 75% を越えるものもある．火砕流堆積物中の本質破片はほとんどの場合，多孔質で非晶質の石基を有し，石基の鉱物の組合せから岩石系を知り得る場合は少ない．しかし，化学分析の結果から Fe－Mg－Na＋K 図型上に plot すれば，少数の例外を除けば，すべて久野 (1950, 1953) の紫蘇輝石質岩系の区域に入る．紫蘇輝石質岩系は本源岩漿が花崗岩質岩石による混成作用を受け，かつ分別結晶作用を行なつた結果生成したものであると解釈されるから，火砕流を生ぜしめた岩漿の殆んどが混成作用を受けたものであることが知れる．混成作用によつて水その他の揮発性物質が岩漿のなかに濃縮すると見られ，このような揮発性物質を特に多量に含んだ岩漿の噴火により火砕流が生ずるものと考えられる．

火砕流の形成と流動の機巧　[ガス放出の過程] 火砕流堆積物の粒度組成，本質破片の形状，円磨度などから判断して，Krakatoa 型灰流 (および V.T.T.S. 型灰流) では発泡が地下深処から始まり，火道を上昇する間に岩漿の大部分は泡立ち，細かく砕かれ，噴出口から烈しい爆発を伴なわずに流出して火砕流を形成すると解釈される．一方 St. Vincent 型灰流では，発泡は火口内からはじまり，火口の縁では岩漿は一部泡立ち，一部液体のままの状態にあり，噴火は爆発的ではあるが，噴出のガス圧力は著しく高くはなく，噴火雲の内部特に外側で分級を受けた重い物質，すなわち粗粒の軽石と結晶粒とが，その重さのために落下して火砕流を形成すると考えられる．中間型火砕流では，

Fig. 16. The Middle Ash-flow of the Kutcharo Volcano. Sp. no. Kc 9, Notoro, Abashiri-shi.

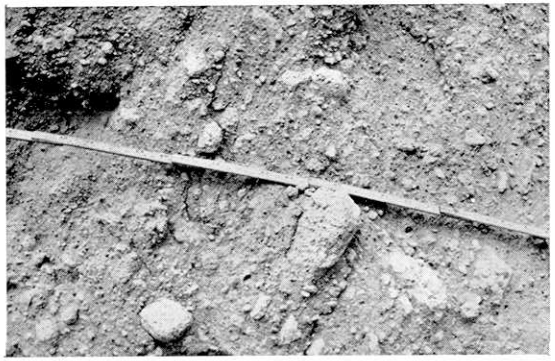

Fig. 18. The Upper Ash-flow of the Kutcharo Volcano. Sp. no. Kc. 6, Hiushinai, Tanno-mura.

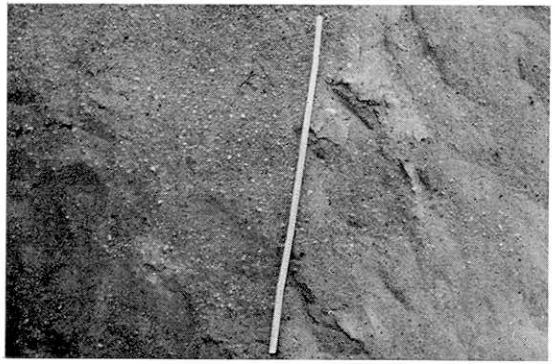

Fig. 17. The Middle Ash-flow of the Kutcharo Volcano. Sp. no. Kc 8, Heiwa, Abashiri-shi.

Fig. 19. The Ash-flow of the Mashu Volcano. Sp. no. Ms 3, Minakami, Koshimizu-machi.

Photographs of pyroclastic flow deposits

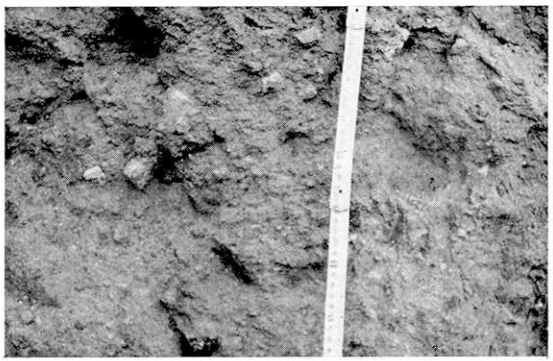

Fig. 20. The Meakandake Pyroclastic Flow of the Akan Volcano. Sp. no. Ak 4, Kamihakuai, Ashoro-machi.

Fig. 22. The 1929 Pyroclastic Flow of the Tokachi-dake Volcano. Sp. no. Tk 6, Bôgakudai.

Fig. 21. Non-welded part of the Tokachi Welded Tuff. Sp. no. TkW 1, Shimizuyama, Furano-machi.

Fig. 23. The Ash-flow and the preceding ash-falls of the Daisetsuzan Volcano. Sp.no. D 2, Ôbako, Kamikawa-machi.

Photographs of pyroclastic flow deposits

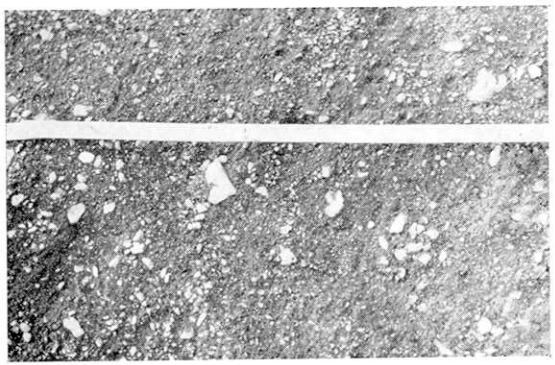

Fig. 24. The Ash-flow of the Shikotsu Volcano. Sp. no. S 7, Tomakomai-shi.

Fig. 26. The Upper Ash-flow of the Toya Volcano. Sp. no. Ty 5, Tateyama, Date-machi.

Fig. 25. The Upper Ash-flow of the Kuttara Volcano. Sp. no. Kt 2, Noboribetsu hot spring.

Fig. 27. The 1929 Ash-flow of the Komagatake Volcano Sp. no. Km 4, Akaigawa, Mori-machi.

Photographs of pyroclastic flow deposits

Fig. 28. The Ash-flow of the Towada Volcano. Sp. no. Tw 14, Nigorigawa, Kosaka-machi.

Fig. 30. The Older Ash-flow of the Towada Volcano. Sp. no. Tw 22, Nenokuchi.

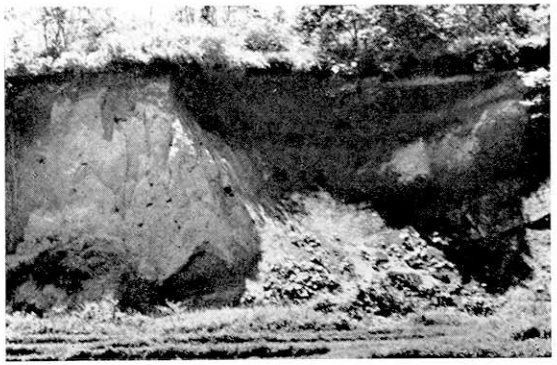

Fig. 29. The Ash-flow and the preceding ash-fall of the Towada Volcano. Sp. nos. 17 and 23, Gonohe-machi.

Fig. 31. The Welded Tuff of the Hakkoda Volcano. Sp. no. Hd 1, Moya, Aomori-shi.

Photographs of pyroclastic flow deposits

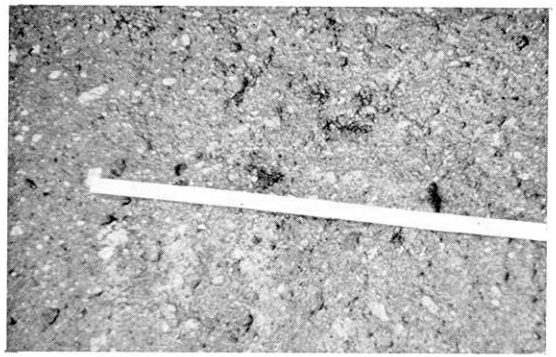

Fig. 32. The Ash-flow of the Osoreyama Volcano. Sp. no. Os 1, Futamata, Mutsu-shi.

Fig. 34. The Ash-flow of the Onikobe Volcano. Sp. no. On 2, Haguro, Furukawa-shi.

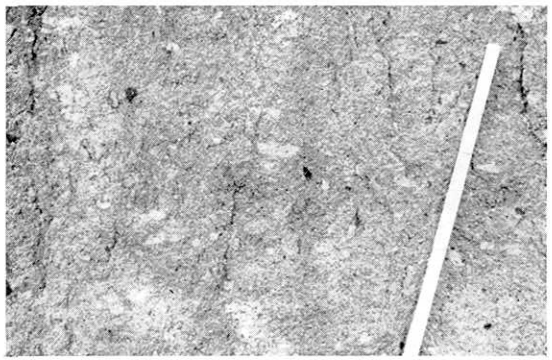

Fig. 33. The Tazawa Welded Tuff. Sendatsu, Obonai-machi.

Fig. 35. The Ash-flow of the Hijiori Volcano. Sp. no. Hj 2, Hikage, Ôkura-mura.

Photographs of pyroclastic flow deposits

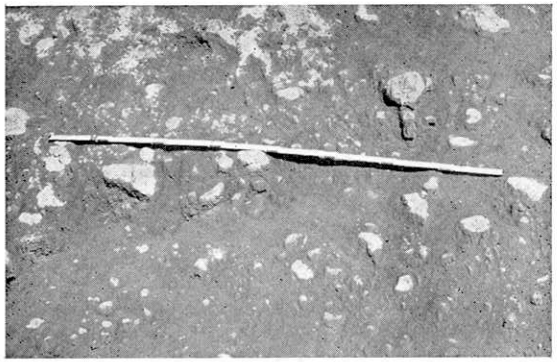

Fig. 36. Non-welded part of the Numajiri Welded Tuff. Sp. no. Nm 1, Nakanosawa, Inawashiro-machi.

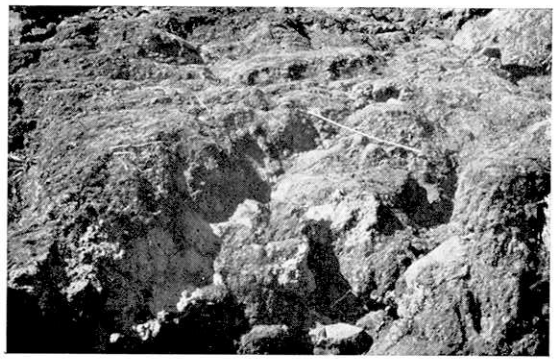

Fig. 38. The Scoria-flow of the Nantai Volcano. Sp. no. Nn 1. Misawa, Nikkô-shi.

Fig. 37. The Ash-flow of the Takaharayama Volcano. Sp. no. Th 1, Hariu, Yaita-machi.

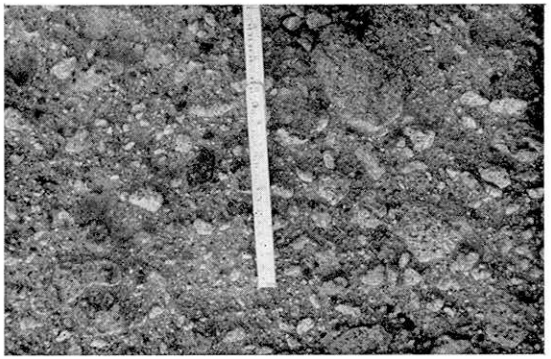

Fig. 39. The Pumice-flow of the Nantai Volcano. Sp. no. Nn 3, Arasawa, Nikkô-shi.

Photographs of pyroclatic flow deposits

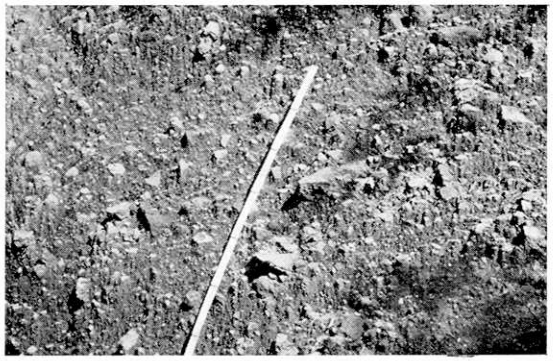

Fig. 40. The Lower Ash-flow of the Haruna Volcano. Sp. no. Hr 1, Ikaho-machi.

Fig. 42. The Ash-flow of the Kusatsu-Shirane Volcano. Sp. nos. SK 3 and 4, Mihara, Tsumagoi-mura.

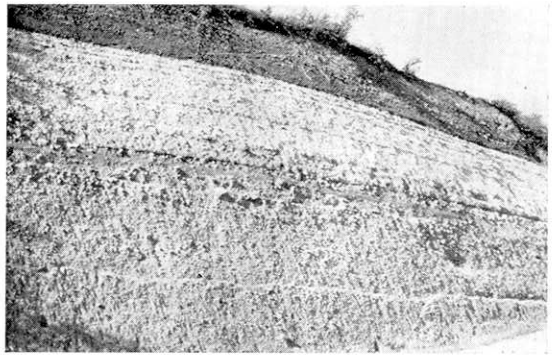

Fig. 41. The Lower and Upper Ash-flows and the preceding pumice-fall of the Haruna Volcano. Sp. nos. Hr 2, 4 and 5, Kurosawa, Shibukawa-shi.

Fig. 43. The Pyroclastic Flow of the Myoko Volcano. Sp. no. My 2, Tsubamegawara, Myôkôkôgen-mura.

Photographs of pyroclastic flow deposits

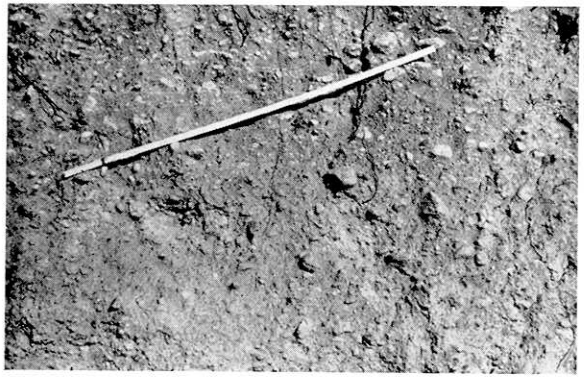

Fig. 44. The Upper Ash-flow of the Asama Volcano. Sp. no. Am 20, Matsubayashi, Komoro-shi.

Fig. 45. The Oiwake Pyroclastic Flow of the Asama Volcano. Sp. no. Am 28, Mitsuya, Miyota-machi.

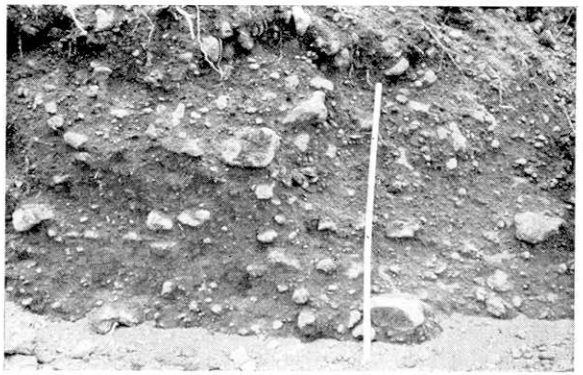

Fig. 46. The Agatsuma Pyroclastic Flow of the 1783 eruption of the Asama Volcano. Sp. no. Am 32, Kuromame-gawara, Naganohara-machi.

Fig. 47. An essential block of the Kambara Nuée Ardente of the 1783 eruption of the Asama Volcano.

Photographs of pyroclastic flow deposits

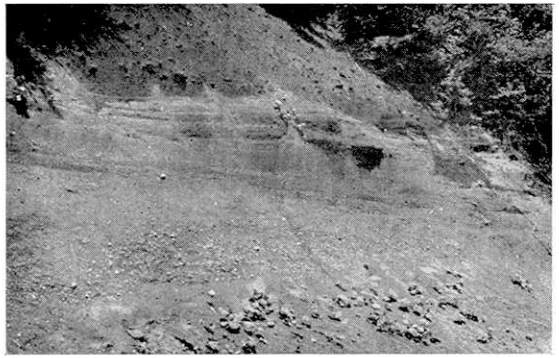

Fig. 48. The Ash-flows of the Hakone Volcano. Sp. nos. Hn 6 and 8, Hakone-machi. The upper layer is scoriaceous and the lower layer is pumiceous.

Fig. 49. The Ash-flow (pumiceous) of the Hakone Volcano. Sp. no. Hn 1, Ashigara, Odawara-shi.

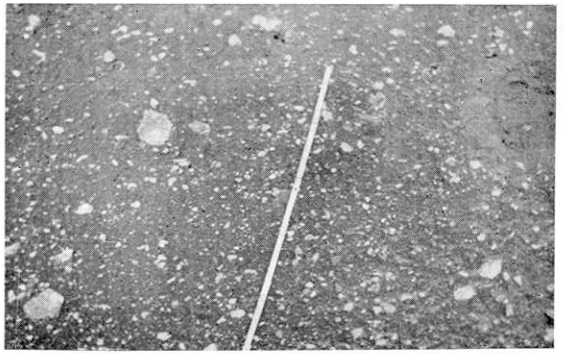

Fig. 50. The Ash-flow (scoriaceous) of the Hakone Volcano. Sp. Hn 10, Mishima-shi.

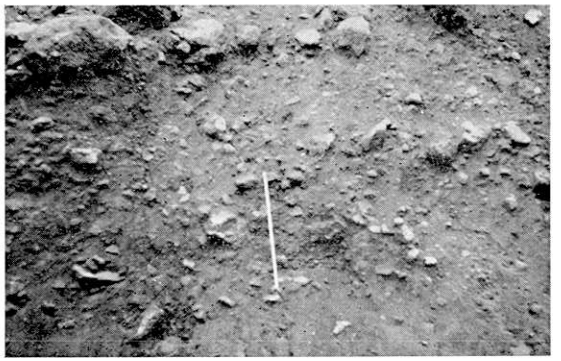

Fig. 51. The Central Cone Pyroclastic Flow of the Hakone Volcano. Sp.Hn 11, Ubako, Sengokuhara-mura.

Photographs of pyroclastic flow deposits

Fig. 52. The Pyroclastic Flow of the Ko-Fuji Volcano. Sp. no. KF 1, Tanukinuma, Fujimiya-shi.

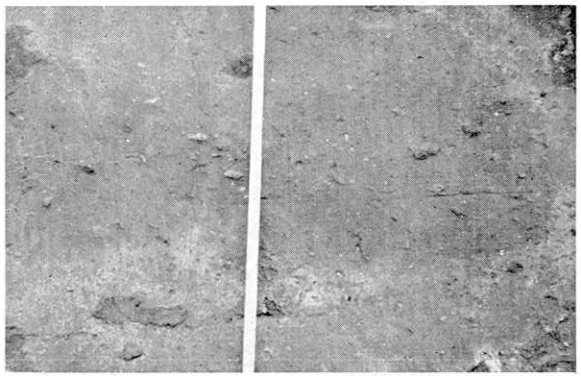

Fig. 53. The Ash-flow of the Aso Volcano. Sp. no. As 2, Hitoyoshi-shi.

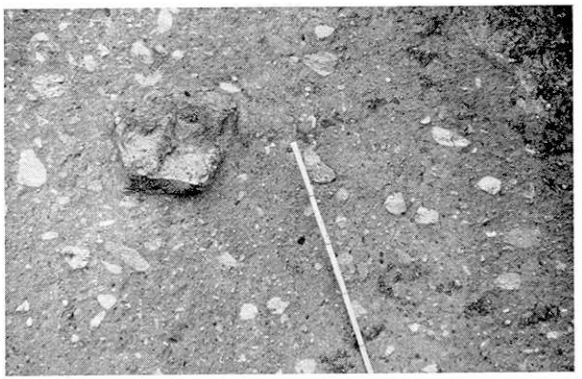

Fig. 54. The Middle Ash-flow of the Aira Volcano. Sp. no. Ai 1, Taguchi, Kirishima-mura.

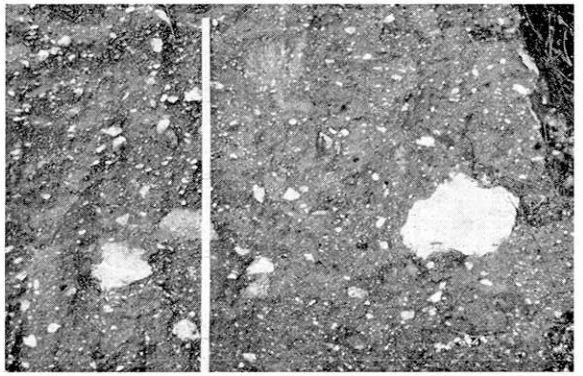

Fig. 55. The Middle Ash-flow of the Aira Volcano. Sp. no. Ai 13, Imaizumi, Ibusuki-shi.

Photographs of pyroclastic flow deposits

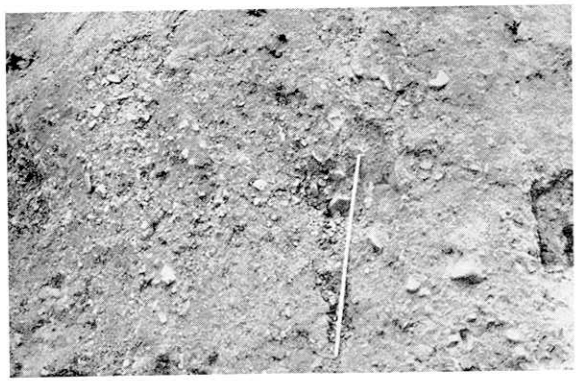

Fig. 56. The Sukawa Mud-flow of the Zaô Volcano. Sp. no. Z 1, Zaô hot spring, Yamagata-shi.

Fig. 57. The 1888 Mud-flow of the Bantai Volcano. Sp. B 3, Kitashiobara-mura.

Fig. 58. A lava flow of Meakandake. Sp. no. Ak 5, Ashoro-machi.

Fig. 59. A lava flow of the Fuji Volcano. Sp. no. F 2, Shimoawakura, Fujimiya-shi.

Photographs of dry mud-flow deposits and auto-brecciated lava flows

岩漿が火口から噴出するさいおよびその後に発泡が起る．この場合，火山灰が火口から垂直に高く抛出されることはなく，噴出物は一団の泡立つ火砕流となつて山腹を流下する．熱雲の場合も，同様に発泡は火砕流の流動の途中に主として起る．

[火砕流の二体性] 多くの学者によつて指摘されているように，火砕流は二つの部分，すなわち下部の粗粒の物質を含む火砕流の本体と，その上部にひろがる火山塵とガスの雲とに分かれて流下する．このような性質は中間型火砕流と熱雲の場合に特に著しい．これは火砕流の流下の途中で烈しい発泡が起るため，すなわち auto-explosion のためである．放出されたガスは滑剤として働らき，火砕流は非常な速度で流動する．灰流の場合では発泡は主として噴出以前あるいは噴出のさいに起るが，しかしガスの放出は流動の間でも続くと考えられるから，同様の性質を示すと見られる．St. Vincent 型灰流では特にこの性質が顕著に認められる．

[分級作用] 火砕流は乱流の状態で烈しく流下し，分級のかなり悪い堆積物をそのあとに残す．しかしこの間に分級作用はある程度有効に働らき，堆積物は特徴的な粒度組成を持つようになる．分級作用は噴出のさいにも火砕流の流下の途中にも起る．St. Vincent 型灰流では，垂直に上昇する噴火雲のなかで重い粒子が分級作用を受けて落下し，火砕流を形成するが，流下の途中でもガスの放出が続いて細粒物質は上空に運ばれ，粗粒の軽石と結晶粒が特に集中した堆積物を生ずる．中間型火砕流および熱雲でも，流下中に起る auto-explosion により多量の細粒物質が上空に運ばれる．Krakatoa 型灰流および V.T.T.S. 型灰流でもある程度の分級作用が働らくと考えられ，粒度組成は Rosin の法則に適合しなくなる．

[dry mud-flow との中間的性質を有するもの] St. Vincent 型灰流堆積物と共通の性質をもち，類質および異質石質破片の比率が極端に高い堆積物が屢々見られる．これは St. Vincent 型灰流に伴なう場合が多く，特にその最下部を構成する場合が多い，おそらく爆発的噴火によつて火山体の一部が破壊され，同時に多量の本質破片が噴出して火砕流を形成したものと解釈される．このようなものは多くの点で火砕流と dry mud-flow との中間的性質を示している．